UNIVERSIDAD NACIONAL AUTÓNOMA DE MEXICO

POSGRADO EN CIENCIA E INGENIERÍA DE MATERIALES
INSTITUTO DE INVESTIGACIONES EN MATERIALES

A NEW DIMENSIONLESS COUPLING CONSTANT IN SUPERCONDUCTIVITY

QUE PARA OPTAR POR EL GRADO DE:
DOCTOR EN CIENCIA E INGENIERÍA DE MATERIALES

PRESENTA:
ISRAEL CHÁVEZ VILLALPANDO

TUTOR PRINCIPAL
DR. MANUEL DE LLANO DE LA GARZA
INSTITUTO DE INVESTIGACIONES EN MATERIALES, UNAM

MIEMBROS DEL COMITE TUTOR
DRA. MARCELA DOLORES GRETHER GONZÁLEZ
FACULTAD DE CIENCIAS, UNAM
DR. FRANCISCO JAVIER SEVILLA PÉREZ
INSTITUTO DE FÍSICA, UNAM

CD.MX. AGOSTO DE 2018

UNIVERSIDAD NACIONAL AUTÓNOMA DE MÉXICO

A NEW DIMENSIONLESS COUPLING CONSTANT IN SUPERCONDUCTIVITY

T E S I S

QUE PARA OBTENER EL GRADO DE:

Doctor en Ciencia e Ingeniería de Materiales

PRESENTA:

M. en C. Israel Chávez Villalpando

Director de Tesis

Dr. Manuel de Llano de la Garza
Instituto de Investigaciones en Materiales, UNAM

Comité tutor

Dr. Marcela Dolores Grether González
Facultad de Ciencias, UNAM

Dr. Francisco Javier Sevilla Pérez
Instituto de Física, UNAM

UNAM POSGRADO
Ciencia e Ingeniería de Materiales

AGOSTO, 2018

A NEW DIMENSIONLESS COUPLING CONSTANT IN SUPERCONDUCTIVITY

THESIS

in order to obtain

Doctoral degree at

Materials Science and Engineering

Presented by

Israel Chávez Villalpando

Materials Research Institute
National Autonomous University of Mexico

Supervisor Committee

Dr. Manuel de Llano Dr. Marcela D. Grether Dr. Francisco J. Sevilla

August, 2018

To Cruzita† and Jorge my beloved parents.
To let me be in this lifetime,
to give me the gift of this lifetime.

In memoriam
Vladimir V. Tolmachev
(1930 – 2018)

"Pluralitas non est ponenda sine necessitate"
("plurality should not be posited without necessity")
William of Ockham (1285–1347/49)

Acknowledgments

I thank to my supervisor committee in the Graduate Program (Posgrado de Ciencia e Ingeniería de Materiales) at National Autonomous University of Mexico (UNAM): Dr. Manuel de Llano, Dr. Marcela Grether, Dr. Mauricio Fortes and Dr. Francisco Sevilla for their guide, their support and patience. Specially, I want to thank to Dr. Manuel de Llano for his support, his guidance, his knowledge and his wisdom; you taught me the simple way of life by using Ockhams's razor. I thank specially to Dr. Marcela Grether by her support, by the opportunity to work with you. Your guidance and knowledge makes me grow up.

I thank to the assigned jury: Dr. Chumin Wang Chen, Dr. Carlos Ramírez Ramos, Dr. Carlos Villarreal Luján, Dr. Frederic Trillaud Pighi and Dr. Manuel de Llano for his suggestions to improve this manuscript.

Many thanks to the graduate staff program: Lic. Esther Carrillo, Lic. Isabel Gómez and Lic. Diana Calzadilla. Thanks to computer technicians at Materials Research Institute: Lic. Caín González Sánchez and Lic. Alberto López Vivas and many thanks to Lic. Jacobo Méndez Ramírez and all administrative staff at Materials Research Institute, UNAM. Many thanks to the graduate program teachers: Dr. Enrique Geoffroy, Dr. Ariel A. Valladares, Dr. Roberto Escudero for their formation and advices. I am grateful with Francisco Zuñiga Frías, for his invaluable help to reading and correcting this ms. Also, I want to extend my acknowledgments to Dr. Jenny D. Vinko and Dr. Zlatko Koinov, you broaden my comprehension on superconductivity.

I thank CONACyT for graduate grant 291001 and PAPIIT-DGAPA-UNAM for completion studies grant #IN116914. I also thank CONACyT (Mexico) grant CB-2016-I #285894.

I am in debt with my family and friends, this achievement is also yours. To Life!

Contents

List of Figures

List of Tables

Abstract

The generalized Bose-Einstein condensation (GBEC) theory is an ideal boson-fermion (BF) ternary gas composed of unbound electrons as fermions, two-electron Cooper pairs (2eCPs) as bosons and explicitly includes two-hole Cooper pairs (2hCPs) also as bosons. GBEC naturally incorporates BF vertex interactions in the resulting ideal BF ternary gas that drive formation/disintegration processes of both kinds of CPs. At thermodynamic equilibrium leads to three coupled transcendental equations, a gap-like equation for 2eCPs and another for 2hCPs, as well as a number equation which guarantees charge conservation which is lacking in BCS theory. Defining the total electron number density as n and made dimensionless with that of unbound electrons at zero temperature, $n_f(T=0) \equiv n_f$ we construct a phase diagram for critical temperature in units of Fermi temperature T_c/T_F. Another diagram for the energy gap dimensionless with Fermi energy at zero temperature $\Delta(0)/E_F$, and another one for the electron chemical potential in units of Fermi energy $\mu(T)/E_F$. These phase diagrams addressed the coupling regimes changing n/n_f, the system evolves from a weak-coupling regime with $n/n_f = 1$ to a strong-coupling regime with $n/n_f \to \infty$, e.g., $n_f \to \infty$, i.e., all electrons are paired into CPs, this being the familiar picture of the BCS-BEC crossover theory, but now n/n_f plays the role of a dimensionless coupling parameter. The dimensionless coupling constant in BCS theory λ_{BCS} is an interaction-model-dependent parameter, while n/n_f is an interaction-model-*independent* parameter just as, e.g., the Pippard coherence length $1/k_F\xi_0$ where k_F is the Fermi wavevector. Within GBEC are subsumed the BCS-BEC crossover as well the BCS and ordinary BEC theories.

Three phases are determined numerically by solving the three coupled transcendental equations which depend on three unknown functions: $\mu(T)$ along with the 2eCP and 2hCP Bose-Einstein (BE) condensate densities $n_0(T) \equiv N_0/L^3$ and $m_0(T) \equiv M_0/L^3$ where N_0 and M_0 are the numbers of 2eCP and 2hCP bosons, respectively, while L^3 is the volume of the gas system in 3D. As mentioned, is subsumed within GBEC as special cases: i) the BCS theory when $n/n_f = 1$ if 2eCPs and 2hCPs are in equal footing, i.e, an ideal perfect symmetry between 2eCPs and 2hCPs, ii) the ordinary BEC theory when $n/n_f \to \infty$, or, e.g., with $n_f \to 0$ meaning that no unbound electrons remain in the system—without, of course, no 2hCPs and iii) we extend the BCS-BEC crossover theory by explicitly including 2hCPs.

Varying n/n_f leads at least, to three extreme situations: i) a perfect ideal symmetry, i.e., 50-50 proportions between 2eCPs and 2hCPs; ii) 100-0 proportions with 2eCPs only; and iii) 0-100 proportions with 2hCPs only. With these three cases one is able to analyze the superconducting energy gap $\Delta(T)$ for some elemental superconductors (SCs) such as Al, In, Sn, Hg, Pb, Nb and Ga, the latter with positive charge carri-

ers. In some cases the 50-50 case reproduces quiet well the empirical data; in other cases, the 100-0 or 0-100 proportions fitting extremely well.

Also, the extended crossover predicts the T_c/T_F values for the aforementioned SCs fitting with experiment, notably, much better than BCS predictions. In turn, these results are compared with theoretical curves associated with the extended crossover at $n/n_f = 1$. Remarkably, for 50-50 symmetry all extended-crossover results lie below the Bogoliubov *et al.* upper limit $\lambda_{BCS} \leq 1/2$ thus justifying this upper limit.

A critical discussion is also given for the lack/inclusion of 2hCPs in comparison with the 50-50 case or even the pure phase of the 100-0 case (2eCPs only) and is analyzed the Ga superconductor having positive-charge carriers, here we choose the 0-100 proportions (2hCPs only) to fit experimental data. We also analyze the resulting energy gap at zero temperature and the gap-to-T_c ratio for the aforementioned superconductors including the so-called "bad actors" of the BCS theory Pb and Hg. In summary, changing n/n_f changes the T_c which is consistent with empirical data of Y.J. Uemura *et al*. [2006] and more recently with I. Božović *et al*. [2016] and of course with the increase of the energy gap as Cohen *et al*. found in 1967.

Published papers

The following papers were published while developing this thesis.

1. I. Chávez, L.A. García, M. Grether, M. de Llano and V.V. Tolmachev, J. Supercond. And Novel Magn. **31**, Issue 3 631-637 (2017) "*BCS-Bose Crossover extended with hole Cooper pairs*"
2. I. Chávez, L.A. García, M. Grether and M. de Llano Int. J. Mod. Phys. B **31**, Issue 25, 1745013 (2017)"*Extended BCS-Bose Crossover*"
3. I. Chávez, L.A. García, M. Grether and M. de Llano Int. J. Mod. Phys. B **31**, Issue 25, 1745004 (2017) "*Role of superconducting energy gap in extended BCS-Bose crossover theory*"
4. I. Chávez, M. Grether and M. de Llano, J. Supercond. Nov. Magn **29**, 691-695 (2016) "*Generalized BEC and Crossover Theories of Superconductors and Ultracold Bosonic and Fermionic Gases*"
5. I. Chávez, M. Grether and M. de Llano, J. Supercond. Novel Magn. **28**, 1279-1283 (2015) "*Multicondensate Superconductivity in a Generalized BEC Formalism with Hole Cooper Pairs*"
6. I. Chávez, M. Grether and M. de Llano, J. Supercond. Novel Magn. **28**, 309-313 (2015) "*Is BCS related with BEC?*"
7. I. Chávez, J. Ortega, M. de Llano and V.V. Tolmachev, in Superconductivity: Properties, Applications and New Developments, Editor: Paulette Grant. Chapter 4: "*Generalized Bose-Einstein Condensation Model of Superconductivity and Superfluidity*" pp. 91-134. ISBN: 978-1-63483-907-5 (Book chapter)

Preparation Manuscripts

- I. Chávez, L.A. García, M. Grether, M. de Llano and V.V. Tolmachev, J. Supercond. And Novel Magn. "*Two-Electron and Two-Hole Cooper Pairs in Superconductivity*" (Submitted)
- I. Chávez, M. Grether, M. de Llano and V.V. Tolmachev, Phys. Rev. Lett. "*Superconductivity with or without hole Cooper pairs in a generalized BEC theory*" (in preparation)
- I. Chávez, M. Grether and M. de Llano, Phys. Rev. B. "*Superconductor Thermodynamic Properties in a BCS-Bose Crossover extended with hole Cooper pairs*" (in preparation)

This work was presented at the following conferences

- 3rd International Conference on Theoretical Condensed Matter Physics. Oral Presentation. New York, October 2017.
- International Conference Superstripes 2017: Quantum Complex Matter. Oral Presentation, Ischia (Naples) Italy, June 2017.
- New^{3}SC: 11th International Conference on New Theories, Discoveries, and Applications. Oral Presentation, Bled Slovenia, September 2016.
- International Conference Superstripes 2016: Quantum Complex Matter. Poster Presentation, Ischia (Naples) Italy, June 2016.

Introduction

The study of high critical temperature superconductors (HTSC) is of great interest because they have a great technological potential in diverse areas. For example, in devices as diverse as magnetic levitation, lossless energy conduction or nuclear magnetic resonance to medical diagnosis. The discovery of room-temperature superconductivity would revolutionize our technology as the industrial revolution did in the XVIII century [1]. Since its discovery, diverse theories have to tried to describe superconductivity (SC) as an intriguing discipline of solid state physics. Such theories have gradually appeared to explain not only how it works, but also how to predict new materials. In this effort, a study of superconducting materials is presented within a generalized formalism that subsumes the five statistical theories of superconductivity.

The transition to the superconducting state occurs below a temperature called the transition temperature or critical temperature (T_c) at which the electrical resistance of the material becomes zero. This discovery was made in Hg by Kammerlingh Onnes in 1911 [2]. Zero resistance can only be measured by laboratory techniques, but the most notable phenomena is the Meissner-Oschenfeld [3] effect in which the magnetic field is totally expelled from the inside of the superconductor and only happens below T_c, becoming a perfect diamagnetic material.

A great variety of SCs [4] exists with a wide range of critical temperatures, from some degrees above zero Kelvin such as Be with $T_c = 0.026$ K or Ti with $T_c = 0.40$ K [5] to as higher than $T_c = 93$K for YBaCuO [6], while the first superconductor, Hg have a $T_c = 4.1$ K. The macroscopic explanation of the Meissner effect appeared in 1933 by the London brothers [7], this theory states the relationship between the superconducting current and the magnetic field, but it does not explain the microscopic origin.

In 1950 Ginzburg and Landau formulate a theory of superconductivity [8], which is combined with the Landau's second order phase transition theory [9]. This theory explains macroscopically the properties of superconductors, predicting two types of superconductors, namely type I and type II. In the former, superconductivity appears suddenly, while in the latter it appears gradually. In 1950 Maxwell and Reynolds [10, 11] find that the critical temperature T_c of a superconductor is related to the atomic mass of the element, called isotopic effect. Frölich in his work of 1950-52 [12, 13] describes the electronic conduction by the dispersion of electrons and vibrations of the ionic network absorbing or emitting energy from the phonon lattice. This description leads to an electron-phonon interaction as the microscopic mechanism responsible for superconductivity.

In 1957, J. Bardeen, L. Cooper and J. Schrieffer (BCS) formulate what is now known as the BCS theory

of superconductivity, a theory that microscopically explains the current in a superconductor through the mechanism of Cooper pairs [14] (CP). Those pairs are bound electrons whenever the difference of energy between the electron states is less than the energy of a phonon ($\hbar\omega$), in this state the superconducting phase can be formed when the attractive interaction surpasses the coulombian repulsion. For the BCS theory, they were awarded with the Nobel Prize in 1972. In 1959 Lev Gor'kov showed that the BCS theory is reduced to the Ginzburg-Landau theory near T_c [15].

Therefore, two key-stages can be identified in the history of superconductivity, one that marks the beginning and study at low temperatures with a highest point being the BCS theory in 1957, on the other hand the second-stage beginning in 1986 with Bednorz and Müller [16] discovering SC above 40 K, higher than the one predicted by BCS theory, and a year later would be $T_c = 93$ K [6]. This last stage can be referred as the discovery of HTSC. A feverish begun to searching SC materials with higher T_c's. This leads, in just seven years, known to date, to the highest-T_c cuprate superconductor, the $HgBaCaCuO$ compound [17] with a $T_c \simeq 164\ K$ under very high pressure ($\simeq 310,000$ atm). More recently, the discovery of the hydride SC compound H_3S [18] with $T_c \simeq 193K$ under ultrahigh pressure ($\simeq 2 \times 10^6$ atm) marked a new record in HTSC. However, we are still far from achieving a room-temperature SC.

On the other hand, the theoretical prediction of Bose-Einstein condensation (BEC) by Einstein in 1925 based on the work by Bose on photons from 1924 was finally observed, in 1995, in laser-cooled magnetically-trapped ultracold *bosonic* atomic clouds with $^{87}_{37}$Rb [19] nuclei. Within weeks, other observations quickly followed, initially with $^{7}_{3}$Li [20] and $^{23}_{11}$Na [21], and somewhat later with $^{1}_{1}$H [22], $^{85}_{37}$Rb[[23], $^{4}_{2}$He [24], $^{41}_{19}$K[[25], $^{133}_{55}$Cs [26], $^{52}_{24}$Cr [27] as well as in two-electron systems such as alkaline-earth and ytterbium atoms with $^{174}_{70}$Yb [28–30] nuclei and with $^{84}_{38}$Sr [31]. A well-known fact is that BEC in an ideal Bose gas which occurs below of T_c whenever the thermal wavelength $\lambda = h/\sqrt{2\pi m_B k_B T}$, with m_B the boson mass, becomes larger than the average interbosonic separation $n_B^{-1/3}$, n_B being the bosonic-atom number density, and h, k_B the Planck and Boltzmann constants, respectively. More specifically, BEC sets in [32] whenever

$$n_B \lambda^3 > \zeta(3/2) \simeq 2.612$$

with a macroscopic number of particles sharing the same lowest quantum state. For a many-fermion system such as a SC one has electron number-densities of $n = 10^{19} - 10^{23} cm^{-3}$ which implies characteristic Fermi temperatures of $T_F = 10^2 - 10^5$ K. On the other hand, an ultracold fermionic BECs with enormous average spacings (compared with interatomic potential ranges) have mass densities of $\rho \simeq 10^{-8} g/cm^3$ so that $T_F < 10^{-6} K$. Then, one can expect that in the strong-coupling limit one has low densities, or interparticle spacings much greater than the diameter of the composite bosons.

In 1963 Schrieffer [33] stated that one must simultaneously solve *two* equations to determine Δ the energy-gap parameter *and* μ the chemical potential which in BCS theory was put equal to the Fermi energy $E_F \equiv k_B T$ which depends only on electron number density. In the mid-60s for the first time Keldysh *et al.* [34] wrote that the weak Coulomb interaction corresponds to the assumption that the mean correlation energy q^2/r_D is much less than E_F, where q is the elemental electron charge and r_D the Debye screening radius,

this condition being satisfied for the relatively small electron number-densities of $n \sim 10^{18} - 10^{19} cm^{-3}$. A year later Popov [35] proposed a theory of a Bose gas produced by bounded pairs of Fermi particles which in the small density limit describes a system *behaving* as a Bose gas whose particles should form a condensate at low-enough temperatures. Popov raised the important question "*What should the chemical potential μ be in order for the density n to be small, that is, for the interaction radius r_0 to be small compared with the mean distance between particles $n^{-1/3}$?*" He concluded that there must exist a nontrivial solution whenever $\mu > -B_2/2$, where B_2 is the (positive) bound-state energy in which a number of bound pairs form a Bose condensate.

In 1967 Friedel *et al*. [36] proposed that "*two equations must be solved in the BCS formalism to obtain the gap equation at $T = 0$*." However, this statement was not elucidated at all, even though it was concluded [36] that all type A_3B SCs must lie between the weak- and strong-coupling regimes. A couple of years later Eagles [37] studied *two* simultaneous equations for the BCS gap Δ and its associated fermionic chemical potential μ. Solutions of these two simultaneous equations for T_c thus defined the so-called "*BCS-BEC crossover*" theory.

Leggett [38] later derived, but only for $T = 0$ [39], the *two* basic equations associated with this crossover picture for *any* many-fermion system of identical particles each of mass m whose pair interaction is described by its S-wave scattering length a. He obtained a $T = 0$, the dimensionless *number equation*

$$\frac{4}{3} = \int_0^\infty d\widetilde{\epsilon}\sqrt{\widetilde{\epsilon}}\left[1 - \frac{\widetilde{\epsilon} - \widetilde{\mu}}{\sqrt{(\widetilde{\epsilon} - \widetilde{\mu})^2 + \widetilde{\Delta}^2}}\right] \tag{1}$$

where tildes mean in units of the Fermi energy $E_F \equiv \hbar^2 k_F^2/2m$ of the associated ideal Fermi gas with μ and Δ being the zero-temperature fermionic chemical potential and energy gap, respectively. Also, he obtained the dimensionless *gap equation* at $T = 0$

$$\frac{\pi}{k_F a} = \int_0^\infty d\widetilde{\epsilon}\left[\frac{1}{\sqrt{\widetilde{\epsilon}}} - \frac{\sqrt{\widetilde{\epsilon}}}{\sqrt{(\widetilde{\epsilon} - \widetilde{\mu})^2 + \widetilde{\Delta}^2}}\right]. \tag{2}$$

These two equations were alternately derived as reported in [40].

Both expressions are coupled transcendental equations to be solved self-consistently for μ and Δ with both quantities implicitly depending on a. The two equations are then valid for *any* coupling—weak, strong or intermediate. For weak coupling $\mu \simeq E_F$ as assumed by BCS [41] is a very good approximation, and whose theory is embodied in a *single* equation, the BCS gap equation. However, for very strong coupling one must have $\mu \simeq -B_2/2$ with B_2 is the two-body (positive) binding energy of a pair *in vacuo*, provided that one assumes the two-body potential supports *one and only one* bound state as, e.g., the BCS model interaction can be shown [42] to effectively do so as well.

In 2D Miyake [43] solved the two crossover equations *exactly* at $T = 0$ for an attractive delta interaction potential between pairs of fermions. This was obviously facilitated because in 2D the density of electronic

states is a *constant* independent of energy. The potential delta well is assumed to support only one bound state of binding energy $B_2 \geqslant 0$ which in turn serves as a measure of coupling. Miyake found the exact expressions $\Delta = \sqrt{2E_F B_2}$ and $\mu = E_F - \frac{1}{2}B_2$ the latter evidently reducing to E_F in weak coupling and to $-B_2/2$ in strong, as should be. Indeed, a 2D [44] as well as a 3D delta-potential well support an infinite number of bound-state levels and this alone would suffice to collapse the many-fermion ground state to infinite binding and density. However, both 2D and 3D delta-potential wells can be *regularized* [45], i.e., constructed so as to allow one and only one bound state characterized by the value of $B_2 \geqslant 0$.

The BCS-Bose crossover was subsequently discussed by Nozières *et al.* [46] (1985); Ranninger *et al.* [47] (1988); Randeria *et al.* [48] (1989); van der Marel [49] (1990); Bar-Yam [50] (1991); Drechsler & Zwerger [51] (1992); Haussmann [52] (1994); Pistolesi & Strinati [53] (1996), and many others.

Note that we denote the crossover by "BCS-Bose" instead of by "BCS-BEC" since a BEC cannot occur in either 2D nor in 1D [54] whereas bosons *can* form in both instances.

Boson-fermion (BF) models of SCs as a BEC go back to the mid-50s, [55–58] pre-dating even the BCS-Bogoliubov theory [59, 60]. Although BCS theory only envisions the presence of *Cooper correlations* of single-electron states, BF models [55–58] [61–70] posit the existence of *actual* bosonic CPs.

Such pair as charge carriers have been observed in magnetic flux quantization experiments on elemental [71, 72] as well as on cuprate [73] superconductors. Clusters larger than pairs, viz., *quartets* or quadruples with charge $4e$, have *not* been unambiguously observed in the bulk of any superconductor (see, however Refs. [74–78]). The presence of quartets in ^3He in aerogel [79] has been suggested. Moreover, no experiment has yet been done, to our knowledge that distinguishes between electron and hole pairs, i.e., that determines the *sign* of $2e$ charge carriers. Cooper pairs it seems to be the single most important universally accepted ingredient of SC, whether conventional or "exotic," of low- or high-transition-temperatures. And yet, in despite of playing a central role in SC they are poorly understood. The fundamental drawback of early [57, 58] BF models, which took two-electron (2e) pairs as analogous to diatomic molecules in a classical atom-molecule gas mixture, is the cumbersome introduction of an electron energy gap $\Delta(T)$. "Gapless" models cannot describe the ordinary superconducting state at all, although they are useful in locating transition temperatures if approached from above, i.e., $T > T_c$. Even so, we are not aware of any calculations with the early BF models attempting to reproduce any empirical T_c values.

The gap first began to appear naturally in later BF models [61, 62], [68, 69, 80] and [81–86]. With two [81, 82] exceptions, however, all BF models neglect the effect of *hole* CPs included on an equal footing with electron CPs to give the "complete" BF model that constitutes the generalized Bose-Einstein condensation (GBEC) theory to be surveyed. It is complete only in that it consists of *both* bosonic CP species coexisting with unbound electrons.

This lead [81, 82, 87, 88] to picture a SC as an ideal *ternary* boson-fermion (BF) gas plus BF interaction vertices that explicitly include 2hCPs alongside 2eCPs. Assuming charge conservation as well as thermodynamic equilibrium leads to three coupled transcendental equations: a single number equation which guarantees total charge conservation plus two gap-like equations. These *three* equations must be solved simultaneously (like Leggett's *two* equations (1) and (2) that lead to the usual $T = 0$ BCS-Bose crossover) but

now performed in the GBEC formalism for *all* $T \geq 0$.

To complete this survey it will be mentioned at least four possible dimensionless coupling constants: i) the usual BCS lambda $\lambda_{BCS} \geq 0$ (huge pairs compared to interelectron spacings) and limited to $1/2$ according to the Bogoliubov school; and four model-independent constants ii) the inverse of the Fermi wavenumber k_F times the S-wave scattering length a_S characterizing the two-body interaction, with $1/k_F a_s$ varying [52] from $-\infty$ (weak-coupling) to $+\infty$ (strong coupling); iii) the well-known Pippard coherence length ξ_0 times the Fermi wavenumber k_F [40,89], which varies from 0 (tiny pairs compared to interelectron spacings) to ∞ (huge pairs compared to interelectron spacings); and iv) a new dimensionless quantity [88], the ratio of total electron number density n with $n_f(T=0)$ the number density of unbound electrons at zero temperature. The ratio n/n_f varies from 1 (when GBEC precisely reduces to the BCS theory) on the other hand when tends to ∞ (strong coupling or tiny, well-separated pairs); it is usable in various BF gas models describing binary or ternary gas mixtures.

This thesis proposes that the dimensionless number density n/n_f plays the role of a dimensionless (model-independent) coupling constant. The ratio n/n_f emerges from an ideal BF mixture with electrons as fermions, two-electron Cooper pairs as bosons and explicitly included two-hole Cooper pairs as well as bosons. When the interaction between particles is "turned on" one has the BF vertex interaction with a dimensionless strength parameter which in turn is related with dimensionless number density. By changing n/n_f one can able to depicts this BF mixture from the weak to strong coupling extremes, and of course the intermediate coupling. Thus, one can recovers the BCS and BEC theories as extreme cases and furthermore describes superconductivity in the crossover region. In principle the dimensionless number density can be related with any other dimensionless coupling constant in superconductivity.

This work is organized as follows: chapter one presents a general review on the aforementioned dimensionless coupling constants of superconductivity; chapter two introduces the GBEC theory deducing the main framework and the grand thermodynamic potential which in turn is used to compute numerically, the thermodynamic properties. Thus, introducing the new dimensionless coupling constant; chapter three presents the dimensionless number density and its correlation with dimensionless coupling constant such as λ_{BCS} of BCS theory or the condensate fraction of BEC theory as well some other thermodynamic properties such as the energy gap; in chapter four we using the dimensionless number density to calculated the critical temperature, the energy gap for some elemental superconductors via the BCS-Bose crossover extended with two-hole Cooper pairs and compared with experimental data and finally the conclusions of this survey and future work.

Chapter 1

Dimensionless coupling constants

The main idea behind a coupling constant is to mediate the force strength in the interaction between particles. In this chapter are listed some dimensionless coupling constants in superconductivity. They are presented for comparison purposes only, and will not be developed or deduced. However, the appropriate references are cited.

Surely, the most known coupling constant is that of BCS theory $\lambda_{BCS} = N(0)V$, where $N(0)$ is the density of states (DOS) at Fermi level and V is the Coulomb repulsion plus the electron-phonon interaction. Sometime later Migdal described fermion interactions with retardation effects, Eliashberg applied this theory to a SC material and found the strong coupling correction to BCS theory. The dimensionless λ_{BCS} is a model-dependent constant while the following dimensionless coupling is not.

In the Pippard theory is found that Cooper pairs must have a physical size to has coherence in a bound state, this is known as the Pippard coherence length $k_F\xi_0$, where k_F is the Fermi wavenumber and ξ_0 the coherence length. Another coupling constant is the S-wave scattering length a_s, when $1/k_F a_s < 0$ one has attractive interaction between particles, whereas $1/k_F a_s > 0$ one has a repulsive interaction; if $k_F a_s \to 0$ one has the so-called Feshbach resonance which has been observed in ultracold fermionic atoms.

Finally, the dimensionless number density n/n_f is presented, where n is the total electron number density and $n_f \equiv n_f(T = 0)$ is that of unbound electrons at zero temperature, which as the previous dimensionless coupling constants is model independent. Here, is studied with great detail.

1.1 The electron-phonon coupling constant from BCS theory

Until the 1950s the mechanism by which superconductivity occurred was unknown. In 1957 the BCS theory described microscopically so far the known superconductors with a second quantization formalism and the variational method. The formalism introduced by BCS is based on the interaction produced by the difference of energy between the superconducting and normal states of the virtual exchange of phonons and the coulombian screening repulsion between electrons. The problem lies in calculating the ground-state and the excited states of the fermion system that interacting via two-bodies potential.

The most significant contribution is a expression where exist a temperature of transition T_c which is predicted the superconducting state and the energy gap as a function of temperature. However, the most peculiar and distinctive effect, the Meissner effect is not depicted by the formalism itself. The first idea in the BCS theory is that there is an effective attraction between electrons near the Fermi surface. This idea was first formulated by Frölich in 1952, and still seems surprising since two electrons "obviously" repel each other.

The second idea is that the electrons interact through an exchange of phonons by the crystal lattice. In the language of Feynmann diagrams, an electron in the Bloch state $\psi_{n\mathbf{k}}(\mathbf{r})$ can excite a phonon lattice with momentum $\hbar\mathbf{q}$, leaving an electron in a state $\psi_{n\mathbf{k}}(\mathbf{r}')$ with momentum $\hbar\mathbf{k}' = \hbar\mathbf{k} - \hbar\mathbf{q}$, then an electron can absorb energy and takes with momentum $\hbar\mathbf{q}$, this is illustrated in Fig.1.1 which corresponds to an effective interaction between electrons.

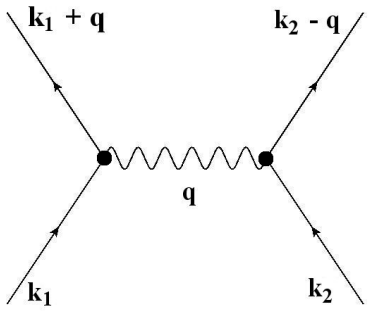

Figure 1.1: Shows the ectron-electron interaction through the exchange of a phonon of the crystal lattice. The net effect is the transfer of momentum $\hbar\mathbf{q}$ from one electron to another electron, implying an effective interaction between electrons.

In the Cooper [14] problem, we suppose a spherical Fermi surface at $T = 0$, where all states $k < k_F$ are occupied, then two extra electrons are placed outside the Fermi surface, those electrons interact via electron-phonon interaction, so that we can construct the wave function of these two-electrons as

$$\psi_0(\mathbf{r}_1 - \mathbf{r}_2) = \sum_{\mathbf{k}} g_{\mathbf{k}} e^{i\mathbf{k}\cdot\mathbf{r}_1} e^{-i\mathbf{k}\cdot\mathbf{r}_2}$$

Inserting this equation into the corresponding Schrödinger equation, it can be shown that the coefficients $g_{\mathbf{k}}$ and the energy eigenvalues are determined, solving

$$(E - 2\epsilon_{\mathbf{k}})\, g_{\mathbf{k}} = \sum_{k' > k_F} V_{\mathbf{k}\mathbf{k}'} g_{\mathbf{k}'} \tag{1.1}$$

In this expression, $\epsilon_{\mathbf{k}}$ are the unperturbed states and $V_{\mathbf{kk}'}$ is the matrix elements of the interaction potential

$$V_{\mathbf{kk}'} = \mathscr{V}^{-1} \int V(\mathbf{r}) e^{i(\mathbf{k}'-\mathbf{k})\cdot\mathbf{r}}\, d\mathbf{r}$$

where $\mathbf{r}$ is the distance between two electrons and $\mathscr{V}$ the normalized volume. $V_{\mathbf{kk}'}$ characterizes the potential strength to scattering an electron pair with momentum $(\mathbf{k}', -\mathbf{k}')$ and $(\mathbf{k}, -\mathbf{k})$. If a set of $g_{\mathbf{k}}$ satisfies (1.1) with $E < 2E_F$, then the bounded pair can exist.

Cooper introduced a very useful approximation, namely that for all $V_{\mathbf{kk}'} = -V$ for the states $\mathbf{k}$ out of the cut-off energy $\hbar\omega_D$, away from E_F, in addition $V_{\mathbf{kk}'} = 0$ beyond $\hbar\omega_D$. Then the right side of (1.1) is a constant, independent of $\mathbf{k}$ and we have

$$g_{\mathbf{k}} = V \frac{\sum g_{\mathbf{k}'}}{2\epsilon_k - E} \tag{1.2}$$

summing both sides and canceling $\sum g_{\mathbf{k}}$, gives

$$\frac{1}{V} = \sum_{k<k_F} (2\epsilon_{\mathbf{k}} - E)^{-1} \tag{1.3}$$

When we replace the sum by an integral, with $N(0)$ the density of states at the Fermi level for electrons with a spin orientation, we have

$$\frac{1}{V} = N(0) \int_{E_F}^{E_F+\hbar\omega_D} \frac{d\epsilon}{2\epsilon - E} = \frac{1}{2} N(0) \ln\left(\frac{2E_F - E + 2\hbar\omega_D}{2E_F - E}\right) \tag{1.4}$$

In most classical superconductors, we find that $N(0)V < 0.3$, this is known as the weak coupling approximation, valid for $N(0)V \ll 1$, then the solution of the above equation is,

$$E \sim 2E_F - 2\hbar\omega_D e^{-2/N(0)V} \tag{1.5}$$

Then we have a bounded state of negative energy with respect to the Fermi surface, made up of electrons with $k < k_F$, that is, with energy exceeding E_F, and its energy is exponentially small when $N(0)V$ is small.

In the BCS solution the energy scale for a superconductor is the Debye energy $\hbar\omega_D$. This may explain why the transition temperatures T_c are so small, compared to such energies in solids. The Debye energy of most materials correspond to scales of order $100 - 300$ K, with a very small exponential factor which leads to a $T_c \sim 1$ K for most metallic superconductors. In BCS theory is taken the case of a reliable coupling, with the assumption that such pair with $\lambda_{BCS} \ll 1$, then $|\Delta|$ is much smaller than all other energy scales, such as E_F and $\hbar\omega_D$.

1.2 The electron-phonon coupling constant from Migdal-Eliashberg theory

At the same time as BCS theory, the Migdal [90] paper pointed out interactions on fermion particles and he claimed that an "excited state of a system with strong interactions cannot be described in terms of quasi-particles." We recall that a quasi-particle only exist in a solid and describes mathematically, the behavior of an electron inside the solid, therefore is not a "real" particle but helps to simplifying the description of a solid. One year latter, his famous paper entitled “Interactions between electrons and lattice vibrations in a normal metal” he develops a method to obtain the electron-energy spectrum and the dispersion of the lattice vibrations without assuming that the interaction is small. His principal aim was to construct a theory which was not limited by the assumption of small interactions then he found an attenuation mechanism due to the interaction between electrons, which resulted from phonon exchange by using Green functions as propagators for fermions as well for phonons and found a perturbation series about the vertex interaction between electrons and phonons. However, his approach cannot be compatible with λ_{BCS} since in BCS theory does not include the correction to electron-phonon interaction.

Some time later, Eliashberg [91] developed a method to find the energy spectrum applying Migdal's theory but now using a perturbation method assuming no small interaction, i.e., he extended the BCS theory to strong coupling regime. In principle, the Eliashberg theory can be reduced to BCS through a number of appropriate approximations [92].

The original text of Eliashberg is not clear when one speak about the strong coupling regime, this coverage was realized by McMillan [93] several years later. With his famous equation where calculated the critical temperature as

$$T_c = \frac{\Theta}{1.45} \exp\left[-\frac{1.04(1+\lambda)}{\lambda - \mu^*(1+0.62\lambda)}\right] \tag{1.6}$$

where the μ^* is the pseudo-coulombian potential of Anderson-Morel [94] and λ is the electron-boson mass-renormalization parameter. To avoid confusions between λ_{BCS} and Migdal-Eliashberg-McMillan (MEM) parameter, we denote it as λ_{MEM} hereafter. The correlation between the dimensionless coupling constants of BCS and MEM theories is

$$N(0)V = \lambda_{BCS} = \frac{\lambda_{MEM} - \mu^*}{1 + \lambda_{MEM}}. \tag{1.7}$$

Nevertheless, the McMillan T_c expression has a correction made by Allen and Dynes [95], they assert that Eliashberg theory is not limited by the phonon frequencies and show that McMillan's $\lambda_{MEM} = 2$ is spurious. Furthermore, they recalculated the critical temperature and became more accurate with respect experimental data. Several studies [92] have confirmed the validity of Migdal-Eliashberg theory such as the so-called "bad actors" of BCS theory, Pb and Hg. These materials behave as strong-coupling superconductors, since $\lambda_{MEM} > 1$ while in BCS theory remains below of the so-called Bogoliubov [96,97] et al. limit $\lambda_{BCS} \leq 1/2$ arguing lattice instabilities. Table 1.1 compares both dimensionless coupling constants for some elemental superconductors including Al, the "poster-child" of BCS theory.

The BCS dimensionless coupling constant has a drawbacks: i) λ_{BCS} is model dependent and ii) has no connection with experiment since V, the interaction matrix, cannot be obtained so far directly from any

Table 1.1: Comparison between the dimensionless coupling constant λ_{BCS} of BCS theory with that of Migdal-Eliashberg-McMillan theory for some elemental superconductors. The λ_{BCS} values were calculted via the weak-coupling BCS formula and λ_{MEM} values were taken from [95] except for aluminium value that was take from [93]. Note that for λ_{BCS} all SC values are below from Bogoliubov et al. upper limit.

	T_c (K)	λ_{BCS}	λ_{MEM}
Al	1.17	0.20	0.38
In	3.41	0.28	0.80
Sn	3.72	0.24	0.72
Hg	4.15	0.31	1.60
Pb	7.19	0.37	1.55
Nb	9.22	0.28	0.85

experiment, also V cannot expand in power series, i.e., cannot expand as a perturbation series. On the other hand, λ_{MEM} has totally been connected with experiment via phonon density of states through the spectral function $\alpha F^2(\omega)$, but μ^* has been strongly questioned as was λ_{BCS}, besides of its experiment validation.

1.3 Pippard coherence length

Before the concept of coherence length, the London penetration length was a key in the understanding of the behavior of the so-called SCs type-I and type-II. It is well known that in type-I SCs, the superconductor state is suddenly destroyed if a (sufficiently strong) external magnetic filed is applied. This field is called the critical magnetic field H_c. In contrast, type-II SCs have two different critical fields denoted as H_{c1} corresponding to the lower critical magnetic field and H_{c2} corresponding to the upper critical magnetic field.

The London & London theory [98] was originally inspired by the two-fluid model of ^{4}He. The London equation is one of the most important equations describing superconductors

$$\mathbf{j} = -\frac{n_s e^2}{m_e}\mathbf{A}$$

where $\mathbf{j}$ is the electrical current density inside of a superconductor, $\mathbf{A}$ the magnetic vector potential, e the electron charge, m_e the electron mass and n_s the number density of superconducting electrons. With the London penetration depth

$$\lambda_L = \left(\frac{m_e}{\mu_0 n_s e^2}\right)^{1/2}$$

which is the distance inside the superconductor where the magnetic field becomes zero, i.e., the Meissner-Oschenfeld effect [3]. The London equation can be rewritten in terms of the magnetic vector potential $\mathbf{j} = -\left(1/\mu_0\lambda_0^2\right)\mathbf{A}$, this implies that the magnetic field can penetrate only a small distance λ decreasing exponentially [99]. Another consequence of the London equations is that n_s is expected to decrease continuously to zero as $T \to T_c$ causing that $\lambda(T)$ diverges at T_c [100], since $\lambda(T) \simeq \lambda_0[1-(T/T_c)^4]^{-1/2}$. The

penetration depth λ_L are always larger than λ_0. Pippard offered a quantitative explanation but this required the introduction of the coherence length ξ_0.

The term "coherence length" appeared the first time in the Pippard *et al.* paper of 1959, they observed that adding an impurity, is shortened the range of "coherence." Furthermore, the remarkable phenomenon that they saw was that the addition of impurity altered considerably the penetration depth in zero magnetic field, without producing a corresponding change in the thermodynamical properties of the material. This leads to review the London brothers theory and consequently their famous superconducting current equation had to be modified to truly describe experimental evidence.

After discussing the experimental data in his paper of 1957, Pippard *et al.* asserted that a parameter having the dimensions of length and of order of 10^{-4}cm should be introduced to the theory of superconductivity, and they realized that the coherence range should vary with temperature just as the penetration depth. Their main function in the theory is to measure the distance over which the effects of a perturbing force is appreciable. Then, the modified current density expression is

$$\mathbf{J} = -\frac{3}{4\pi\xi_0\Lambda}\int \frac{\mathbf{r}(\mathbf{r}\cdot\mathbf{A})\exp[-\mathbf{r}/\xi]}{r^4}d\tau$$

which is analogous to that of London theory for the supercurrent, with ξ_0 is the coherence range (length). Adding to this, the coherence length decreases with the introduction of impurities and leads to the correct explanation on the magnitude of the penetration length and its variation with impurity contents.

In their original paper, Pippard *et al.* analyzed two points: the first one being the difficulty to apply the previous equation to very small particles and the second one being the magnitude of the London penetration depth λ_0 in different pure metals. They proposed the solution that the coherence length must be dependent of the size of particles and of course independent of temperature. The second solution is that the penetration depth must be varying inversely with respect critical temperature since Λ_n takes different values for different metals. Pippard suggested that "the behavior of a superconductor is in some aspects controlled by a long range interaction (called the 'range of coherence') within the electron assembly," i.e., that the superconducting wave function should have a similar characteristic dimensions of ξ_0. This length is defined as $\xi_0 = a\hbar v_F/k_B T_c$ where a is a numerical constant parameter with unit order, v_F the Fermi velocity of electron and k_B the Boltzmann's constant. After BCS theory, the coherence length can be related with the energy gap value as

$$\xi_0 = \frac{\hbar v_F}{\pi\Delta}. \tag{1.8}$$

The interpretation of the coherence length is that represents *the physical size of the Cooper pair bound state* in BCS theory.

1.4 Scattering length

The scattering length a_s is often used to show the transition from a weak-coupling system to a strong-coupling one. The crossover BCS-BEC theory addressed such transition. One of the best pictures is shown

in Fig 1.1 of Ref. [101] (reproduced here for comparison purposes), a qualitative phase diagram of T/T_F *vs.* $1/k_F a$ from normal Fermi liquid to normal Bose liquid, traversing the unitary regime of superfluidity. In chapter three, the phase diagram of the GBEC theory will be shown and coincides qualitatively with this picture.

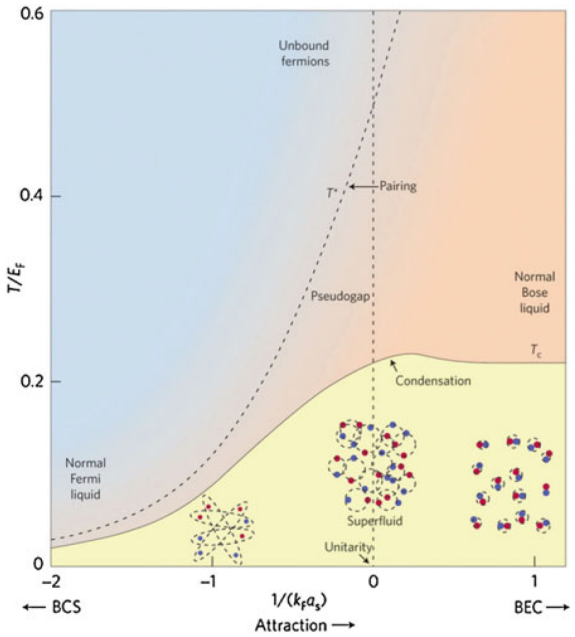

Figure 1.2: Qualitative phase diagram [101] of the BCS to BEC as a function of the temperature T/T_F and the dimensionless coupling $1/(k_F a_s)$, where k_F is the Fermi wave number and a_s the scattering length. Here shows schematically, the evolution of the ground state from the BCS limit with large, spatially overlapping Cooper pairs to the BEC limit with tightly bound molecules at the ground state with $1/(k_F a_s) = 0$ has strongly interacting pairs with size comparable to $1/k_F$. As a function of increasing attraction the pair-formation crossover scale T^* diverges away from the transition temperature T_c below which a condensated exists (Figure from Ref. [102])

The basics on the scattering length a_s lies in the dispersion/attraction of particles under a repulsive/attractive potential, respectively. This is illustrated in Fig. 1.3. It shows four cases for the dispersion length a_s, namely

i) $a_s > 0$, purely dispersive,

ii) attractive potential but so weak, that has no bound state,

iii) $a_s = \pm\infty$ an attractive potential with a bound state S and bound energy equals to zero and,

iv) $a_s > 0$ an attractive potential with negative energy

Some authors [40] have solved the crossover equations at zero temperature to find out how the scattering dispersion in the crossover extremes is working. A great interest for discussion arises here, since one of our main propositions will be that the dimensionless number density n/n_f plays the role of a model-independent dimensionless coupling constant. As mentioned previously in the introduction, the crossover

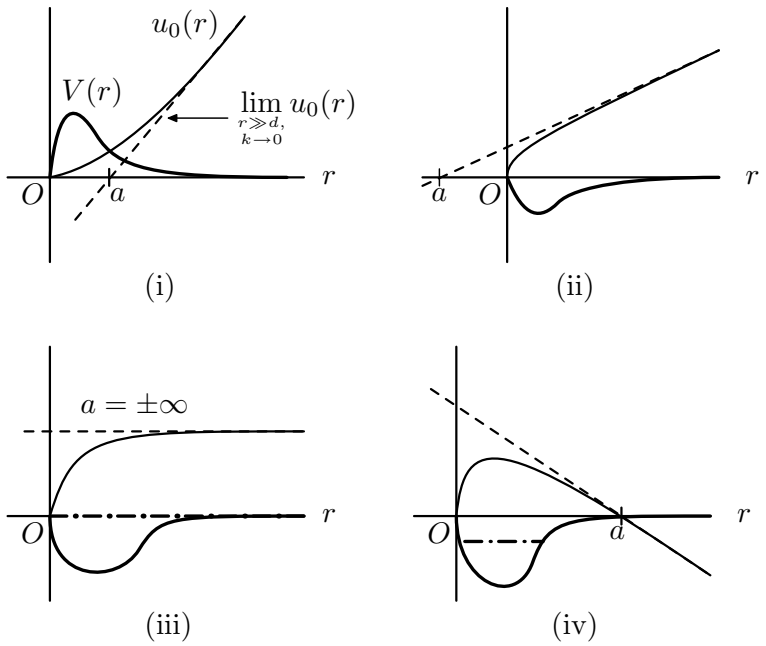

Figure 1.3: $V(r)$ (thick lines) *vs.* r along with $u_0(R)$ (thin lines). Depicts the scattering length a where the function $u_0(r)$ is null exactly, dashed lines is the extrapolating curve. One has the cases: i) $a < 0$ a purely dispersive, ii) weak atractive potential, iii) atractive potential with bound energy and iv) atractive potential with negative energy. Figure taken from [103].

theory is composed by two equations: the gap equation and the number equation; from the latter one can extract the chemical potential μ of the system. However, in BCS theory it was assume that $\mu = E_F$. In [40] as well as in this survey, this assertion will not be assumed.

The number and gap equations (7) and (19) in [40] was solved simultaneously and numerically for $-\infty < 1/\lambda < +\infty$ where $\lambda = k_F a_s$ with k_F the Fermi wavenumber and a_s the S-wave scattering length. The results for the energy gap and chemical potential at zero temperature is displayed in Fig. 2 and 3 of [40] and reproduced here in Fig. 1.4.

The behavior of the energy gap at zero temperature depending on the scattering length a_s shows two extremes well defined as the weak-coupling (BCS) regime where $\Delta/E_F \ll 1$ and the strong-coupling (BEC) regime where $\Delta/E_F \to \lambda^{-1/2}$, the first condition leads to a number equation that reduces to $\mu = E_F$ as shown in Fig. 1.4(b) on the other hand the chemical potential $\mu \to -\infty$ when $1/\lambda \to +\infty$ as shown in Fig. 1.4(b). When the dimensionless scattering length $k_F a_s \to 0$, one recovers the weak-coupling limit, namely one has a highly repulsive system such as the correlated electrons in BCS theory. On the other hand when $k_F a_s \to 0$ one has a system attractive highly such as the ideal Bose gas.

Some other authors [104] have observed condensation of fermionic atom pairs in the BCS-BEC crossover regime. They have been measured the scattering length in ultracold atoms, performing experiments near the unitary zone. They conclude that their measurements prove the pairing in the strong coupling regime.

In Fig. 1.5 illustrates the weak coupling (BCS) extreme where pairs (blue-dotted circles) severely overlap, the strong coupling (BEC) extreme where all pairs (blue-full-line circle) composed by two-fermions are

well defined and of course the intermediate (crossover) coupling. Below it shows at least four dimensionless coupling constants in superconductivity: i) the well-known $\lambda_{BCS} = N(0)\,V$ of BCS theory, where $N(0)$ is the electronic DOS at Fermi energy and V the potential interaction, for weak interaction $\lambda_{BCS} << 1$, strong coupling $\lambda \geq 1$, ii) the dimensionless scattering length $1/k_F\,a_s$ where a_s the S-wave scattering length and k_F the Fermi wave vector, the weak coupling occurs when $1/k_F a_s \to -\infty$ and the strong coupling $1/k_F a_s \to \infty$, iii) the dimensionless coherence length $1/k_F\xi_0$ with xi_0 the Pippard coherence length, weak coupling occurs when $1/k_F\xi_0 << 1$ and the strong coupling $1/k_F\xi_0 >> 1$ and iv) the dimensionless number density n/n_f which appears from a boson-fermion model and presented here with $n/n_f = 1$ as the weak coupling extreme and $n/n_f \to \infty$ as the strong coupling extreme.

So far the coupling constants presented here, offer the main idea that if one appropriately change, the entire system evolves from a weak coupling regime to a strong coupling regime, this the basics of a crossover theory. In the next chapter we address the main framework of the GBEC theory and deduced the three transcendental equations which appear from thermodynamic equilibrium conditions and is presented the dimensionless number density n/n_f which will play the role of the dimensionless coupling constant (model independent) in GBEC theory.

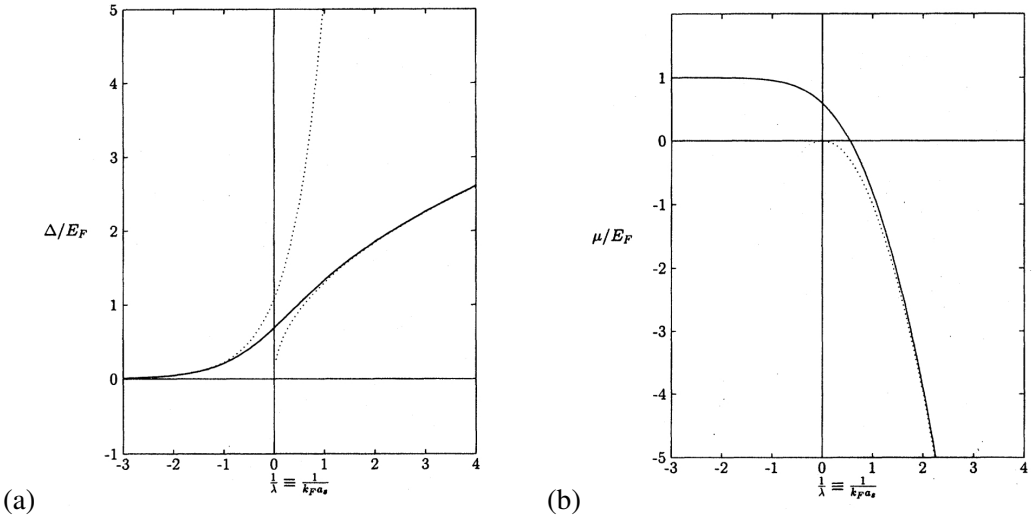

(a) (b)

Figure 1.4: (a) Energy gap Δ/E_F *vs.* $1/\lambda \equiv 1/k_F a_s$ at zero temperature. Left dotted curve is the weak-coupling BCS result from eq. (25) of Ref. [40]; right dotted curve is the strong-coupling limit $\Delta/E_F \to \lambda^{-1/2}$ discussed in [40]. (b) Chemical potential μ/E_F vs $1/\lambda \equiv 1/k_F a_s$ at zero temperature. The weak coupling extreme ($1/\lambda \to -\infty$) value of unity, as the coupling increases to the strong extreme ($1/\lambda \to +\infty$); dotted curve is strong coupling limit of $-1/\lambda^2$ as shown in (28) from Ref. [40].

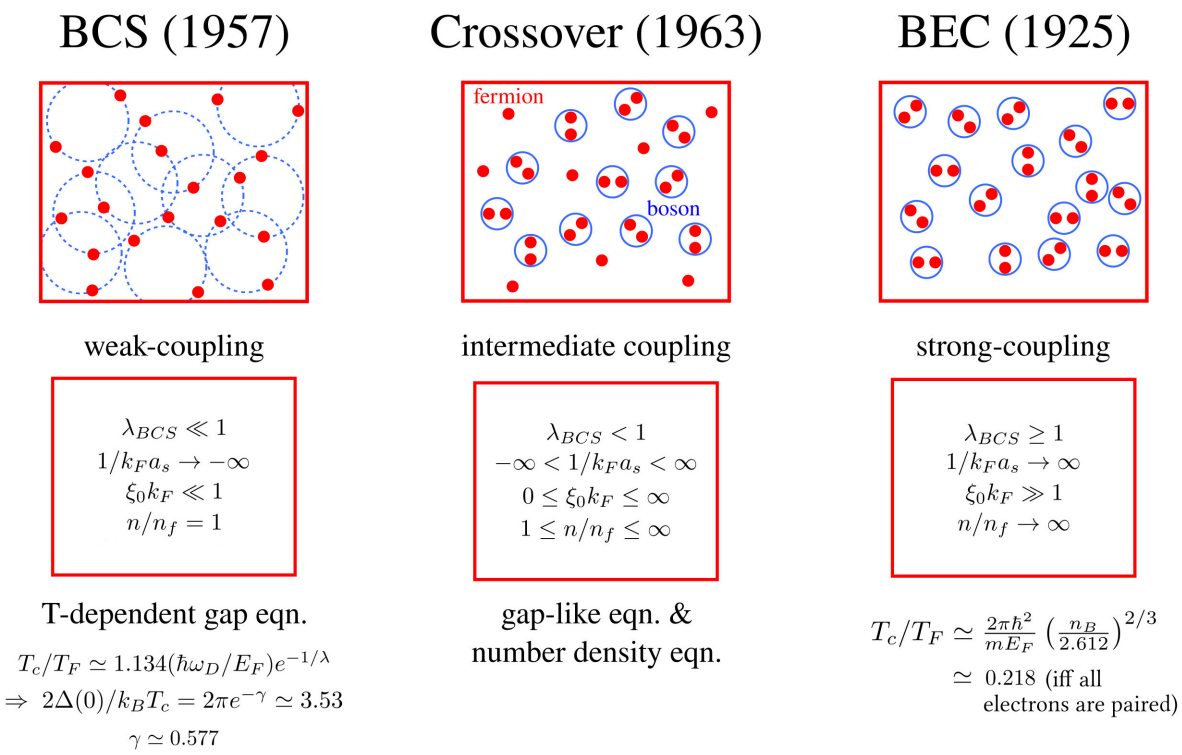

Figure 1.5: Shown at least, four dimensionless coupling constants in superconductivity. The electron-phonon dimensionless coupling constant of BCS theory λ_{BCS} which is model dependent. The scattering length a_s, the Pippard coherence length ξ_0 and the dimensionless number density of the GBEC theory n/n_f. In the weak coupling extreme, dotted (blue-online) circles represents the BCS pairs as correlated pairs, instead a Cooper Pairs as real bosons full-line (blue-online) circle. At bottom, shows the characteristic equations at such extremes to calculated the critical temperature; the gap equation in the weak-coupling approximation, which rules in the BCS regime, and the number equation with n_B the number of condensed bosons with the well-known limit of $T_c/T_F \simeq 0.218$ where all fermions are paired as bosons and of course the crossover region with both equations.

Chapter 2

Generalized Bose-Einstein Condensation Theory

In this chapter will be introduced the main framework of the Generalized Bose-Einstein Condensation (GBEC) theory in order to get the new dimensionless coupling constant which emerges from the result of mechanical statistics and made dimensionless with the number of unbound electrons at zero temperature. Later in the chapter, it will be deduce the thermodynamic potential in order to find out the thermodynamic properties of the system. Finally, by minimizing the Helmholtz free energy, one obtains the gap-like equations for two-electron Cooper pairs and two-hole Cooper pairs, the last ones will be crucial to describing superconductivity. The contents of this chapter is based on Ref. [105].

2.1 GBEC Hamiltonian

The generalized Bose-Einstein condensation theory describes in detail the properties of a quantum statistical many-fermion system. For this purpose we assume that our system has three kinds of individual charged micro-particles, unbound particles (here, electrons), two-electron Cooper pairs (2eCPs) and two-hole Cooper pairs (2hCPs) both kinds are postulated to be bosons. In this system there are interactions between unbound electrons or holes with 2eCPs or 2hCPs. We omit the interactions between 2eCPs and 2hCPs as well as e-h interactions. We take into account very specific direct interactions between fermions and 2eCPs and 2hCPs due to elementary processes of decay of 2eCPs or 2hCPs into their unbound constituents of electrons or holes, and the inverse elementary processes of formation of both kinds of pairs.

We first describe the *kinematic properties* of the many-fermion system. Assume that the many-fermion system is contained in a vessel of macroscopic dimensions of volume L^d where d is the system dimensionality. One-particle states of unbound individual particles are described by plane-wavefunctions

$$\phi_{\mathbf{k},s}(\mathbf{r},\sigma_z) = L^{-d/2} e^{i\mathbf{k}\cdot\mathbf{r}}\, \delta_{s,\sigma_z} \tag{2.1}$$

which are characterized by values of the fermion momentum wavevector $\mathbf{k}$ and by its projection of spin

$s = \pm\frac{1}{2}$ on z-axis. These states have energies

$$\epsilon_k \equiv \frac{\hbar^2 k^2}{2m} \tag{2.2}$$

where m is the effective electron mass. One-particle states of the center-of-mass motion of individual 2eCPs are described by the plane waves

$$\Phi_{\mathbf{K}}(\mathbf{R}) = L^{-d/2} \exp[i\mathbf{K} \cdot \mathbf{R}] \tag{2.3}$$

which are characterized by values $\mathbf{K}$ of the total, or center-of-mass momentum (CMM), wave-vectors of electron Cooper pairs. These states have energies

$$E_+(K) \equiv E_+(0) + \varepsilon_K \tag{2.4}$$

where $E_+(0)$ is the positive energy of *motionless* (i.e., zero-CMM) 2eCP and ε_K is the non-negative excitation energy (or, dispersion relation) of the *moving* (i.e., with nonzero-CMM) CP. This would be simply

$$\varepsilon_K \equiv \hbar^2 K^2/2(2m) \tag{2.5}$$

if we assumed that 2eCPs with a mass of $2m$ moved *in vacuo* as does, say, a deuteron with an average nucleon mass of m. In fact, the original CPs propagating slowly in the Fermi sea are *linearly-dispersive*, namely, $\varepsilon_K = 2\Delta + b(d)\lambda\hbar v_F K + \mathcal{O}(K^2)$ with $b(d) = 1, \frac{1}{2}, \pi$ and $\frac{1}{4}$ for $d = 1$ [106], 2 [107] and 3 [108], respectively, Δ is the zero-temperature BCS energy gap, and λ a dimensionless interfermionic coupling constant, e.g., the BCS model interaction coupling constant associated with pair formation. Note the notational difference between *fermion* (2.2) ϵ and *boson* (2.5) ε dispersion energies. In this study we take both as a quadratic dispersion relation.

As the second quantization basic functions of one-particle states of CMM motion of individual 2hCPs, we also take the plane waves (2.3) but referring to CMM values $\mathbf{K}$ of 2h-CPs. These states have energies

$$E_-(K) \equiv E_-(0) - \varepsilon_K \tag{2.6}$$

where $E_-(0)$ is the positive energy of *motionless* 2hCP. We assume here that the mass of the 2hCP equals to $2m$, the same for 2eCP. For simplicity, we also assume that a 2eCP as well as a 2hCP have only *one* discrete internal bound state.

Now let us use the the second quantization representation periodic boundary conditions on the walls of the vessel of volume L^d for all wave functions of our many-fermion system, which we consider. They are satisfied automatically, when $\mathbf{k}$ of individual fermions, the $\mathbf{K}$ of individual 2eCPs, and $\mathbf{K}$ of individual 2hCPs take those values which are the *nodes* of simple lattice in k-space (reciprocal space), the elementary cell of the lattice has volume $(2\pi/L)^d$ (Born-von Karman boundary conditions [109, p. 135]).

The fermion second-quantized creation (annihilation) operators in their one-particle states with momentum $\mathbf{k}$ and spin projection s are designated by $a^\dagger_{\mathbf{k},s}$ ($a_{\mathbf{k},s}$), respectively, and satisfy the *anti*commutation

relations

$$\begin{aligned}\{a^\dagger_{\mathbf{k},s}, a^\dagger_{\mathbf{k}',s'}\} &\equiv a^\dagger_{\mathbf{k},s}a^\dagger_{\mathbf{k}',s'} + a^\dagger_{\mathbf{k}',s'}a^\dagger_{\mathbf{k},s} = 0,\\ \{a_{\mathbf{k},s}, a_{\mathbf{k}',s'}\} &= 0\\ \{a_{\mathbf{k},s}, a^\dagger_{\mathbf{k}',s'}\} &= \delta_{\mathbf{k}',\mathbf{k}}\delta_{s',s}\end{aligned} \tag{2.7}$$

where $\delta_{\mathbf{k}',\mathbf{k}}$ and $\delta_{s',s}$ are Kronecker symbols.

The 2eCPs second-quantized creation (annihilation) operators in their one-*particle* states of CMM with wavevector $\mathbf{K}$ are designated by $b^\dagger_{\mathbf{K}}$ ($b_{\mathbf{K}}$), respectively. We *postulate* them to be Bose operators (see appendix A), i.e., they satisfy the commutation relations

$$\begin{aligned}[b^\dagger_{\mathbf{K}}, b_{\mathbf{K}'}] &\equiv b^\dagger_{\mathbf{K}}b_{\mathbf{K}'} - b_{\mathbf{K}'}b^\dagger_{\mathbf{K}} = 0\\ [b_{\mathbf{K}}, b_{\mathbf{K}'}] &= 0\\ \left[b_{\mathbf{K}}, b^\dagger_{\mathbf{K}'}\right] &= \delta_{\mathbf{K}',\mathbf{K}}.\end{aligned} \tag{2.8}$$

Note that the last relation differs from the corresponding one associated with the *BCS pair operators* $b_{\mathbf{kK}} \equiv a_{\mathbf{k}_2,\downarrow}a_{\mathbf{k}_1,\uparrow}$ and $b^\dagger_{\mathbf{kK}} \equiv a^\dagger_{\mathbf{k}_1,\uparrow}a^\dagger_{\mathbf{k}_2,\downarrow}$ (for which only the $\mathbf{K} = 0$ case was discussed by them). That relation is

$$\left[b_{\mathbf{kK}}, b^\dagger_{\mathbf{k}'\mathbf{K}}\right] = (1 - n_{\mathbf{K}/2-\mathbf{k},\downarrow} - n_{\mathbf{K}/2+\mathbf{k},\uparrow})\delta_{\mathbf{kk}'} \tag{2.9}$$

where $n_{\mathbf{K}/2\pm\mathbf{k},s} \equiv a^\dagger_{\mathbf{K}/2\pm\mathbf{k},s}a_{\mathbf{K}/2\pm\mathbf{k},s}$ are Fermi number operators. Since (2.9) are not precisely Bose commutation rules, it has been claimed [41] correctly, that the BCS operators do *not* stand, strictly speaking, for true bosons. Similarly to (2.8), the 2hCPs second-quantized creation (annihilation) operators $c^\dagger_{\mathbf{K}}$ ($c_{\mathbf{K}}$) (see appendix A) in their one-*hole* states of CMM wavevector $\mathbf{K}$ are also postulated to be Bose operators and thus satisfy the relations

$$[c^\dagger_{\mathbf{K}}, c^\dagger_{\mathbf{K}'}] = 0, \qquad [c_{\mathbf{K}}, c_{\mathbf{K}'}] = 0, \qquad [c_{\mathbf{K}}, c^\dagger_{\mathbf{K}'}] = \delta_{\mathbf{K}',\mathbf{K}}. \tag{2.10}$$

It is precisely the inclusion of hole pairs along with the usual electron pairs that makes the present BF model a "*complete*" one. To our knowledge [110], no one has yet succeeded in constructing CP creation and annihilation operators that obey Bose commutation relations, starting from fermion creation $a^\dagger_{k_1,s}$ and annihilation $a_{k_1,s}$ operators. Nevertheless, later it will be shown that this kind of particles (2e/2hCPs) obey the Bose distribution.

By postulating both kinds of pairs one accounts for the factor of 2 in the smallest or elementary fluxon $\hbar/2e$ found in magnetic-flux quantization experiments in both conventional [71,72] as well as in cuprate [73] superconductors. Here e is the *magnitude* of the charge of a single electron as, to our knowledge [111], these measurements do not determine the sign of the charge on the pair charge carriers. Although the vast majority of superconductors have *hole* charge carriers in the normal state [112], as determined empirically from *positive* Hall coefficients, there are London magnetic-moment measurements [113] establishing —at

least according to one interpretation [114]— electron pairs in the condensates of superconductors as diverse as Pb (p-type above T_c), $BaPb_{0.8}Bi_{0.2}O_3$ (n-type) and $YBa_2Cu_3O_{7-\delta}$ (p-type), regardless of whether the single charge carriers in the normal state above T_c are electrons or holes. Related to this, there is a wealth of experimental data [115–117] on the Hall-coefficient sign-reversal in various cuprates, but we shall not attempt to address in detail this phenomenon here.

We assume that creation and annihilation operators for particles of different kinds, i.e., of fermions $(a^\dagger_{\mathbf{k},s}, a_{\mathbf{k},s})$ and of 2eCPs $(b^\dagger_{\mathbf{K}}, b_{\mathbf{K}})$, and of 2hCPs $(c^\dagger_{\mathbf{K}}, c_{\mathbf{K}})$ *commute* with each other. This is equivalent to assuming that the b and c operators describe *kinematically independent* composite bosons. Here we use for the unbound-electron Fermi operators and for the 2e- and 2h-CP Bose operators the so-called "electronic" representation, see Appendix A.

As to the postulated *dynamical properties* of the many-fermion system, they are described by the total Hamiltonian $H = H_0 + H_{int}$, namely, the sum of an unperturbed or zero-order Hamiltonian H_0 plus an interaction Hamiltonian H_{int}. Let us suppose further, that the unperturbed Hamiltonian itself corresponds to a noninteracting BF mixture and is equal to a sum of energy operators of unbound fermions, of 2e-CPs, and of 2h-CPs, respectively. Specifically

$$H_0 = \sum_{\mathbf{k}_1,s} \epsilon_{k_1} a^\dagger_{\mathbf{k}_1,s} a_{\mathbf{k}_1,s} + \sum_{\mathbf{K}} E_+(K) b^\dagger_{\mathbf{K}} b_{\mathbf{K}} - \sum_{\mathbf{K}} E_-(K) c^\dagger_{\mathbf{K}} c_{\mathbf{K}}. \tag{2.11}$$

As the Fröhlich (or Dirac) interaction Hamiltonian for a BF mixture of phonons (or photons) and electrons, it is natural to suppose that the Hamiltonian for the specific interaction between unbound fermions or holes and 2eCPs and 2hCPs has the form

$$\begin{aligned} H_{int} &= L^{-d/2} \sum_{\mathbf{k},\mathbf{K}} f_+(k) \left(a^\dagger_{\mathbf{k}+\frac{1}{2}\mathbf{K},\uparrow} a^\dagger_{-\mathbf{k}+\frac{1}{2}\mathbf{K},\downarrow} b_{\mathbf{K}} + a_{-\mathbf{k}+\frac{1}{2}\mathbf{K},\downarrow} a_{\mathbf{k}+\frac{1}{2}\mathbf{K},\uparrow} b^\dagger_{\mathbf{K}} \right) \\ &+ L^{-d/2} \sum_{\mathbf{k},\mathbf{K}} f_-(k) \left(a^\dagger_{\mathbf{k}+\frac{1}{2}\mathbf{K},\uparrow} a^\dagger_{-\mathbf{k}+\frac{1}{2}\mathbf{K},\uparrow} c^\dagger_{\mathbf{K}} + a_{-\mathbf{k}+\frac{1}{2}\mathbf{K},\downarrow} a_{\mathbf{k}+\frac{1}{2}\mathbf{K},\uparrow} c_{\mathbf{K}} \right). \end{aligned} \tag{2.12}$$

In the first summation, we characterize by some phenomenological function $f_+(k)$ which describes the following elementary processes: a) of simultaneous annihilation of 2eCPs with momentum wavevectors $\mathbf{K}$ and creation of two unbound fermions with momenta wavevectors $\mathbf{k}_1 \equiv \mathbf{k}+\frac{1}{2}\mathbf{K}$ and $\mathbf{k}_2 \equiv -\mathbf{k}+\frac{1}{2}\mathbf{K}$—so that $\mathbf{k}_1+\mathbf{k}_2 \equiv \mathbf{K}$ and $\mathbf{k} \equiv \frac{1}{2}(\mathbf{k}_1 - \mathbf{k}_2)$— and with the opposite spin projections; and b) of simultaneous creation of a two-fermion molecule with momentum wavevector $\mathbf{K}$ and annihilation of two unbound fermions with momentum wavevectors $-\mathbf{k}+\frac{1}{2}\mathbf{K}$ and $\mathbf{k}+\frac{1}{2}\mathbf{K}$ and with opposite spin projections. These two elementary processes are analogous to the spontaneous decay (creation) of a two-fermion "molecule" into (from) two dissociated fermions. The same process takes place in the second sum of (2.12), which we also characterize by some phenomenological function $f_-(k)$, describing the opposite elementary processes: a) simultaneous creation of two-hole molecules with momentum $\mathbf{K}$ and annihilation of two holes with momenta $-\mathbf{k}+\frac{1}{2}\mathbf{K}$ and $\mathbf{k}+\frac{1}{2}\mathbf{K}$ and with opposite spin projections. (This is an elementary process of creation of two-hole molecule during collision of two holes); b) simultaneous annihilation of a 2hCP with momentum $\mathbf{K}$ and creation of two

fermions with momenta: $\mathbf{k}+\frac{1}{2}\,\mathbf{K}$ and $-\mathbf{k}+\frac{1}{2}\mathbf{K}$ with opposite spin projections (this is an elementary process of spontaneous *decay* of two-holes molecules into two holes). In each of four elementary processes depicted in Fig. 2.1, the total momentum and total spin projection of all particles which participate before and after as an elementary process are conserved, can be seen immediately from (2.12). Also, each elementary process of the *total* number of fermions is conserved. The physical meaning of the phenomenological functions $f_+(k)$ and $f_-(k)$ is the Fourier-transform functions of the internal wavefunctions of the *bound* 2eCPs and 2hCPs, respectively.

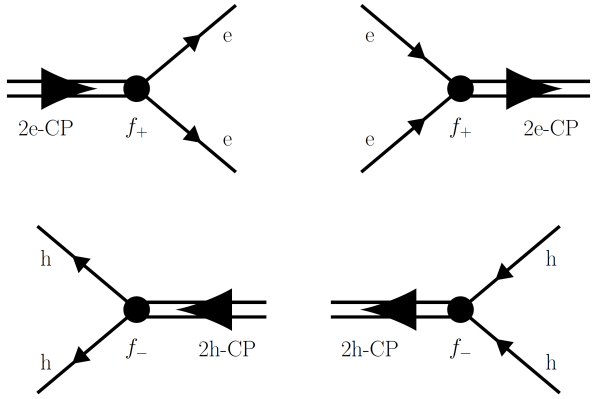

Figure 2.1: The BF Hamiltonian interaction (2.12) consists of four vertices each with two-fermion/one-boson creation-annihilation operators representing how unbound electrons (+) and/or holes (-) bind to form 2eCPs or 2hCPs, and disintegrate into two unbound fermions. Here, $f_\pm$ represents the BF interaction functions as mentioned in text.

Note that (2.11) plus (2.12) is quite different from the BCS Hamiltonian

$$H^{BCS} \equiv H_0^{BCS} + H_{int}^{BCS} = \sum_{\mathbf{k}_1,s_1} \epsilon_{k_1} a^\dagger_{k_1,s_1} a_{k_1,s_1} + \sum_{\mathbf{k}_1\mathbf{l}_1} V_{\mathbf{k}_1,\mathbf{l}_1} a^\dagger_{\mathbf{k}_1\uparrow} a^\dagger_{-\mathbf{k}_1\downarrow} a_{-\mathbf{l}_1\downarrow} a_{\mathbf{l}_1\uparrow} \tag{2.13}$$

with, say, the *BCS model interaction*

$$V_{\mathbf{k}_1,\mathbf{l}_1} = \begin{cases} -V/L^d & \text{if } \mu - \hbar\omega_D < \epsilon_{k_1},\ \epsilon_{l_1} < \mu + \hbar\omega_D \\ 0 & \text{otherwise} \end{cases} \tag{2.14}$$

with $V \geqslant 0$. We shall consider the GBEC Hamiltonian (2.11) plus (2.12) and later, when we writing down the precise conditions under which the GBEC theory contains the BCS theory as a special case we will specify the interaction condition.

2.2 GBEC Thermodynamic Potential

We now discuss the *thermodynamic properties* of the postulated many-fermion system. Although the *volume properties* of this many-fermion system are independent of the specific kind of macroscopic environment like

any statistical system, it is necessary from the beginning to chose a definite type of environment in order to perform precise statistical-thermodynamics calculations.

We place the system in a macroscopic vessel of constant macroscopically large volume $\mathcal{V} \equiv L^d$. This vessel is in turn placed in an *environment* which we shall characterize by a given constant absolute temperature T, and by some given value of fermion chemical potential μ, i.e., let us assume that the walls of the vessel are *permeable* for heat but we maintain at all times a constant temperature T on them, and furthermore the walls are *permeable* for fermions so that one can maintain a definite constant value of the fermion chemical potential μ. Thus, let us allow our many-fermion system to freely exchange with its environment both, heat and fermions.

Hence the *environment* is characterized by L^d, T and μ. In any statistical thermodynamic problem we must always suppose to have performed, at some step in the reasoning, a so-called *statistical limiting process* to an infinite system in which the volume of the system, its total energy, its total heat capacity, the total number of particles in the system, and in general any other so-called *extensive* thermodynamic quantity tends to infinity in such a way that volume density of energy, of thermodynamic potential, volume density of number of particles and, generally, the *volume density* of any extensive thermodynamic quantity remain *constant*. Such a limiting process, is the *thermodynamic limit*, whereas $L^d \to \infty$ and $N \to \infty$, assuming that L^d is the volume of the system and N its the number of particles. For our many-fermion system we shall suppose that this statistical limiting process is performed. In particular, all sums over momentum must be replaced by the corresponding integrals over momenta, namely

$$\begin{aligned} \sum_{\mathbf{k}} &\longrightarrow \left(\frac{L}{2\pi}\right)^d \int d^d k \equiv A_d \int dk\, k^{d-1} \\ \sum_{\mathbf{K}} &\longrightarrow \left(\frac{L}{2\pi}\right)^d \int d^d K \equiv A_d \int dK\, K^{d-1} \end{aligned} \tag{2.15}$$

for nonnegative k or K, where

$$A_d \equiv L^3/2\pi^2,\ L^2/2\pi \text{ and } L/\pi \tag{2.16}$$

for $d = 3$, 2 and 1, respectively. These replacements are an obvious consequence of the fact that the volume in 3D, or area in 2D, or length in 1D, of the elementary "cell" in momentum space is equal to $(2\pi/L)^d$ and tends to zero when $L^d \to \infty$.

Putting our many-fermion system in the environment L^d, T, μ, then it will stay in some *thermodynamic equilibrium state*, i.e., in a state which is characterized by the values of thermodynamics parameters L^d, T, μ, where T is the environment absolute temperature. According to the *basic recipe of statistical thermodynamics* the thermodynamic (or "grand") potential $\Omega(T, L^d, \mu)$ corresponds to the environment L^d, T, μ. It is related to the system pressure P, internal energy E and entropy S by $\Omega = -PL^d = F - \mu N \equiv E - TS - \mu N$, where F is the Helmholtz free energy. Then, the thermodynamic potential is defined as

$$\Omega(T, L^d, N, \mu) = -k_B T \ln\Big(Tr[\exp\{-\beta(\hat{H} - \mu\hat{N})\}]\Big) \tag{2.17}$$

where $\beta \equiv 1/k_B T$, Tr the "trace" of the diagonalized system, k_B the Boltzmann constant, and H is the *full* Hamiltonian of the system. Here $\hat{N}$ is the operator for the *total* number N of fermions in the system. Therefore, for the BF system is just

$$\hat{N} = \sum_{\mathbf{k}_1,s} a^\dagger_{\mathbf{k}_1,s} a_{\mathbf{k}_1,s} + 2\sum_{\mathbf{K}} b^\dagger_{\mathbf{K}} b_{\mathbf{K}} - 2\sum_{\mathbf{K}} c^\dagger_{\mathbf{K}} c_{\mathbf{K}}. \tag{2.18}$$

The total number of fermions in the many-fermion system is the number of unbound electrons, plus the number of electrons paired into 2eCPs, *minus* the number of holes paired into 2hCPs, while the latter have opposite charge to electrons. Thus, as a hole carries with a charge of $+e$, if we multiply (2.18) throughout the fermion charge $-e$ the result expresses the *charge conservation* of the system. From (2.11), (2.12) and (2.18) we immediately conclude that the full Hamiltonian $H = H_0 + H_{int}$ of our many-fermion system commutes with the operator $\hat{N}$ for the total number of electrons in the system.

The Gibbs identity for the thermodynamic potential Ω (2.17) is

$$d\Omega = -Pd\mathcal{V} - SdT - Nd\mu \tag{2.19}$$

where P is the pressure, S the entropy, and N the total number of electrons for that equilibrium state of the system when one has a constant volume L^d and is in contact with the environment, held at constant temperature T and the electron chemical potential μ. As immediate consequences we have the familiar relations

$$P = -\left(\frac{\partial\Omega}{\partial\mathcal{V}}\right)_{T,\mu} \qquad S = -\left(\frac{\partial\Omega}{\partial T}\right)_{\mathcal{V},\mu} \qquad N = -\left(\frac{\partial\Omega}{\partial\mu}\right)_{T,\mathcal{V}} \tag{2.20}$$

we assumed that the macroscopic environment of our many-fermion system is characterized by thermodynamic parameters L^d, T, and μ.

However, the characterization of the environment of a real superconductor at thermodynamic equilibrium experiment to measure, e.g., its specific heat, or critical magnetic field, when the superconductor carries no electric charge and characterizing their environment by the value of the electron chemical potential is unphysical. In such kind of experiments we have no free exchange of electrons between the superconductor and its environment. Physically, it is more correct to fix, in such traditional thermodynamic equilibrium conditions, not the value of chemical chemical potential μ of the environment but the value of the total number N of electrons in our many-electron system. Thus, we shall do this in such a way that the system volume L^d, its temperature T, and its total number N of electrons are each held fixed. Thus we define our *environment* by L^d, T, N instead. In the thermodynamic limit the total electron number-density n remains constant, or

$$n = \frac{N}{L^d} \equiv const. \tag{2.21}$$

The main thermodynamic quantities for our many-fermion system in the environment characterized by T, L^d, n are then: the pressure $P = P(T,n)$, the entropy $S(T,n)$ per unit volume $s(T,n)$ and the constant-volume specific heat $C_{\mathcal{V}}(T,n)$ per unit volume $c_{\mathcal{V}}(T,n)$. These quantities are clearly functions of the total

number density n of electrons, and of the temperature T, namely

$$\frac{S}{\mathcal{V}} \equiv s(T,n), \qquad \frac{C_{\mathcal{V}}}{\mathcal{V}} \equiv c_{\mathcal{V}}(T,n). \tag{2.22}$$

To ensure diagonalizability of the total Hamiltonian, we follow to Bogoliubov [59] and we allow the possibility that such condensates of 2eCPs and 2hCPs be in the state $\mathbf{K} = 0$ as follows. We shall go to reduce the formulation of our mathematical quantum statistical problem as follows. One can writes the full Hamiltonian (2.11) plus (2.12) as $\hat{H} - \mu\hat{N}$, giving

$$\begin{aligned}
\hat{H} - \mu\hat{N} &= \sum_{\mathbf{k},s}(\varepsilon_{\mathbf{k}} - \mu)a^{\dagger}_{\mathbf{k},s}a_{\mathbf{k},s} + [E_{+}(0) - 2\mu]\, b^{\dagger}_{0}b_{0} + \sum_{\mathbf{K}\neq 0}[E_{+}(K) - 2\mu]\, b^{\dagger}_{\mathbf{K}}b_{\mathbf{K}} \\
&+ [2\mu - E_{-}(0)]\, c^{\dagger}_{0}c_{0} - \sum_{\mathbf{K}\neq 0}[2\mu - E_{-}(K)]\, c^{\dagger}_{\mathbf{K}}c_{\mathbf{K}} \\
&+ L^{-3/2}\sum_{\mathbf{k}} f_{+}(k)\left(a^{\dagger}_{\mathbf{k},\uparrow}a^{\dagger}_{-\mathbf{k},\downarrow}b_{0} + a_{-\mathbf{k},\downarrow}a_{\mathbf{k},\uparrow}b^{\dagger}_{0}\right) \\
&+ L^{-3/2}\sum_{\mathbf{k}} f_{-}(k)\left(a^{\dagger}_{\mathbf{k},\uparrow}a^{\dagger}_{-\mathbf{k},\downarrow}c^{\dagger}_{0} + a_{-\mathbf{k},\downarrow}a_{\mathbf{k},\uparrow}c_{0}\right) \\
&+ L^{-3/2}\sum_{\mathbf{k},\mathbf{K}\neq 0} f_{+}(k)\left(a^{\dagger}_{\mathbf{k}+\frac{1}{2}\mathbf{K},\uparrow}a^{\dagger}_{-\mathbf{k}+\frac{1}{2}\mathbf{K},\downarrow}b_{\mathbf{K}} + a_{-\mathbf{k}+\frac{1}{2}\mathbf{K},\downarrow}a_{\mathbf{k}+\frac{1}{2}\mathbf{K},\uparrow}b^{\dagger}_{\mathbf{K}}\right) \\
&+ L^{-3/2}\sum_{\mathbf{k},\mathbf{K}\neq 0} f_{-}(k)\left(a^{\dagger}_{\mathbf{k}+\frac{1}{2}\mathbf{K},\uparrow}a^{\dagger}_{-\mathbf{k}+\frac{1}{2}\mathbf{K},\downarrow}c^{\dagger}_{\mathbf{K}} + c_{-\mathbf{k}+\frac{1}{2}\mathbf{K},\downarrow}a_{\mathbf{k}+\frac{1}{2}\mathbf{K},\uparrow}c_{\mathbf{K}}\right).
\end{aligned}$$

here we are separating the boson operator with CMM $K = 0$ from the bosons with CMM $\mathbf{K} \neq 0$. In [118–121] addressed two-electrons CPs with nonzero CMM via two-time Green functions and conclude that a pseudo-gap appears owing to this nonzero CMM CPs. Ignoring bosons with CMM $\mathbf{K} \neq 0$ we can construct a new so-called *reduced* full Hamiltonian operator $\hat{H}_{red} = \hat{H} - \mu\hat{N}$

$$\begin{aligned}
\hat{H}_{red} &\simeq \sum_{\mathbf{k},s}(\varepsilon_{\mathbf{k}} - \mu)a^{\dagger}_{\mathbf{k},s}a_{\mathbf{k},s} + [E_{+}(0) - 2\mu]\, b^{\dagger}_{0}b_{0} + \sum_{\mathbf{K}\neq 0}[E_{+}(K) - 2\mu]\, b^{\dagger}_{\mathbf{K}}b_{\mathbf{K}} \\
&+ [2\mu - E_{-}(0)]\, c^{\dagger}_{0}c_{0} - \sum_{\mathbf{K}\neq 0}[2\mu - E_{-}(K)]\, c^{\dagger}_{\mathbf{K}}c_{\mathbf{K}} \\
&+ L^{-3/2}\sum_{\mathbf{k}} f_{+}(k)\left(a^{\dagger}_{\mathbf{k},\uparrow}a^{\dagger}_{-\mathbf{k},\downarrow}b_{0} + a_{-\mathbf{k},\downarrow}a_{\mathbf{k},\uparrow}b^{\dagger}_{0}\right) \\
&+ L^{-3/2}\sum_{\mathbf{k}} f_{-}(k)\left(a^{\dagger}_{\mathbf{k},\uparrow}a^{\dagger}_{-\mathbf{k},\downarrow}c^{\dagger}_{0} + a_{-\mathbf{k},\downarrow}a_{\mathbf{k},\uparrow}c_{0}\right)
\end{aligned}$$

We following the Bogoliubov [122] recipe, *exact* in the thermodynamic limit [123], we shall allow for a possible BEC of the 2eCPs and 2hCP bosons with $\mathbf{K} = 0$ by replacing both creation and annihilation Bose operators $b^{\dagger}_{0}$, b_{0}, respectively for 2eCPs by the c-number N_0 (N_0 being the number of BE-condensed 2eCPs, i.e., with $\mathbf{K} = 0$) and Bose operators $c^{\dagger}_{0}$, c_{0}, respectively for 2hCPs by another c-number M_0 (M_0 being the

number of BE-condensed 2hCPs also with $\mathbf{K} = 0$). "*Note that this recipe goes beyond mean-field theory since one can show that the replacement implies no approximation provided one imposes the conditions of thermodynamic equilibrium"* [82]. So we shall redefine our Hamiltonian as

$$\begin{aligned}\hat{H}_{red} &\equiv [E_+(0) - 2\mu]N_0 + [2\mu - E_-(0)]M_0 + \sum_{\mathbf{k}}(\epsilon_k - \mu)a^\dagger_{\mathbf{k},s}a_{\mathbf{k}s} \\ &+ \sum_{\mathbf{K}\neq 0}[E_+(K) - 2\mu]b^\dagger_{\mathbf{K}}b_{\mathbf{K}} + \sum_{\mathbf{K}\neq 0}[2\mu - E_-(K)]c^+_{\mathbf{K}}c_{\mathbf{K}} \\ &+ \sum_{\mathbf{k}}[\sqrt{n_0}f_+(k) + \sqrt{m_0}f_-(k)]\left(a^\dagger_{\mathbf{k},\uparrow}a^\dagger_{-\mathbf{k}\downarrow} + a_{-\mathbf{k}\downarrow}a_{\mathbf{k}\uparrow}\right) \end{aligned} \tag{2.23}$$

therefore, the new interaction Hamiltonian H'_{int} is now

$$\begin{aligned}\hat{H}'_{int} &\equiv L^{-d/2}\sum_{\mathbf{k},\mathbf{K}\neq 0} f_+(k)\left(a^\dagger_{\mathbf{k}+\frac{1}{2}\mathbf{K},\uparrow}a^\dagger_{-\mathbf{k}+\frac{1}{2}\mathbf{K},\downarrow}b_{\mathbf{K}} + a_{-\mathbf{k}+\frac{1}{2}\mathbf{K},\downarrow}a_{\mathbf{k}+\frac{1}{2}\mathbf{K},\uparrow}b^\dagger_{\mathbf{K}}\right) \\ &+ L^{-d/2}\sum_{\mathbf{k},\mathbf{K}\neq 0} f_-(k)\left(a^\dagger_{\mathbf{k}+\frac{1}{2}\mathbf{K},\uparrow}a^\dagger_{-\mathbf{k}+\frac{1}{2}\mathbf{K},\downarrow}c^\dagger_{\mathbf{K}} + a_{-\mathbf{k}+\frac{1}{2}\mathbf{K},\downarrow}a_{\mathbf{k}+\frac{1}{2}\mathbf{K},\uparrow}c_{\mathbf{K}}\right) \end{aligned} \tag{2.24}$$

i.e., excluding the $\mathbf{K} = 0$ terms now included in (2.23). Note that $\hat{H}_{red}$ in (2.23) now depends *explicitly* on the numbers N_0 and M_0 which we have introduced as independent parameters.

Let us now insert the Hamiltonian $\hat{H}$ in the form $\hat{H}_{red}$, namely ignoring $\mathbf{K} \neq 0$ (eq. 2.24) in the basic statistical thermodynamic formula (2.17) and calculate the corresponding so-called modified thermodynamic potential

$$\Omega(T, L^d, \mu, N_0, M_0) = -k_B T \ln\left(Tr[\exp\{-\beta\hat{H}_{red}\}]\right) \tag{2.25}$$

which now depends on the independent thermodynamic variables T, L^d, μ, N_0, M_0. It is related to the system pressure P, the internal energy E and the entropy S by

$$\Omega = -PL^d = F - \mu N = E - TS - \mu N$$

where $F \equiv F(T, L^d, \mu, N_0, M_0)$ is the Helmholtz free energy. We fix the values of the numbers N_0 and M_0 in the following way. A thermodynamically stable state requires that for these values, the derivative of the Helmholtz free energy F, taken for a fixed T, L^d, μ wrt N_0 and M_0 has a minimum value. In other words, let us demand that satisfy

$$\left(\frac{\partial F}{\partial N_0}\right)_{L^d,\mu,T,M_0} = 0 \qquad \left(\frac{\partial F}{\partial M_0}\right)_{L^d,\mu,T,N_0} = 0 \qquad \text{and} \qquad \left(\frac{\partial \Omega}{\partial \mu}\right)_{L^d,T,N_0,M_0} = -N \tag{2.26}$$

where the first partial derivatives are taken at constant T, L^d, μ, while the third derivative is the well-known result of mechanical statistics. Solving the system of eqs. (2.26) in respect to N_0 and M_0, we shall construct

the following functions

$$N_0/L^d \equiv n_0 = n_0(T, L^d, \mu) \qquad M_0/L^d \equiv m_0 = m_0(T, L^d, \mu) \tag{2.27}$$

Solving the equation system (2.26) we obtain specific n_0 and m_0 for each set of values of independent thermodynamic parameters: T, L^d and μ, while the third equation in (2.26) ensures the charge conservation of the system, i.e., gauge invariance [124], which lacking in BCS theory.

Let us now substitute the functions (2.27) into the thermodynamic potential (2.25) in order to obtain some expression for the true thermodynamic potential of our many-fermion system in the environment characterized by T, L^d and μ. Explicitly, we have

$$\Omega(T, L^d, \mu) \equiv \Omega[T, L^d, \mu, \, n_0(T, L^d, \, \mu), \, m_0(T, L^d, \mu)] \tag{2.28}$$

which depends now on the variables T, L^d and μ only. The equation (2.28) allows us to go from the independent variables T, μ to the independent variables T, n. To do so, we use $-(\partial\Omega/\partial N)_{T,L^d} = \mu$ in order to determine the function

$$\mu = \mu(n, T). \tag{2.29}$$

2.2.1 GBEC Eigenstates

Although the many-electron system to be considered in this section is quite unrealistic, it is very simple and serves as a prelude in dealing with our full many-fermion system. Let us omit in the full dynamic operator (2.23) and (2.24) all interactions between unbound fermions and condensed ($\mathbf{K} = \mathbf{0}$) as well as excited ($\mathbf{K} \neq 0$) bosonic CPs of both kinds, namely 2eCPs and 2hCPs. Thus, the ideal boson-fermion model is defined by

$$\begin{aligned} H_0' - \mu\hat{N} &= [E_+(0) - 2\mu]N_0 + [2\mu - E_-(0)]M_0 + \sum_{\mathbf{k},s}(\epsilon_k - \mu)a^\dagger_{\mathbf{k},s}a_{\mathbf{k},s} \\ &+ \sum_{\mathbf{K}\neq 0}[E_+(K) - 2\mu]\, b^\dagger_{\mathbf{K}}b_{\mathbf{K}} + \sum_{\mathbf{K}\neq 0}[2\mu - E_-(K)]c^\dagger_{\mathbf{K}}c_{\mathbf{K}}. \end{aligned} \tag{2.30}$$

This follows from (2.23) by putting $f_+(k) = f_-(k) = 0$. The operator H_0' is clearly in diagonal form. Its *exact* eigenstates can be enumerated with the sets of occupation numbers $\{...n_{\mathbf{k},s}...N_{\mathbf{K}}...M_{\mathbf{K}}...\}$ where $n_{\mathbf{k},s}$ characterize one-particle electron states and take on two values 0 and 1, while one-boson occupation numbers $N_{\mathbf{K}}$ of 2eCPs and $M_{\mathbf{K}}$ of 2hCPs with momentum $\mathbf{K} \neq 0$, can take on values $0, 1, 2, \cdots \infty$. The exact eigenstates of the Hamiltonian $H_0' - \mu\hat{N}$ are then

$$|\, ...n_{\mathbf{k},s}...N_{\mathbf{K}}...M_{\mathbf{K}}...\rangle = \prod_{\mathbf{k},s}(a^\dagger_{\mathbf{k},s})^{n_{\mathbf{k},s}} \prod_{\mathbf{K}\neq 0}\frac{1}{\sqrt{N_{\mathbf{K}}!}}\left(b^\dagger_{\mathbf{K}}\right)^{N_{\mathbf{K}}} \prod_{\mathbf{K}\neq 0}\frac{1}{\sqrt{M_{\mathbf{K}}!}}\left(c^\dagger_{\mathbf{K}}\right)^{M_{\mathbf{K}}}|0\rangle \tag{2.31}$$

where $|0\rangle$ is the vacuum state for electrons and simultaneously for 2eCP and 2hCP creation and annihilation operators. Specifically

$$a_{\mathbf{k},s}|0\rangle \equiv b_{\mathbf{K}}|0\rangle \equiv c_{\mathbf{K}}|0\rangle \equiv 0. \tag{2.32}$$

The exact eigenvalues of the unperturbed Hamiltonian H_0' are then

$$\begin{aligned} E_{\{...n_{\mathbf{k},s}...N_{\mathbf{K}}...M_{\mathbf{K}}...\}} &= [E_+(0) - 2\mu]N_0 + [2\mu - E_-(0)]M_0 + \sum_{\mathbf{k},s}(\epsilon_k - \mu)n_{\mathbf{k},s} \\ &+ \sum_{\mathbf{K}\neq 0}[E_+(K) - 2\mu]N_{\mathbf{K}} + \sum_{\mathbf{K}\neq 0}[2\mu - E_-(K)]M_{\mathbf{K}}. \end{aligned} \tag{2.33}$$

Let us now calculate for $H_0' - \mu\hat{N}$ the modified thermodynamic potential Ω_0' with the help of its definition (2.25). In addition to (2.4) and (2.6), we shall define

$$\begin{aligned} U_0 &\equiv [E_+(0) - 2\mu]N_0 + [2\mu - E_-(0)]M_0 \\ \xi_k &\equiv \epsilon_k - \mu \end{aligned} \tag{2.34}$$

for $Tr\left(\exp\left[-\beta(H_0' - \mu\hat{N})\right]\right)$ one immediately obtains

$$\begin{aligned} &\sum_{...n_{\mathbf{k},s}...N_{\mathbf{K}}...M_{\mathbf{K}}...} \langle ...n_{\mathbf{k},s}...N_{\mathbf{K}}...M_{\mathbf{K}}... \mid \exp\left[-\beta(H_0' - \mu\hat{N})\right] \mid ...n_{\mathbf{k},s}...N_{\mathbf{K}}...M_{\mathbf{K}}...\rangle \\ &= \exp[-\beta U_0] \sum_{...n_{\mathbf{k},s}...N_{\mathbf{K}}...M_{\mathbf{K}}...} \exp[-\beta\xi_k n_{\mathbf{k},s}] \exp\left[-\beta \sum_{\mathbf{K}\neq 0}[E_+(\mathbf{K}) - 2\mu]\, N_{\mathbf{K}}\right] \\ &\times \exp\left[-\beta \sum_{\mathbf{K}\neq 0}[2\mu - E_-(K)]M_{\mathbf{K}}\right] \\ &= \exp[-\beta U_0] \prod_{\mathbf{k},s}\left[\sum_{n_{\mathbf{k},s}=0}^{1} \exp\left[-\beta\xi_k n_{\mathbf{k},s}\right]\right] \prod_{\mathbf{K}\neq 0}\left[\sum_{\mathbf{K}\neq 0} \exp\left[-\beta[E_+\mathbf{K} - 2\mu]N_{\mathbf{K}}\right]\right] \\ &\times \prod_{\mathbf{K}\neq 0}\left[\sum_{\mathbf{K}\neq 0} \exp[-\beta[2\mu - E_-(K)]\, M_{\mathbf{K}}]\right] \\ &= \exp[-\beta U_0] \prod_{\mathbf{k},s}[1 + \exp(-\beta\xi_k)] \prod_{\mathbf{K}\neq 0}[1 - \exp[-\beta\,(E_+\mathbf{K} - 2\mu)]]^{-1} \\ &\times \prod_{\mathbf{K}\neq 0}[1 - \exp\{-\beta[2\mu - E_-(K)]\}]^{-1}. \end{aligned} \tag{2.35}$$

Since $\Omega_0' = -k_B T \ln\left(Tr[\exp\{-\beta(H_0' - \mu\hat{N})\}]\right)$ one has

$$\begin{aligned}\Omega_0' &= U_0 - 2k_BT\sum_{\mathbf{k}}\ln(1+\exp[-\beta\xi_k]) + k_B\,T\sum_{\mathbf{K}\neq 0}\ln\left(1-\exp[-\beta(E_+(K)-2\mu)]\right) \\ &\quad + k_BT\sum_{\mathbf{K}\neq 0}\ln\left(1-\exp[-\beta(2\mu-E_-(K)]\right) \qquad (2.36)\end{aligned}$$

using (2.15) this quantity per unit volume $\mathcal{V} \equiv L^d$ becomes

$$\begin{aligned}\Omega_0'(T,\mu,n_0,m_0)/L^d &= [E_+(0)-2\mu]n_0 + [2\mu - E_-(0)]m_0 \\ &- 2k_BT\left(\frac{A_d}{L^d}\right)\int_0^\infty k^{d-1}dk\ln(1+\exp[-\beta\xi_k]) \\ &+ k_BT\left(\frac{A_d}{L^d}\right)\int_{0^+}^\infty K^{d-1}dK\ln\left(1-\exp[-\beta(E_+(K)-2\mu)]\right) \\ &+ k_BT\left(\frac{A_d}{L^d}\right)\int_{0^+}^\infty K^{d-1}dK\ln\left(1-\exp[-\beta(2\mu-E_-(K))]\right). \qquad (2.37)\end{aligned}$$

In general, for the system pressure P, the internal energy E and the entropy S, one has $\Omega(T, L^d, \mu, N_0, M_0) = -PL^d = F - \mu N = E - TS - \mu N$ where F is the Helmholtz free energy. For the thermodynamic potential (2.37) we now require the conditions

$$\begin{aligned}\frac{\partial}{\partial n_0}\left(\frac{F_0'}{L^3}\right)_{T,\mu,m_0} &\equiv [E_+(0)-2\mu] = 0 \\ \frac{\partial}{\partial m_0}\left(\frac{F_0'}{L^3}\right)_{T,\mu,m_0} &\equiv [2\mu - E_-(0)] = 0 \qquad (2.38)\end{aligned}$$

while

$$\begin{aligned}n &\equiv -\frac{\partial}{\partial\mu}\left(\frac{\Omega_0'}{L^3}\right)_{T,n_0,m_0} \\ &= 2n_0 - 2m_0 + 2\left(\frac{A_d}{L^d}\right)\int_0^\infty k^{d-1}dk\left[\exp[\beta\xi_k]+1\right]^{-1} \\ &+ 2\left(\frac{A_d}{L^d}\right)\int_0^\infty K^{d-1}dK\left[\exp[\beta(E_+(K)-2\mu)]-1\right]^{-1} \\ &- 2\left(\frac{A_d}{L^d}\right)\int_0^\infty K^{d-1}dK\left[\exp[\beta(2\mu-E_-(K))]-1\right]^{-1} \qquad (2.39)\end{aligned}$$

where the first two relations are necessary conditions for thermodynamic stability while the third relation ensures constancy of the initial number of particles in the system. From (2.34) we have

$$\frac{\partial\xi}{\partial\mu} = -1 \qquad \frac{\partial[E_+(K) - 2\mu]}{\partial\mu} = -2 \qquad \frac{\partial[2\mu - E_-(K)]}{\partial\mu} = 2. \tag{2.40}$$

Note that the first equality of (2.38) in a real situation is satisfied only when the minimum of the thermodynamic potential is reached when $n_0 \neq 0$ and $m_0 \neq 0$ are simultaneously satisfied, i.e., the available values are strictly $n_0 > 0$ and $m_0 > 0$. When the minimum is reached for $n_0 = 0$ and $m_0 \neq 0$, or for $n_0 \neq 0$ and $m_0 = 0$, or $n_0 = 0$ and $m_0 = 0$, i.e., on the range *boundaries* are indicated, one of the first two equations of (2.38) or both must be omitted.

2.3 GBEC with Reduced BF Vertex Interaction

Let us omit in the full modified Hamiltonian $\hat{H}_{red}$ (2.23), (2.24) the interaction operator $\hat{H}'_{int}$, and approximately put $\hat{H}_{red} \simeq \hat{H}'_0$. So we omit all the interaction between the fermions and excited 2eCps and 2hCPs, this interactions are studied in [118–120]. Thus, we take into account only those BF interactions between the unbound electrons or holes, and the 2eCPs and 2hCPs in their respective condensates.

The modified dynamical operator $\hat{H}'_0$ is given by the formula (2.23). This operator is a *quadratic form* in the fermion operators and consequently not difficult to determine *exactly* its eigenstates and eigenvalues. We need only transform the old creation and annihilation fermion operators $a^\dagger_{\mathbf{k},s}$ and $a_{\mathbf{k},s}$ to new creation and annihilation quasi-particle operators $\alpha^\dagger_{\mathbf{k},s}$ and $\alpha_{\mathbf{k},s}$ via the Bogoliubov-Valatin [125, 126] canonical (i.e., that preserve the form of Fermi anticommutation relations) u, v-transformation. Specifically

$$\begin{aligned} a_{\mathbf{k},s} &\equiv u_k\,\hat{\alpha}_{\mathbf{k},s} + 2s\,v_k\,\hat{\alpha}^\dagger_{-\mathbf{k},-s'} \\ a^\dagger_{\mathbf{k},s} &\equiv u_k\,\hat{\alpha}^\dagger_{\mathbf{k},s} + 2s\,v_k\,\hat{\alpha}_{-\mathbf{k},-s'} \end{aligned} \tag{2.41}$$

where $s = \pm\frac{1}{2}$ the particle spin, namely

$$\begin{aligned} \hat{a}_{\mathbf{k},\uparrow} &\equiv u_{\mathbf{k}}\alpha_{\mathbf{k},\uparrow} + v_{\mathbf{k}}\alpha^\dagger_{-\mathbf{k},\downarrow} \\ \hat{a}^\dagger_{\mathbf{k},\uparrow} &\equiv u_{\mathbf{k}}\alpha^\dagger_{\mathbf{k},\uparrow} + v_{\mathbf{k}}\alpha_{-\mathbf{k},\downarrow} \\ \hat{a}_{\mathbf{k},\downarrow} &\equiv u_{\mathbf{k}}\alpha_{\mathbf{k},\downarrow} - v_{\mathbf{k}}\alpha^\dagger_{-\mathbf{k},\uparrow} \\ \hat{a}^\dagger_{\mathbf{k},\downarrow} &\equiv u_{\mathbf{k}}\alpha^\dagger_{\mathbf{k},\downarrow} - v_{\mathbf{k}}\alpha_{-\mathbf{k},\uparrow} \end{aligned} \tag{2.42}$$

where the new operators $\alpha, \alpha^\dagger$ follows the commutation rules $\{\alpha_k, \alpha^\dagger_{k'}\} = \delta_{k,k'}$ and $\{\alpha_k, \alpha_{k'}\} = \{\alpha^\dagger_k, \alpha^\dagger_{k'}\} = 0$. Substituting (2.41) in the first and the interaction term of (2.23) gives

$$\begin{aligned}
\hat{H}_{red} &\equiv \sum_{\mathbf{k},s}(\epsilon_k-\mu)\left[(u_k\alpha^\dagger_{k,s}+v_k\alpha_{-k,s})(u_k\alpha_{k,s}+v_k\alpha^\dagger_{-k,s})\right] \\
&+ [E_+(0)-2\mu]N_0+\sum_{\mathbf{K}\neq 0}[E_+(K)-2\mu]b^\dagger_{\mathbf{K}}b_{\mathbf{K}}+[2\mu-E_-(0)]M_0+\sum_{\mathbf{K}\neq 0}[2\mu-E_-(K)]c^+_{\mathbf{K}}c_{\mathbf{K}} \\
&+ \sum_{\mathbf{k}}\left[f_+(k)\sqrt{n_0}+f_-(k)\sqrt{m_0}\right]\left[\ (u_k\alpha^\dagger_{k,\uparrow}+v_k\alpha_{-k,\downarrow})(u_k\alpha^\dagger_{-k,\downarrow}-v_k\alpha_{-k,\uparrow})\right. \\
&+ \left.(u_k\alpha_{-k,\downarrow}-v_k\alpha^\dagger_{k,\uparrow})(u_k\alpha_{k,\uparrow}+v_k\alpha^\dagger_{-k,\downarrow})\ \right] \qquad (2.43)
\end{aligned}$$

expanding terms

$$\begin{aligned}
\hat{H}_{red} &\equiv \sum_{\mathbf{k},s}(\epsilon_k-\mu)\left[u_k^2\alpha^\dagger_{k,s}\alpha_{-k,s}+u_kv_k\alpha^\dagger_{k,s}\alpha^\dagger_{-k,s}+v_k^2\alpha_{-k,s}\alpha_{-k,s}+u_kv_k\alpha_{-k,s}\alpha_{k,s}\right] \\
&+ [E_+(0)-2\mu]N_0+\sum_{\mathbf{K}\neq 0}[E_+(K)-2\mu]b^\dagger_{\mathbf{K}}b_{\mathbf{K}} \\
&+ [2\mu-E_-(0)]M_0+\sum_{\mathbf{K}\neq 0}[2\mu-E_-(K)]c^+_{\mathbf{K}}c_{\mathbf{K}} \\
&+ \sum_{\mathbf{k}}\left[f_+(k)\sqrt{n_0}+f_-(k)\sqrt{m_0}\right]\left[\ (u_k^2\alpha^\dagger_{k,\uparrow}\alpha^\dagger_{-k,\downarrow}-u_kv_k\alpha^\dagger_{k,\uparrow}\alpha_{k,\uparrow}-v_k^2\alpha^\dagger_{-k,\downarrow}\alpha_{k,\uparrow}+u_kv_k\alpha_{-k,\downarrow}\alpha^\dagger_{-k,\downarrow})\right. \\
&+ \left.(u_k^2\alpha_{-k,\downarrow}\alpha_{k,\uparrow}-u_kv_k\alpha^\dagger_{-k,\downarrow}\alpha_{k,\uparrow}+v_k^2\alpha_{k,\uparrow}\alpha^\dagger_{-k,\downarrow}+u_kv_k\alpha_{k,\uparrow}\alpha_{k,\uparrow})\ \right] \qquad (2.44)
\end{aligned}$$

Rewriting $\xi_k \equiv \varepsilon_k-\mu$ and $f_+(k)\sqrt{n_0}+f_-(k)\sqrt{m_0}\equiv\Delta_k$ and rearranging terms, the operator $\hat{\Omega}=\hat{H}_{red}$ gives

$$\begin{aligned}
\hat{\Omega} &\simeq \sum_{\mathbf{k},s}\xi_k\left[u_k^2\alpha^\dagger_{k,s}\alpha_{k,s}+2s\left(2s\,v_k^2\{1-\alpha^\dagger_{-k,s}\alpha_{k,s}\}-2s\,u_kv_k\{\alpha^\dagger_{k,s}\alpha^\dagger_{-k,s}+\alpha_{k,s}\alpha_{k,s}\}\right)\right] \\
&+ [E_+(0)-2\mu]N_0+\sum_{\mathbf{K}\neq 0}[E_+(K)-2\mu]\,\hat{b}^\dagger_{\mathbf{K}}\hat{b}_{\mathbf{K}} \\
&+ [2\mu-E_-(0)]M_0+\sum_{\mathbf{K}\neq 0}[2\mu-E_-(K)]\ \hat{c}^\dagger_{\mathbf{K}}\hat{c}_{\mathbf{K}} \\
&+ \sum_{\mathbf{k}}\Delta_k\{u_k^2\left(\alpha^\dagger_{k,\uparrow}\alpha^\dagger_{-k,\downarrow}+\alpha_{-k,\downarrow}\alpha_{k,\uparrow}\right)-v_k^2\left(\alpha^\dagger_{-k,\downarrow}\alpha_{k,\uparrow}+\alpha_{k,\uparrow}\alpha^\dagger_{-k,\downarrow}\right) \\
&+ u_kv_k\left(\alpha^\dagger_{-k,\downarrow}\alpha_{-k,\downarrow}+\alpha_{-k,\downarrow}\alpha_{k,\downarrow}-\alpha^\dagger_{k,\uparrow}\alpha_{k,\uparrow}-\alpha_{k,\uparrow}\alpha_{k,\uparrow}\right)\} \qquad (2.45)
\end{aligned}$$

Hereafter, we ignore the second order terms as usual in mean field approximation theory. Thus, simpli-

fying terms one has

$$\begin{aligned}
\hat{\Omega} &\simeq \sum_{\mathbf{k},s}\left[\xi_k(u_k^2-v_k^2)-2\Delta_k u_k v_k\right]\alpha_{k,s}^{\dagger}\alpha_{k,s} \\
&+ \sum_{\mathbf{k},s} 2s\left[\xi_k u_k v_k+\frac{1}{2}\Delta_k(u_k^2-v_k^2)\right]\left(\alpha_{k,s}^{\dagger}\alpha_{-k,-s}^{\dagger}+\alpha_{k,s}\alpha_{-k,-s}\right) \\
&+ \sum_{\mathbf{k},s} 2\left[\xi_k^2+\Delta_k u_k v_k\right] \\
&+ [E_+(0)-2\mu]N_0+\sum_{\mathbf{K}\neq 0}\left[E_+(K)-2\mu\right]\hat{b}_{\mathbf{K}}^{\dagger}\hat{b}_{\mathbf{K}} \\
&+ [2\mu-E_-(0)]M_0+\sum_{\mathbf{K}\neq 0}\left[2\mu-E_-(K)\right]\hat{c}_{\mathbf{K}}^{\dagger}\hat{c}_{\mathbf{K}}
\end{aligned} \tag{2.46}$$

To diagonalized $\hat{\Omega}$ one must have

$$\xi_k u_k v_k+\tfrac{1}{2}\Delta_k\left(u_k^2-v_k^2\right)\equiv 0 \tag{2.47}$$

if one defines the energy E_k as

$$E_k\equiv\xi_k\left(u_k^2-v_k^2\right)-2\Delta_k u_k v_k \tag{2.48}$$

substituting in (2.47) gives

$$u_k^2-v_k^2=\frac{E_k\xi_k}{\xi_k^2+\Delta_k^2} \tag{2.49}$$

with the condition $u_k^2+v_k^2=1$ one has

$$u_k^2=\tfrac{1}{2}\left[1+\frac{E_k\xi_k}{\xi_k^2+\Delta_k^2}\right] \tag{2.50}$$

$$v_k^2=\tfrac{1}{2}\left[1-\frac{E_k\xi_k}{\xi_k^2+\Delta_k^2}\right] \tag{2.51}$$

substituting (2.50) and (2.51) in (2.47) gives the energy

$$E_k\equiv\sqrt{\xi_k^2+\Delta_k^2} \tag{2.52}$$

then

$$u_k^2=\tfrac{1}{2}\left[1+\frac{\xi_k}{\sqrt{\xi_k^2+\Delta_k^2}}\right] \tag{2.53}$$

$$v_k^2=\tfrac{1}{2}\left[1-\frac{\xi_k}{\sqrt{\xi_k^2+\Delta_k^2}}\right] \tag{2.54}$$

substituting (2.52), (2.53) and (2.54) in (2.46) gives

$$H_0' - \mu\hat{N} = U_{00} + \sum_{\mathbf{k},s} E_k \alpha^\dagger_{\mathbf{k},s}\alpha_{\mathbf{k},s} + \sum_{\mathbf{K}\neq 0}[E_+(K) - 2\mu] b^\dagger_{\mathbf{K}} b_{\mathbf{K}} + \sum_{\mathbf{K}\neq 0}[2\mu - E_-(K)] c^\dagger_{\mathbf{K}} c_{\mathbf{K}}. \quad (2.55)$$

This is because we have now *two-* instead of four-fermion operators as in the original BCS Hamiltonian, so that no need to discard terms not in the form $\alpha^\dagger_{\mathbf{k},s}\alpha_{\mathbf{k},s}$. Here U_{00} is the ordinary number defined by

$$U_{00} \equiv [E_+(0) - 2\mu]N_0 + [2\mu - E_-(0)]M_0 + \sum_{\mathbf{k}}(\xi_k - E_k) \quad (2.56)$$

which differs from the previous number U_0 given in (2.34).

The exact eigenstates $|...\nu_{\mathbf{k},s}...N_{\mathbf{K}}...M_{\mathbf{K}}...\rangle$ and eigenvalues $E_{\{...\nu_{\mathbf{k},s}...N_{\mathbf{K}}...M_{\mathbf{K}}...\}}$ of the dynamical operator $H_0' - \mu\hat{N}$ (2.55) are then

$$|...\nu_{\mathbf{k},s}...N_{\mathbf{K}}...M_{\mathbf{K}}...\rangle = \prod_{\mathbf{k},s}(\alpha^\dagger_{\mathbf{k},s})^{\nu_{\mathbf{k},s}} \prod_{\mathbf{K}\neq 0}\frac{1}{\sqrt{N_{\mathbf{K}}!}}\left(b^\dagger_{\mathbf{K}}\right)^{N_{\mathbf{K}}} \prod_{\mathbf{K}\neq 0}\frac{1}{\sqrt{M_{\mathbf{K}}!}}\left(c^\dagger_{\mathbf{K}}\right)^{M_{\mathbf{K}}}|\mathbf{0}\rangle \quad (2.57)$$

and

$$E_{[...\nu_{\mathbf{k},s}...N_{\mathbf{K}}...M_{\mathbf{K}}...]} = U_{00} + \sum_{\mathbf{k},s} E_k \nu_{\mathbf{k},s} + \sum_{\mathbf{K}\neq 0}[E_+(K) - 2\mu]N_{\mathbf{K}} + \sum_{\mathbf{K}\neq 0}[2\mu - E_-(K)]M_{\mathbf{K}}. \quad (2.58)$$

Here $|\mathbf{0}\rangle$ is the vacuum state for new quasi-fermion creation $\alpha^\dagger_{\mathbf{k},s}$ and annihilation $\alpha_{\mathbf{k},s}$ operators, and simultaneously for the creation and annihilation 2eCP and 2hCP operators; it is different from the previous vacuum state $|0\rangle$ defined in (2.31). Namely,

$$\alpha_{\mathbf{k},s}|\mathbf{0}\rangle \equiv b_{\mathbf{K}}|\mathbf{0}\rangle \equiv c_{\mathbf{K}}|\mathbf{0}\rangle \equiv 0. \quad (2.59)$$

The symbol $[...\nu_{\mathbf{k},s}...N_{\mathbf{K}}...M_{\mathbf{K}}...]$ designates a *set* of values of the occupation numbers $\nu_{\mathbf{k},s}$ (which take only the two values, 0 or 1) of the *new* single quasi-fermion states $\mathbf{k}, s$, and the values of the occupation numbers $N_{\mathbf{K}}$ and $M_{\mathbf{K}}$ of the single-boson states with $\mathbf{K} \neq 0$ of 2eCPs and of 2hCPs, respectively, which

take all values $0, 1, 2, \cdots, \infty$. Substituting (2.58) into (2.25) gives

$$\begin{aligned}
\Omega_0'(T, L^d, \mu, N_0, M_0) &= -k_B T \ln\left(Tr \exp\left[-\beta(H_0' - \mu\hat{N})\right]\right) \\
&= -k_B T \ln \sum_{...\nu_{\mathbf{k},s}...N_{\mathbf{K}}...M_{\mathbf{K}}...} \langle ...\nu_{\mathbf{k},s}...N_{\mathbf{K}}...M_{\mathbf{K}}... \mid \\
&\times \exp\left[-\beta(H_0' - \mu\hat{N})\right] \mid ...\nu_{\mathbf{k},s}...N_{\mathbf{K}}...M_{\mathbf{K}}...\rangle \\
&= [E_+(0) - 2\mu]N_0 + [2\mu - E_-(0)]M_0 \\
&+ \sum_{\mathbf{k}} (\xi_k - E_k) - 2k_B T \sum_{\mathbf{k}} \ln\left(1 + \exp[-\beta E_k]\right) \\
&+ k_B T \sum_{\mathbf{K}\neq 0} \ln\left(1 - \exp\left[-\beta(E_+(K) - 2\mu)\right]\right) \\
&+ k_B T \sum_{\mathbf{K}\neq 0} \ln\left(1 - \exp\left[-\beta(2\mu - E_-(K))\right]\right). \qquad (2.60)
\end{aligned}$$

Then the grand potential (2.28) becomes

$$\begin{aligned}
\Omega(T, L^d, \mu, N_0, M_0)/L^d &= [E_+(0) - 2\mu]n_0 + [2\mu - E_-(0)]m_0 \qquad (2.61) \\
&+ \int_0^\infty d\epsilon N(\epsilon)[\epsilon - \mu - E(\epsilon)] \\
&- 2k_B T \int_0^\infty d\epsilon N(\epsilon) \ln\left(1 + \exp[-\beta E(\epsilon)]\right) \\
&+ k_B T \int_{0^+}^\infty d\varepsilon M(\varepsilon) \ln\left(1 - \exp[-\beta(E_+(0) + \varepsilon - 2\mu)]\right) \\
&+ k_B T \int_{0^+}^\infty d\varepsilon M(\varepsilon) \ln\left(1 - \exp[-\beta(2\mu - E_-(0) + \varepsilon)]\right)
\end{aligned}$$

where $E(\epsilon) \equiv \sqrt{(\epsilon - \mu)^2 + \Delta^2(\epsilon)}$ whit $\Delta(\epsilon) \equiv \sqrt{n_0} f_+(\epsilon) + \sqrt{m_0} f_-(\epsilon)$ and the functions $f_+(\epsilon)$ and $f_-(\epsilon)$ are attainable from the initial functions $f_+(k)$ and $f_-(k)$ using $k = \sqrt{2m\epsilon}/\hbar$. With

$$N(\epsilon) = m^{3/2}\sqrt{\epsilon}/2^{1/2}\pi^2\hbar^3, \qquad M(\varepsilon) = 2m^{3/2}\sqrt{\varepsilon}/\pi^2\hbar^3 \qquad (2.62)$$

the density of states of electrons, and the bosonic density-of-states, respectively, evaluated at the energies $\epsilon = \hbar^2 k^2/2m$ and $\varepsilon = \hbar^2 K^2/4m$, respectively.

One can rewrite these two expressions by using the first of the identities

$$2/(e^x + 1) \equiv 1 - \tanh\left(\tfrac{x}{2}\right) \qquad \text{and} \qquad 2/(e^x - 1) \equiv \coth\left(\tfrac{x}{2}\right) - 1. \qquad (2.63)$$

Therefore, the first two transcendental system equations become

$$2\sqrt{n_0}[E_+(0)-2\mu] = \int_0^\infty d\epsilon N(\epsilon)\frac{\Delta(\epsilon)\,f_+(\epsilon)}{E(\epsilon)}\tanh\tfrac{1}{2}\beta E(\epsilon) \tag{2.64}$$

$$2\sqrt{m_0}[2\mu-E_-(0)] = \int_0^\infty d\epsilon N(\epsilon)\frac{\Delta(\epsilon)\,f_-(\epsilon)}{E(\epsilon)}\tanh\tfrac{1}{2}\beta E(\epsilon). \tag{2.65}$$

Taking the partial derivative of the modified thermodynamic potential Ω/L^d wrt μ for fixed values of n_0, m_0 and T one gets

$$\begin{aligned} n &= -\frac{\partial}{\partial\mu}\left(\frac{\Omega}{L^d}\right)_{T,n_0,m_0} \\ &= -\int_0^\infty d\epsilon N(\epsilon)\left(1+\frac{\partial E(\epsilon)}{\partial\mu}\right)+2\int_0^\infty d\epsilon N(\epsilon)\frac{\exp[-\beta E(\epsilon)]}{1+\exp[-\beta E(\epsilon)]}\left(\frac{\partial E(\epsilon)}{\partial\mu}\right) \\ &- 2n_0+\int_0^\infty d\varepsilon M(\varepsilon)\frac{\exp[-\beta(E_+(0)-2\mu+\varepsilon)]}{1-\exp[-\beta(E_+(0)-2\mu+\varepsilon)]}\left(\frac{\partial(E_+(0)-2\mu+\varepsilon]}{\partial\mu}\right) \\ &+ 2m_0+\int_0^\infty d\varepsilon M(\varepsilon)\frac{\exp[-\beta(2\mu-E_-(0)+\varepsilon)]}{1-\exp[-\beta(2\mu-E_-(0)+\varepsilon)]}\left(\frac{\partial[2\mu-E_-(0)+\varepsilon]}{\partial\mu}\right) \end{aligned} \tag{2.66}$$

one has that

$$\begin{aligned} \left(\frac{\partial E(\epsilon)}{\partial\mu}\right)_{T,n_0,m_0} &= -\frac{\epsilon-\mu}{E(\epsilon)}, \\ \left(\frac{\partial[E_+(0)-2\mu+\varepsilon]}{\partial\mu}\right)_{T,n_0,m_0} &= -2, \\ \left(\frac{\partial[E_+(0)-2\mu+\varepsilon]}{\partial\mu}\right)_{T,n_0,m_0} &= 2 \end{aligned} \tag{2.67}$$

so that (2.66) becomes

$$\begin{aligned} n &= \int_0^\infty d\epsilon N(\epsilon)\left(1-\frac{\epsilon-\mu}{E(\epsilon)}\right)+2\int_0^\infty d\epsilon N(\epsilon)\frac{\epsilon-\mu}{E(\epsilon)}\left(\exp[\beta E(\epsilon)\}+1]^{-1}\right) \\ &+ 2n_0(T)+2\int_{0+}^\infty d\varepsilon M(\varepsilon)\left(\exp[\beta(E_+(0)-2\mu+\varepsilon)]-1\right)^{-1} \\ &- 2m_0(T)-2\int_{0+}^{+\infty} d\varepsilon M(\varepsilon)\left(\exp[\beta(2\mu-E_-(0)+\varepsilon)]-1\right)^{-1}. \end{aligned} \tag{2.68}$$

The third transcendental equation becomes the *number equation*

$$n = 2n_B(T) - 2m_B(T) + n_f(T). \tag{2.69}$$

defining

$$\begin{aligned} n_B(T) &\equiv n_0(T) + \int_{0^+}^{\infty} d\varepsilon M(\varepsilon)[\exp\beta[E_+(0) - 2\mu + \varepsilon] - 1]^{-1} && (2.70)\\ &\equiv n_0(T) + n_{B+}(T) \\ m_B(T) &\equiv m_0(T) + \int_{0^+}^{\infty} d\varepsilon M(\varepsilon)[\exp\beta[2\mu - E_-(0) + \varepsilon] - 1]^{-1} && (2.71)\\ &\equiv m_0(T) + m_{B+}(T) \\ n_f(T) &\equiv \int_0^{\infty} d\epsilon N(\epsilon)\left(1 - \frac{\epsilon - \mu}{E(\epsilon)}\tanh\tfrac{1}{2}\beta E(\epsilon)\right) && (2.72) \end{aligned}$$

where $n_{B+}(T)$ and $m_{B+}(T)$ can be termed as the total number-density of nonzero-CMM excited or "pre-formed" 2eCPs and 2hCPs, respectively, and $n_f(T)$ the number-density of unbound electrons, all at absolute temperature T. The system of *three* coupled integral equations (2.64), (2.65) and (2.69) consequently enables us to determine the *three* quantities $n_0 = n_0(T, n, \mu)$, $m_0 = m_0(T, n, \mu)$ and $\mu = \mu(T, n)$. The latter quantity can then be eliminated to give us $n_0 = n_0(T, n)$ and $m_0 = m_0(T, n)$. The thermodynamic properties can be obtained such as the entropy per unit volume $s(T, n)$ and the specific heat per unit volume $c_{\mathcal{V}}(T, n)$.

The preformed bosonic particles *above* the condensate, apparently by first time have been deduced to exist from the gigahertz-frequency complex conductivity studies [127, 128] in $Bi_2Sr_2CaCu_2O_{8+\delta}$. The energy of these pairs has more energy than two unbound electrons, this condition have appeared in previous BF models [118–121] where the authors addressed two-electrons CPs with nonzero CMM as bosonic excitations via two-time Green functions and conclude that a pseudo-gap appears owing to this bosonic pairs. In Ref. [107] it's analyzed the infinite-lifetime two-particle bound-state if two-hole CPs are ignored concluding that two-electron CPs has a positive-energy *resonant-state* CPs with a finite lifetime for nonzero CMM. Also is proposed that a pre-formed CPs [129] emerges naturally as the nonzero-total CMM CPs that are entirely neglected in the ordinary BCS theory [41]. Although in [130] argued that these excited pairs has a total energy $E_K(T) \equiv 2\mu(T) - \Delta_K(T)$ with binding energy $\Delta_K(T) \geq 0$ with $\mu(T)$ the fermionic chemical potential, do not confuse Δ_K with the BCS energy gap $\Delta(T)$. Their expression for bosonic excited pairs resembles the energy for 2eCPs presented here.

In Ref. [131] the authors addresses the Bose-Einstein condensation of "pairons". That study shows that a pairon composed by two fermions can undergo a BE condensation transition. An important difference is the dispersion relation, while the pairons hold a linear-dispersive relation our treatment is on the quadratic-

dispersive relation. Furthermore, pairons do not overlap in space since the interpairon distance is several times greater than the pairon size, see eq. (9.5.5); meaning that BE condensation takes place before the free pairon picture breaks down.

Furthermore in [132] discussed a model of charged bosons (2e) and fermions (1e), this system with *pre-formed* (local) pairs can be described by a Hamiltonian of hard-core charged bosons on a lattice [63,133,134], they have main features, among others the origin of the energy gap can be distinct from BCS, the ratio $2\Delta(0)/k_BT_c$ is not universal, it varies around the BCS value of 3.53 as the relative proportions of pre-formed pairs and this local pairs exist above T_c, later will be addressed.

2.3.1 Symmetrical-Step Reduced BF Interaction

Consider now a reduced BF vertex interaction of symmetrical step-like form

$$f_+(\epsilon) = \begin{cases} f & \text{if} \quad E_f < \epsilon < E_f + \delta\epsilon \\ 0 & \text{otherwise} \end{cases} \tag{2.73}$$

$$f_-(\epsilon) = \begin{cases} f & \text{if} \quad E_f - \delta\epsilon < \epsilon < E_f \\ 0 & \text{otherwise.} \end{cases} \tag{2.74}$$

This particular form will allow us to making an one-to-one correspondence between the BF vertex (two-fermion) interaction and the familiar Cooper/BCS two-parameter model interelectron (four-fermion) interaction in the appropriate limits, as we will see below, and through this association we obtain the BCS gap equation precisely. Both step functions are perfectly adjacent to each other at a given characteristic energy E_f, have the same height f and the same width $\delta\epsilon$.

Instead of dealing with the phenomenological zero-CMM energies $E_+(0)$ and $E_-(0)$, respectively associated with the 2eCPs and 2hCPs postulated to exist in the normal state, we define two alternative *positive* energies

$$E_f \equiv \tfrac{1}{4}[E_+(0) + E_-(0)] \tag{2.75}$$

and

$$\delta\epsilon \equiv \tfrac{1}{2}[E_+(0) - E_-(0)]. \tag{2.76}$$

The latter is positive provided only when $E_+(0) > E_-(0)$. Note that this is *not* satisfied by the original definition of CPs by Cooper based on the ideal Fermi gas "sea," where $E_+(0) < 0$ while $E_-(0) > 0$, but *is* satisfied by the Bethe-Salpeter treatments of Refs. [107] in 2D and [108] in 3D which are based on the BCS ground-state Fermi sea. Thus, the two energies E_f and $\delta\epsilon$ replace $E_+(0)$ and $E_-(0)$ as our fundamental dynamical phenomenological parameters related to the 2eCPs and 2hCPs. Both (2.75) and (2.76) implying that

$$E_\pm(0) \equiv 2E_f \pm \delta\epsilon. \tag{2.77}$$

The energy gap $\Delta(T)$ now becomes

$$\Delta(T) = \begin{cases} f\sqrt{n_0(T)} & \text{if } E_f < \epsilon < E_f + \delta\epsilon \\ f\sqrt{m_0(T)} & \text{if } E_f - \delta\epsilon < \epsilon < E_f \\ 0 & \text{otherwise,} \end{cases} \tag{2.78}$$

thus the electron energies become the gapped spectra

$$E(\epsilon) = \begin{cases} \sqrt{(\epsilon-\mu)^2 + f^2\, n_0} & \text{if} \quad E_f < \epsilon < E_f + \delta\varepsilon \\ \sqrt{(\epsilon-\mu)^2 + f^2\, m_0} & \text{if} \quad E_f - \delta\epsilon < \epsilon < E_f \\ |\epsilon - \mu| & \text{otherwise.} \end{cases} \tag{2.79}$$

For a BF interaction as (2.60) and (2.61), our basic system of three transcendental equations (2.64) to (2.65) becomes, in view of (2.77), gives

$$[2E_f + \delta\varepsilon - 2\mu(T)] = \tfrac{1}{2}f^2 \int_{E_f}^{E_f+\delta\varepsilon} d\epsilon N(\epsilon) \frac{\tanh\left(\frac{1}{2}\beta\sqrt{[\epsilon-\mu(T)]^2 + f^2 n_0(T)}\right)}{\sqrt{[\epsilon-\mu(T)]^2 + f^2 n_0(T)}} \tag{2.80}$$

$$[2\mu(T) - 2E_f + \delta\varepsilon] = \tfrac{1}{2}f^2 \int_{E_f-\delta\varepsilon}^{E_f} d\epsilon N(\epsilon) \frac{\tanh\left(\frac{1}{2}\beta\sqrt{[\epsilon-\mu(T)]^2 + f^2 m_0(T)}\right)}{\sqrt{[\epsilon-\mu(T)]^2 + f^2 m_0(T)}} \tag{2.81}$$

and

$$n = 2n_0(T) + 2n_{B+}(T) - 2m_0(T) - 2m_{B+}(T) + n_f(T) \tag{2.82}$$

the boson number densities can be rewritten as

$$n_{B+}(T) \equiv \int_{0^+}^{\infty} d\varepsilon M(\varepsilon) \left(\exp[\beta(\varepsilon + 2E_f + \delta\epsilon - 2\mu) - 1]^{-1}\right) \tag{2.83}$$

$$m_{B+}(T) \equiv \int_{0^+}^{\infty} d\varepsilon M(\varepsilon) \left(\exp[\beta(\varepsilon - 2E_f + \delta\epsilon + 2\mu) - 1]^{-1}\right). \tag{2.84}$$

while the number density of the unbound electrons is

$$n_f(T) \equiv \int_0^{\infty} d\epsilon N(\epsilon \left(1 - \frac{\epsilon-\mu}{E(\epsilon)} \tanh\left[\tfrac{1}{2}\beta E(\epsilon)\right]\right) \equiv 2\sum_{\mathbf{k}} v_{\mathbf{k}}^2(T). \tag{2.85}$$

Note, that the $v_{\mathbf{k}}^2(T)$ are the finite-T generalization of $v_{\mathbf{k}}^2 \equiv 1 - u_{\mathbf{k}}^2$ coefficients that first appeared in the BCS

trial wavefunction for singlet pairing given by

$$\prod_{\mathbf{k}}(u_{\mathbf{k}}+v_{\mathbf{k}}a^{\dagger}_{\mathbf{k},\uparrow}a^{\dagger}_{-\mathbf{k},\downarrow})|0\rangle$$

where $|0\rangle$ is the BCS vacuum. The $u_{\mathbf{k}}$ and $v_{\mathbf{k}}$ also appear in the Bogoliubov-Valatin transformation equations (2.41), (2.50), (2.51) and (2.52).

2.4 Special Cases Subsumed in GBEC

In this section we describe how the GBEC theory subsumes the five statistical theories of superconductivity as special cases. These five theories follow from GBEC in three principal branches; the first one: arbitrary proportions between 2eCPs and 2hCPs taking the 2eCP-gap-like equation, the 2hCP-gap-like equation plus the number equation; the second branch is the *symmetrical* case with equal footing between 2eCPs and 2hCPs, this implies to consider the gap-like equation as well the number equation; and the third branch is the asymmetrical case, taking only 2eCPs and putting $f=0$.

2.4.1 Extended BCS-Bose crossover

The BCS-Bose crossover extended with hole Cooper pairs contains the familiar BCS-Bose crossover, namely

- 2eCPs gap-like eqn. + number eqn. (**extended** with 2hCPs) specifically $n=2n_B(T)-2m_B(T)+n_f(T)$
- 2hCPs gap-like eqn. + number eqn. (**extended** with 2hCPs)
- Mixed general case of arbitrary proportions: 2eCPs gap-like eqn. + 2hCPs gap-like eqn. + number eqn. (**extended** with 2hCPs)
- Special case: Ideal perfect symmetry: $2n_B(T)=2m_B(T)$ leads to one gap-like eqn. + number eqn. which simplify to $n=n_f(T)$ referring to the total number of *unbound* electrons, giving the usual BCS-Bose crossover picture.

All cases remain as a ternary BF gas.

2.4.2 BCS-Bose (1967) Crossover

From the number equation (2.82), if one takes the perfect ideal 50-50 proportions between 2eCPs and 2hCPs, i.e., $n_0(T)=m_0(T)$ one has

$$n_0(T)=m_0(T)=\Delta^2(T)/4f^2.$$

Adding (2.80) and (2.80) gives

$$\delta\epsilon = \tfrac{1}{2} f^2 \int_{E_f-\delta\epsilon}^{E_f+\delta\epsilon} d\epsilon N(\epsilon) \frac{\tanh\left(\tfrac{1}{2}\beta\sqrt{[\epsilon-\mu(T)]^2+\Delta^2(T)}\right)}{\sqrt{[\epsilon-\mu(T)]^2+\Delta^2(T)}}.$$

Furthermore, $n_{B+}(T) = m_{B+}(T)$ for all T implies from (2.80) and (2.81) that

$$E_+(0) + \varepsilon_K - 2\mu = 2\mu - E_-(0) + \varepsilon_K$$

which in turn implies that

$$E_f = \mu.$$

Thus one arrives at

$$1 = \frac{f^2}{\delta\epsilon} N(0) \int_0^{\delta\varepsilon} d\xi \frac{1}{\sqrt{\xi^2+\Delta^2(T)}} \tanh\left(\tfrac{1}{2}\beta\sqrt{\xi^2+\Delta^2(T)}\right) \tag{2.86}$$

where $\xi = \epsilon - \mu$, which is *precisely* the BCS gap equation (Ref. [41] eq. 3.27) in disguise, for all temperature T and for all coupling, iff one makes the identification

$$\delta\epsilon \equiv \hbar\omega_D \quad \text{and} \quad f^2/2\delta\epsilon \equiv V.$$

This allows to introduce the BCS dimensionless coupling parameter λ, namely

$$\frac{f^2}{\hbar\omega_D} N(0) \equiv V N(0) \equiv \lambda \geqslant 0.$$

Thus, one has

$$1 = \lambda \int_0^{\hbar\omega_D} d\xi \frac{1}{\sqrt{\xi^2+\Delta^2(T)}} \tanh\left(\tfrac{1}{2}\beta\sqrt{\xi^2+\Delta^2(T)}\right) \tag{2.87}$$

which is the more familiar form of the BCS gap equation.

In (2.82) $n_B(T) = m_B(T)$ makes that first two terms cancel implying

$$n_f(T) \equiv \int_0^{\infty} d\epsilon N(\epsilon) \left(1 - \frac{\xi}{\sqrt{\xi^2+\Delta^2(T)}} \tanh\left[\tfrac{1}{2}\beta\sqrt{\xi^2+\Delta^2(T)}\right]\right) = n \equiv \frac{N}{L^d}. \tag{2.88}$$

Note that the two coupled equations (2.87) and (2.88) for $\Delta(T)$ and $\mu(T)$ define the "*BCS-Bose crossover* picture" first introduced by Friedel [36] *et al.* (1967). It was subsequently developed by Eagles [37] (1969); Leggett [38] (1980); Miyake [43] (1983); Nozières [46] (1985); Ranninger, Micnas & Robaszkiewicz [62] (1988); Randeria *et al.* [48] (1989); van der Marel [49] (1990); Bar-Yam [50] (1991); Drechsler & Zwerger [51] (1992); Haussmann [52] (1993); Pistolesi & Strinati [53] (1996) and many others.

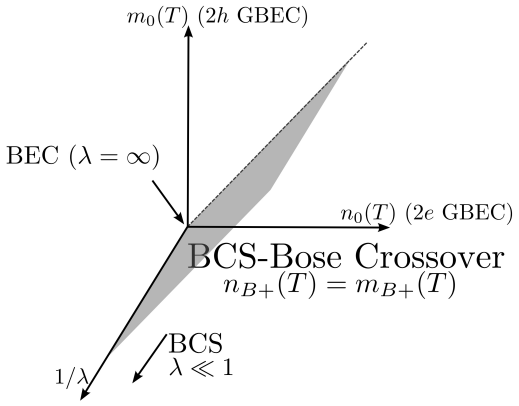

Figure 2.2: Parameter octant defined by the two condensate densities $n_0(T) \geq 0$ and $m_0(T) \geq 0$ as well as the (also non-negative) inverse $1/\lambda \geq 0$ of the interelectronic BCS dimensionless coupling $\lambda \geq 0$, and applicable in principle to all temperature T. GBEC describes a ternary gas and applies in the entire octant. The familiar BCS-Bose crossover theory applies only on the shaded plane defined by $n_0(T) = m_0(T)$ provided the additional restriction$n_{B+}(T) = m_{B+}(T)$ is imposed whereby the total number of 2e (two-electron) noncondensate CPs equals that of 2h (two-hole) CPs. BCS theory is valid *only* along the forefront of the shaded plane where $\lambda \ll 1$ of the shaded BCS-Bose crossover plane since weak coupling then justifies $\mu \simeq E_F$ as assumed by BCS which reduces the number equation to a triviality leaving only the gap equation. This plot was inspired by the celebrated Bronstein cube [135].

2.4.3 BCS (1957) Theory

Ordinary BCS theory is characterized by a single equation, namely, the gap equation for all coupling $\lambda \equiv VN(0)$ and temperature T. The auxiliary (number) equation is replaced by the assumption that $\mu \simeq E_F$. If $\xi \equiv \epsilon - \mu$, and $\hbar\omega_D << \mu$,

$$1 \simeq VN(\mu) \int_0^{\hbar\omega_D} d\xi \frac{1}{\sqrt{\xi^2 + \Delta(T)^2}} \tanh\left[\tfrac{1}{2}\beta\sqrt{\xi^2 + \Delta(T)^2}\right]$$

is BCS gap equation (3.27) in 1957 BCS paper [41].

For *weak coupling* $\Delta \ll E_F$ and $\mu \simeq E_F$ as assumed in ordinary BCS theory, since

$$\begin{aligned} n &= \int_0^\infty d\epsilon N(\epsilon)\left(1 - \frac{\epsilon - \mu}{E(\epsilon)}\tanh\left[\tfrac{1}{2}\beta E(\epsilon)\right]\right) \equiv n_f(T) \\ n_f(T) &\underset{\Delta \to 0}{\longrightarrow} \int_0^\infty d\epsilon N(\epsilon)\left(1 - \tanh\tfrac{1}{2}\beta[\epsilon - \mu]\right) \equiv 2\int_0^\infty d\epsilon N(\epsilon)\left(\exp[\beta(\epsilon - \mu(T))] + 1\right)^{-1} \end{aligned}$$

given that $|x|^{-1}\tanh|x| \equiv x^{-1}\tanh x$ for all $-\infty < x < \infty$ and $1 - \tanh\frac{1}{2}x \equiv 2/(\exp^x + 1)$, and

similarly $\coth\frac{1}{2}(x-1)\equiv 2/(e^x-1)$ so that

$$\begin{aligned} n &= 2\int_0^{\mu(0)} d\epsilon N(\epsilon) = 2\left(\frac{m^{3/2}}{2^{1/2}\pi^2\hbar^3}\right)\int_0^{E_F} d\epsilon\sqrt{\epsilon} = \frac{2\sqrt{2}m^{3/2}E_F^{3/2}}{3\pi^2\hbar^3} \quad \Rightarrow \\ E_F &\equiv \frac{\hbar^2\left(3\pi^2 n\right)^{2/3}}{2m}. \end{aligned}$$

Thus, the BCS gap equation in GBEC can be viewed as the condition for a thermodynamic phase equilibrium between two *pure* BEC phases of 2eCPs and 2hCPs, if coupling is weak. The energy gap equation at $T=0$ readily integrated exactly gives

$$\Delta(0) = \frac{\hbar\omega_D}{\sinh(1/\lambda)} \underset{\lambda\to 0}{\longrightarrow} 2\hbar\omega_D \exp\left(-1/\lambda\right),$$

where dimensionless coupling parameter $\lambda \equiv f^2 N(E_F)/2\hbar\omega_D \equiv VN(E_F)$.

Finally, at $\Delta(T_c)=0$ leads to

$$\frac{1}{\lambda} = \int_0^{\hbar\omega_D/2k_BT_c} dx\,\frac{\tanh x}{x}$$

or the weak-coupling BCS T_c formula

$$k_BT_c \underset{\lambda\to 0}{\longrightarrow} (2e^\gamma/\pi)\hbar\omega_D \exp\left(-1/\lambda\right) \simeq 1.134\hbar\omega_D \exp\left(-1/\lambda\right)$$

if $\Theta_D/2T_c \gg 1$, where $\Theta_D \equiv \hbar\omega_D/k_B$ is the Debye temperature [136]. This implies the gap-to-T_c ratio

$$\frac{2\Delta(0)}{k_BT_c} = 2\pi\exp(-\gamma) \simeq 3.53$$

with the Euler constant $\gamma \simeq 0.5772$.

2.4.4 Friedberg-T.D. Lee (1989) BEC Theory

We take now the third branch of GBEC, the complete asymmetrical case with only 2eCPs, i.e., if one sets $m_B(T)\equiv 0$ and $m_0(T)=0$ implying $f_-(\epsilon)\equiv 0$, therefore (2.81) drops out from the set {(2.80), (2.81), (2.88)}. If one assumes the interaction

$$f_+(\epsilon) = \begin{cases} f & \text{if } \; E_f < \epsilon < E_f + \delta\varepsilon \\ 0 & \text{otherwise} \end{cases}$$

with $E_f = E_+(0)/2$. Then (2.80) becomes

$$4[E_f - \mu] = f^2 \int_{E_f}^{E_f+\delta\varepsilon} d\epsilon \frac{N(\epsilon)}{\sqrt{(\epsilon-\mu)^2 + f^2 n_0}} \tanh\left(\tfrac{1}{2}\beta\sqrt{(\epsilon-\mu)^2 + f^2 n_0}\right) \tag{2.89}$$

Also, (2.88) reduces to $n = 2n_B(T) + n_f(T)$, or

$$\begin{aligned} n &= 2n_0 + 2\int_{0^+}^{\infty} d\varepsilon M(\varepsilon)\left(\exp[\beta(2E_f + \delta\epsilon - 2\mu)] - 1\right)^{-1} \\ &+ \int_0^{\infty} d\epsilon N(\epsilon)\left(1 - \frac{\epsilon-\mu}{E(\epsilon)}\tanh\left[\tfrac{1}{2}\beta E(\epsilon)\right]\right) \end{aligned} \tag{2.90}$$

with

$$E(\epsilon) = \begin{cases} \sqrt{(\epsilon-\mu)^2 + f^2 n_0} & \text{if } E_f < \epsilon < E_f + \delta\varepsilon \\ |\epsilon - \mu| & \text{otherwise.} \end{cases}$$

Eqs. (2.89) and (2.90) are *precisely* (4.3) and (4.4) of Friedberg and Lee (1989) with the following notational changes (GBEC $\Rightarrow$ F-T.D. Lee)

$$E_+(0) \Rightarrow 2\nu_0 \qquad L^3 \Rightarrow \Omega \qquad f \Rightarrow g \qquad n_0 \Rightarrow |B|^2 \qquad n \Rightarrow \rho.$$

2.4.5 Ideal BF Model of Casas *et al.* (1998-2002)

The ideal BF model of Casas *et al*. [70, 130, 137] is a simple statistical model treating CPs as non-interacting bosons in thermal and chemical equilibrium with unbound fermions. In this model appears a boson number which is strongly coupling and temperature-dependent. This model naturally suggest a more convenient definition of the boson chemical potential whereby the generate Fermi region of positive fermion chemical potential can be accessed unlike previous treatments. The authors provide support for a widespread conjecture (or 'paradigm') that superconductivity in general is a Bose-Einstein condensation of charged Cooper pairs.

For *noninteracting* or ideal BF model (IBFM), i.e., for $f = 0$, $E(\epsilon) = |\epsilon - \mu|$ and (2.89) implies $E_f = \mu$; so $E_+(K) - 2\mu = 2(E_f - \mu) + \varepsilon \ = \varepsilon$ and hence only (2.88) is left with $\Delta = 0$, namely

$$n = 2\,n_0 + 2\int_{0^+}^{\infty} d\varepsilon M(\varepsilon)\left(\exp[\beta\varepsilon] - 1\right)^{-1} + 2\int_0^{\infty} d\epsilon N(\epsilon)\left(\exp[\beta(\epsilon - E_f)] + 1\right)^{-1}$$

or more briefly

$$n = 2n_B(T) + n_f(T).$$

Not that in 2D

$$\begin{aligned} n_f(T) \underset{f\to 0}{\longrightarrow} n_f(T) &\equiv 2\left(\frac{m}{2\pi\hbar^2}\right)\int_0^\infty d\epsilon\,(\exp[\beta(\epsilon - E_f)] + 1)^{-1} \\ &= \left(\frac{m}{\pi\hbar^2}\right)\left(E_f + \beta^{-1}\ln\{1+\exp[-\beta E_f]\}\right) \\ &\equiv n_f\left(1 + \left(\frac{T}{T_f}\right)\ln\{1+\exp[-T_f/T]\}\right) \geqslant n_f \end{aligned}$$

exactly, where $n_f \equiv mE_f/\pi\hbar^2$. Clearly, this model might be useful in locating the superconducting singularity in temperature T_c as the system is cooled down, but it cannot describe the superconducting phase as such since the gap is zero.

2.4.6 Original BEC Theory (1925)

Critical temperature T_c —defined as that value of T below which $n_0(T)$ *just ceases to be zero* as the system is cooled and obtained by putting $n_0(T_c) = 0$, or

$$\begin{aligned} 2n_B(T_c) &\equiv 0 + 2\int_{0^+}^\infty d\varepsilon M(\varepsilon)\,(\exp[\beta_c\varepsilon] - 1)^{-1} \\ &= n - 2\int_0^\infty d\epsilon N(\epsilon)\,(\exp[\beta_c(\epsilon - E_f)] + 1)^{-1} \equiv n - n_f(T_c) \end{aligned}$$

with $\beta_c \equiv 1/k_B T_c$ and $n_f(T_c)$ is the *number density of unbound electrons* in the IBFM at T_c. If $M(\varepsilon) \equiv (2m^{3/2}/\pi^2\hbar^3)\sqrt{\varepsilon}$, we get

$$\int_0^\infty dx \frac{\sqrt{x}}{e^x - 1} = \Gamma(3/2)\zeta(3/2)$$

then

$$\begin{aligned} T_c &\simeq \left(\frac{2\pi}{(2.612)^{2/3}}\right)\left(\frac{\hbar^2}{2mk_B}\right)\left(\frac{n - n_f(T_c)}{2}\right)^{2/3} \equiv \left(\frac{2\pi}{(2.612)^{2/3}}\right)\left(\frac{\hbar^2}{2mk_B}\right) n_B(T_c)^{2/3} \\ &\simeq 3.31\left(\frac{\hbar^2}{2mk_B}\right) n_B(T_c)^{2/3}. \end{aligned}$$

Since there are still a very tiny fraction of unbound electrons in the BF gas the expression here is an *implicit* formula for the ideal boson gas (IBG) with boson particle density $n_B(T_c) \equiv \frac{1}{2}[n - n_f(T_c)]$; otherwise, it is precisely the same *form* as the ordinary BEC T_c-formula. Note that

$$n_f(T) \simeq n_f\left(1 + \frac{T}{T_f}\exp[-T/T_f] + \cdots\right) \geq n_f$$

This can also be thought of as an *extreme strong-coupling* regime whereby $n_f(T)$ vanishes, so that $n_B(T_c) = n/2$ and one recovers the familiar limit

$$\frac{T_c}{T_F} \simeq 0.218.$$

In Fig.2.3 depicts how the GBEC theory subsumes the five statistical theories of superconductivity. Also is subsumed the BCS-Bose crossover extended with hole Cooper pairs. The flowchart can be summarized as follows: one branch with an asymmetric case if one takes 2eCPs only, leads to Friedberg & T.D. Lee BEC model and taking $f = 0$ (null interactions) leads to the well-known BEC theory of 1925; a second branch with perfect ideal symmetry between 2eCPs and 2hCPs leads to the familiar BCS-Bose crossover picture with a gap equation and the number equation, if one takes precisely $f = \sqrt{2\hbar\omega_D V}$ and putting $\mu = E_F$ one recovers the BCS theory; a third branch with arbitrary proportions between 2eCPs and 2hCPs leads to the extended BCS-Bose crossover with one gap-like equation for 2eCPs and another one for 2hCPs and the number equation, assuming of course that $\mu \neq E_F$.

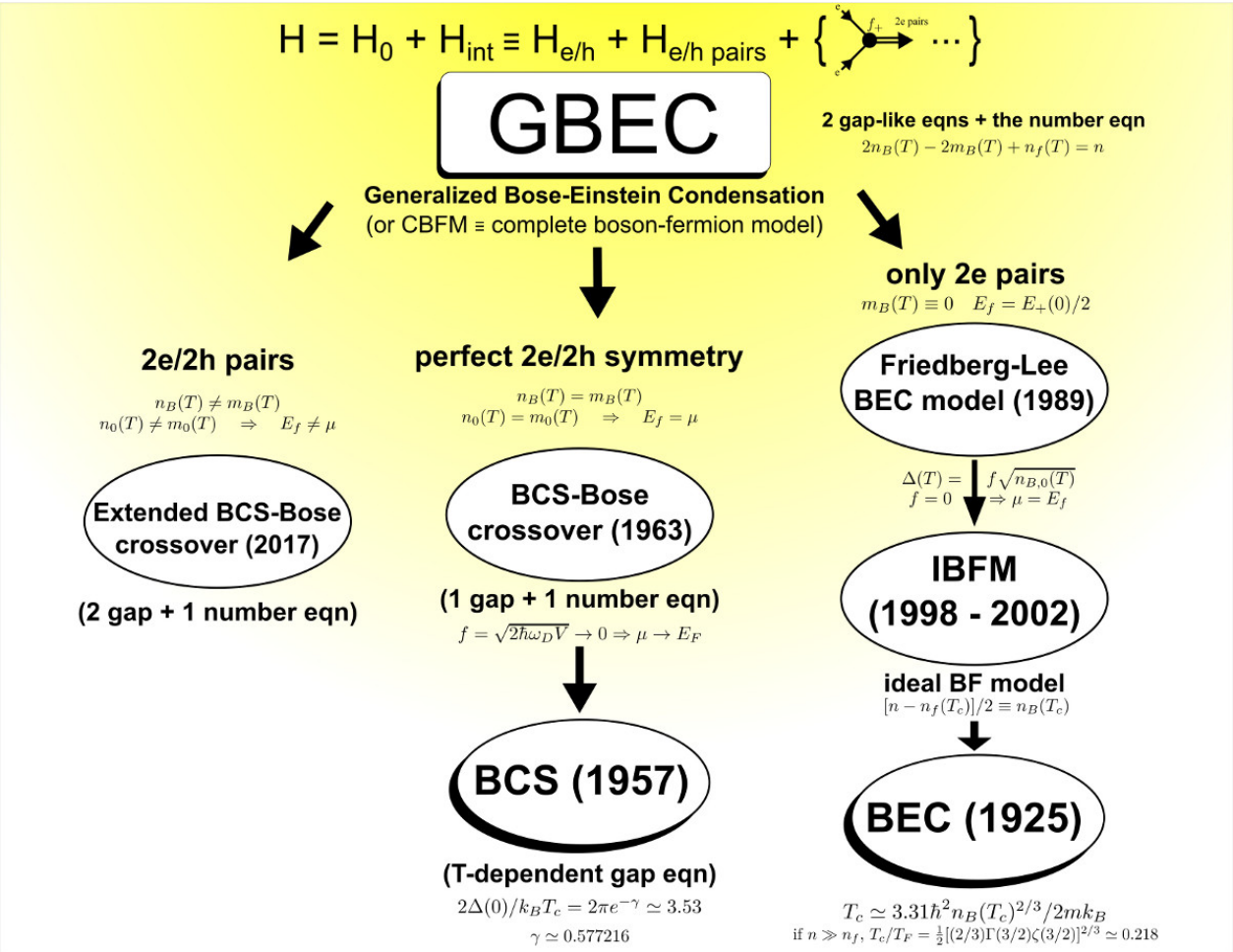

Figure 2.3: Flowchart illustrating conditions under which the GBEC formalism reduces to, or subsumes, all five statistical theories of superconductivity (ovals). Three branches each one assuming different conditions: asymmetric case, taking only 2eCPs, this lead to the BEC theory of 1925. Here ideal boson-fermion model (IBFM) is the *binary* case of GBEC corresponding to the unperturbed Hamiltonian (2.11) only. Here $\zeta(3/2) \simeq 2.612$ is the Zeta function of order 3/2; a perfect ideal symmetry between 2eCPs and 2hCPs leads to familiar BCS-Bose crossover with the gap and number equations, if one putting $\mu = E_F$ and assuming $f = \sqrt{2\hbar\omega_D V}$ one recovers the BCS theory; the arbitrary proportions between 2eCPs and 2hCPs which leads to the extended BCS-Bose crossover with three equations instead of two, a gap-like equation for 2eCPs another one for 2hCPs and the number equation.

Chapter 3

GBEC Dimensionless Number Density

In this chapter the thermodynamic properties of the GBEC will be presented such as the critical temperature and energy gap. Also, it will be introduce a new dimensionless coupling constant, the dimensionless number density n/n_f. This quantity emerges as a ratio between the total number of particles n with that of unbound electrons at zero temperature $n_f(T=0) \equiv n_f$. The dimensionless number density will play the role as a dimensionless coupling constant, since the weak coupling regime occurs at $n/n_f = 1$ while the strong coupling regime is on $n/n_f \to \infty$ and of course the intermediate (crosssover) regime when $1 < n/n_f < \infty$.

3.1 Phase Diagram

To construct the phase diagram of GBEC theory one must solve simultaneously the gap-like equations (2.80) and (2.81) plus number equation (2.88). Thus, made dimensionless with the number density of unbound electrons at zero temperature $n_f(T=0) \equiv n_f$, (2.88) gives

$$\begin{aligned}
\frac{n}{n_f} &= \frac{2n_0(T)}{n_f} - \frac{2m_0(T)}{n_f} \\
&+ \frac{3}{4}\left(\frac{n}{n_f}\right)\int_0^\infty d\tilde{\epsilon}\,\sqrt{\tilde{\epsilon}}\left[1 - \frac{\tilde{\epsilon}-\tilde{\mu}}{\sqrt{(\tilde{\epsilon}-\tilde{\mu})^2+\tilde{\Delta}^2}}\tanh\left(\frac{\sqrt{(\tilde{\epsilon}-\tilde{\mu})^2+\tilde{\Delta}^2}}{2\tilde{T}}\right)\right] \\
&+ \frac{6}{2^{3/2}}\left(\frac{n}{n_f}\right)\int_0^\infty d\tilde{\varepsilon}\,\left[\frac{\sqrt{\tilde{\varepsilon}}}{\exp\left(\frac{\tilde{\varepsilon}+2(n/n_f)^{-2/3}+\delta\tilde{\epsilon}-2\tilde{\mu}}{\tilde{T}}\right)-1}\right] \\
&- \frac{6}{2^{3/2}}\left(\frac{n}{n_f}\right)\int_0^\infty d\tilde{\varepsilon}\,\left[\frac{\sqrt{\tilde{\varepsilon}}}{\exp\left(\frac{\tilde{\varepsilon}-2(n/n_f)^{-2/3}+\delta\tilde{\epsilon}+2\tilde{\mu}}{\tilde{T}}\right)-1}\right]
\end{aligned} \tag{3.1}$$

where tilde means dimensionless with respect to Fermi energy and the useful relation $n/n_f = (E_F/E_f)^{3/2}$. Rewriting the first two terms as

$$\frac{2n_0(T)}{n_f} = \frac{3}{8}\frac{\tilde{\Delta}_n^2}{\tilde{G}}\left(\frac{n}{n_f}\right) \qquad \text{and} \qquad \frac{2m_0(T)}{n_f} = \frac{3}{8}\frac{\tilde{\Delta}_m^2}{\tilde{G}}\left(\frac{n}{n_f}\right) \tag{3.2}$$

where $\tilde{\Delta}_n = f\sqrt{n_0(T)}/E_F$ and $\tilde{\Delta}_m = f\sqrt{m_0(T)}/E_F$ are the energy gap of 2eCPs and 2hCPs, respectively, the number equation becomes

$$\begin{aligned} 1 &= \frac{3}{8}\frac{\tilde{\Delta}_n^2}{\tilde{G}} - \frac{3}{8}\frac{\tilde{\Delta}_m^2}{\tilde{G}} \\ &+ \frac{3}{4}\int_0^\infty d\tilde{\epsilon}\,\sqrt{\tilde{\epsilon}}\left[1 - \frac{\tilde{\epsilon}-\tilde{\mu}}{\sqrt{(\tilde{\epsilon}-\tilde{\mu})^2+\tilde{\Delta}^2}}\tanh\left(\frac{\sqrt{(\tilde{\epsilon}-\tilde{\mu})^2+\tilde{\Delta}^2}}{2\tilde{T}}\right)\right] \\ &+ \frac{6}{2^{3/2}}\int_0^\infty d\tilde{\varepsilon}\,\sqrt{\tilde{\varepsilon}}\left[\exp\left(\frac{\tilde{\varepsilon}+2(n/n_f)^{-2/3}+\delta\tilde{\epsilon}-2\tilde{\mu}}{\tilde{T}}\right)-1\right]^{-1} \\ &- \frac{6}{2^{3/2}}\int_0^\infty d\tilde{\varepsilon}\,\sqrt{\tilde{\varepsilon}}\left[\exp\left(\frac{\tilde{\varepsilon}-2(n/n_f)^{-2/3}+\delta\tilde{\epsilon}+2\tilde{\mu}}{\tilde{T}}\right)-1\right]^{-1} \end{aligned} \tag{3.3}$$

where the last two terms are the excited bosons 2eCPs, 2hCPs, i.e., $2n_{B+}(T)$ and $2m_{B+}(T)$ respectively. Clearly follows a BE statistics.

Then, dimensionless wrt Fermi energy, the gap-like equation for 2eCPs becomes

$$(n/n_f)^{-2/3} + \frac{\delta\tilde{\epsilon}}{2} - \tilde{\mu} = \tilde{G}\int_{(n/n_f)^{-2/3}}^{(n/n_f)^{-2/3}+\delta\tilde{\epsilon}} d\tilde{\epsilon}\,\frac{\sqrt{\tilde{\epsilon}}}{\sqrt{(\tilde{\epsilon}-\tilde{\mu})^2+\tilde{\Delta}_n^2}}\tanh\left(\frac{\sqrt{(\tilde{\epsilon}-\tilde{\mu})^2+\tilde{\Delta}_n^2}}{2\tilde{T}}\right) \tag{3.4}$$

analogously for 2hCPs

$$-(n/n_f)^{-2/3} + \frac{\delta\tilde{\epsilon}}{2} + \tilde{\mu} = \tilde{G}\int_{(n/n_f)^{-2/3}-\delta\tilde{\epsilon}}^{(n/n_f)^{-2/3}} d\tilde{\epsilon}\,\frac{\sqrt{\tilde{\epsilon}}}{\sqrt{(\tilde{\epsilon}-\tilde{\mu})^2+\tilde{\Delta}_m^2}}\tanh\left(\frac{\sqrt{(\tilde{\epsilon}-\tilde{\mu})^2+\tilde{\Delta}_m^2}}{2\tilde{T}}\right). \tag{3.5}$$

The expressions (3.3), (3.4) and (3.5) are the equations of the BCS-Bose crossover *extended* with hole Cooper pairs [138]. Thus, one must be able to solve this system to find out the solutions to the chemical potential μ and to the energy gap Δ at any temperature T. In the extended crossover, one has the following cases:

i) 100-0 (2eCPs only) case, i.e., solving the number equation (3.3) and the gap-like equation (3.4),

ii) 0-100 (2hCPs only) case, i.e, solving the number equation (3.3) and the gap-like equation (3.5) and

iii) 50-50 case, the ideal perfect symmetry between 2eCPs and 2hCPs, namely, $n_0(T) = m_0(T)$ and $n_{B+}(T) = m_{B+}(T)$.

In Fig.3.1 is plotted the solutions of the chemical potential dimensionless with Fermi energy $\mu(T)/E_F$, (a) at $T = 0$ and (b) for $T = T_c$. Each above case must be solved simultaneously with the set of equations {(3.3), (3.4), (3.5)}. In Fig. 3.1a, at $T = 0$ and $n/n_f = 1$, i.e., all particles are unbound (or correlated as BCS theory), the chemical potential is the Fermi energy, just as BCS theory supposed. Thus, one has recovered the weak-coupling extreme. On the other hand, the chemical potential tends to zero when $n/n_f \to \infty$, e.g., $n_f \to 0$ no unbound electron remains in the system, all electrons are paired and one has an ideal Bose gas composed by 2eCPs, this is the strong coupling extreme. Here was used $\delta\tilde{\epsilon} = 10^{-3}$ and $\tilde{G} = 10^{-4}$.

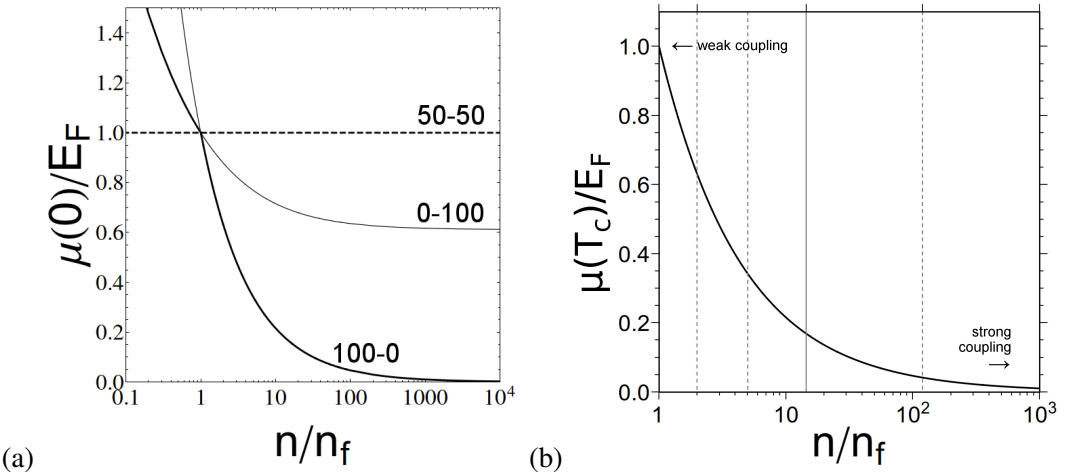

Figure 3.1: Chemical potential *vs.* dimensionless number density n/n_f. (a) $T = 0$, dashed curve is for 50-50 proportions, thick curve for 100-0 (2eCPs only) and thin curve for 0-100 (2hCPs only), all curves crossing at $n/n_f = 1$ which is precisely $\mu(0)/E_F = 1$ just as BCS theory supposed. (b) $T = T_c$ the curve is the same for three cases. Note that at zero temperature the 100-0 case behaves as an ideal Bose gas since $\mu(0)/E_F \to 0$ as $n/n_f \to \infty$, e.g., $n_f \to$ no unbound electrons remain in the system. Three cases has the same behavior at $T = T_c$. Here was used $\delta\tilde{\epsilon} = 10^{-3}$ and $\tilde{G} = 10^{-4}$.

The solution for the energy gap at zero temperature dimensionless with Fermi energy $\Delta(T = 0)/E_F$ *vs.* n/n_f is shown in Fig.3.2. For 100-0 case, when $n/n_f = 1$ the energy gap has the value $\Delta(0)/E_F = 9.11 \times 10^{-6}$, which is near to experimental data (later it will be shown), when $n/n_f \to \infty$ the energy gap tends to $\Delta(0)/E_F \to 0.016$ this increase of the energy gap is in accordance with the crossover picture. At weak coupling regime, i.e, near $n/n_f = 1$ the energy gap is near to experimental data for some elemental superconductors. The 50-50 proportions coincides precisely with experiment instead of the 100-0 proportions, this suggest that 2hCPs play an important role in superconductivity as will show later. On the other hand, when $n/n_f \to \infty$, the energy gap increases for 100-0 case only, the other cases will be analyzed after. Thus, two extremes emerge from analyzing the chemical potential and energy gap: i) the weak coupling regime at precisely $n/n_f = 1$; ii) the strong coupling extreme when $n/n_f \to \infty$ and of course the intermediate

(crossover) $1 < n/n_f < \infty$. Therefore, if one changes n/n_f, the chemical potential and the energy gap changes.

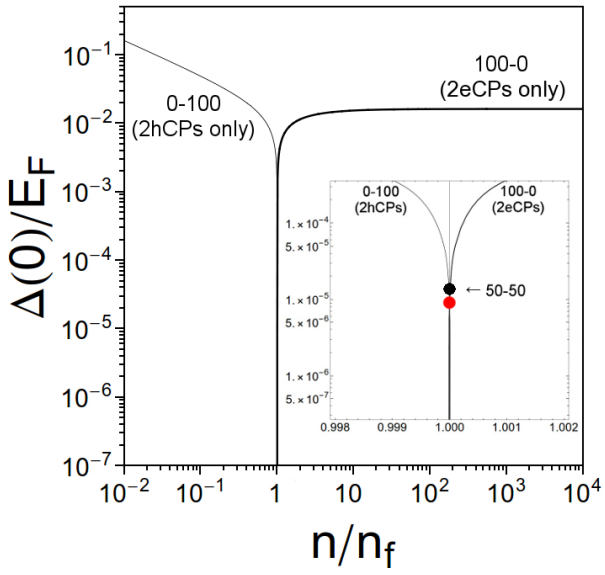

Figure 3.2: Energy gap at zero temperature dimensionless with Fermi energy $\Delta(0)/E_F$ *vs.* n/n_f. For the 100-0 (thick curve) case when $n/n_f \to \infty$ one has $\Delta(0)/E_F \to 0.016$, all electrons are paired, i.e., no unbound electrons remain in the system, while for 0-100 (thin curve) case when $n/n_f \to 0$ one has $\Delta(0)/E_F \to +\infty$, this result it will be discuss later. Inset shows the behavior of three cases near $n/n_f = 1$, the energy gap for the perfect ideal symmetry (black dot) appears only in $n/n_f = 1$, red dot marks the cross between the 100-0 and the 0-100 cases at $\Delta(0)/E_F = 9.11 \times 10^{-6}$, while for 50-50 case is $\Delta(0)/E_F = 1.13 \times 10^{-5}$. Here was used $\delta\tilde{\epsilon} = 10^{-3}$ and $\tilde{G} = 10^{-4}$.

In GBEC there is a dimensionless "strength" [81, 82] parameter $G \equiv f^2 m^{3/2}/2^{5/2}\pi^2\hbar^3 E_f^{1/2}$ which in turn can be related with the dimensionless number density n/n_f, this is illustrated in Fig. 3.3. Furthermore, G and n/n_f can be related with λ_{BCS} the dimensionless coupling constant of BCS theory. In Fig. 3.3 is plotted the λ_{BCS} via the BCS weak-coupling formula $k_B T_c \simeq 1.134\,\hbar\omega_D \exp(-1/\lambda_{BCS})$ and the 50-50 proportions curve of the extended crossover, namely, if one summing (3.4) plus (3.5) gives

$$1 = \frac{2\tilde{G}}{\delta\tilde{\epsilon}} \int_{(n/n_f)^{-2/3}-\delta\tilde{\epsilon}}^{(n/n_f)^{-2/3}+\delta\tilde{\epsilon}} d\tilde{\epsilon}\, \frac{\sqrt{\tilde{\epsilon}}}{\sqrt{(\tilde{\epsilon}-\tilde{\mu})^2 + \tilde{\Delta}^2}} \tanh\left(\frac{\sqrt{(\tilde{\epsilon}-\tilde{\mu})^2 + \tilde{\Delta}^2}}{2\tilde{T}}\right) \tag{3.6}$$

and the number equation is

$$1 \;=\; \frac{3}{4}\int_0^{\infty} d\tilde{\epsilon}\, \sqrt{\tilde{\epsilon}} \left[1 - \frac{\tilde{\epsilon}-\tilde{\mu}}{\sqrt{(\tilde{\epsilon}-\tilde{\mu})^2 + \tilde{\Delta}^2}} \tanh\left(\frac{\sqrt{(\tilde{\epsilon}-\tilde{\mu})^2 + \tilde{\Delta}^2}}{2\tilde{T}}\right)\right] \tag{3.7}$$

here $\tilde{\Delta} = (f_+\sqrt{n_0} + f_-\sqrt{m_0})/E_F$. Also, is plotted the special case 100-0 (2eCPs only) with a slight

change in the dimensionless number density $n/n_f = 1.0001$ and $n/n_f = 0.9999$. Here, the 50-50 curve and BCS exact curve, eq. (3.27) from [41] coincide, while the BCS weak-coupling formula only coincides at relatively low critical temperatures and $\lambda \ll 1$. Remarkably the 100-0 (2eCPs only) with a slight change in the dimensionless number density as $n/n_f = 1.0001$ increases the critical temperature with respect to the BCS exact solution, even for the same value of λ_{BCS}. This suggests that changing the dimensionless number density can increase the T_cs.

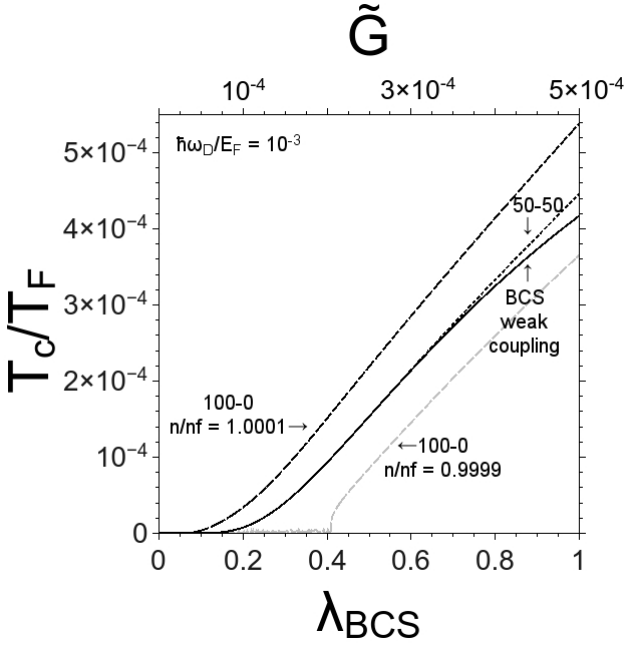

Figure 3.3: T_c/T_F *vs.* λ_{BCS} compared with $\tilde{G}$ the dimensionless strength parameter of GBEC. The solid curve is the BCS weak-coupling formula $k_B T_c \simeq 1.134\,\hbar\omega_D \exp(-1/\lambda_{BCS})$, short-dashed curve is the exact BCS formula which coincides precisely with the 50-50 curve of the extended crossover with $n/n_f = 1$, dashed curve is the 100-0 (2eCPs only) curve with $n/n_f = 1.0001$ and the gray-dashed curve is for 100-0 case with $n/n_f = 0.9999$. BCS weak-coupling curve coincides with 50-50 curve only at relatively low critical temperatures. Note that changing the dimensionless number density increase the critical temperature, even for same coupling. This suggests that changing the dimensionless number density can increase the T_cs. Here were used $\hbar\omega_D/E_F = 10^{-3}$.

In §2.4.3 one recovers the gap equation of BCS theory from the 50-50 symmetry, if one takes (3.6) one has the following correlation between $G^{\ddagger}$ and λ_{BCS} via the dimensionless number density n/n_f given by

$$\lambda_{BCS} = 2G\left(\frac{E_F}{\hbar\omega_D}\right)(n/n_f)^{1/3} \tag{3.8}$$

where $G \equiv (f^2 m^{3/2})/(2^{5/2}\pi^3\hbar^3 E_f^{1/2})$, with f the BF vertex function interaction, thus G is the original dimensionless strength parameter in GBEC [81, 82].

[‡]The GBEC original strength parameter G is related with the dimensionless number density n/n_f, and made dimensionless with Fermi energy E_F instead of E_f implies that $G = \tilde{G}(n/n_f)^{-1/3}$

Thus, to compare the BCS coupling constant with the dimensionless number density n/n_f in Fig. 3.4 is plotted λ_{BCS} *vs.* n/n_f, here was used $\hbar\omega_D/E_F = 10^{-3}$ since λ_{BCS} is related with $\tilde{G}$ in (3.8). For $\lambda_{BCS} = 1/5$ one sees that $n/n_f = 1$, e.g., *all* electrons are unbound or correlated as in BCS theory. Hypothetically, if $\lambda_{BCS} \to \infty$, $n/n_f \to \infty$, e.g., $n_f \to 0$ which means that no unbound electrons remain in the system implying that one has an ideal Bose gas composed of 2eCPs only (strong coupling).

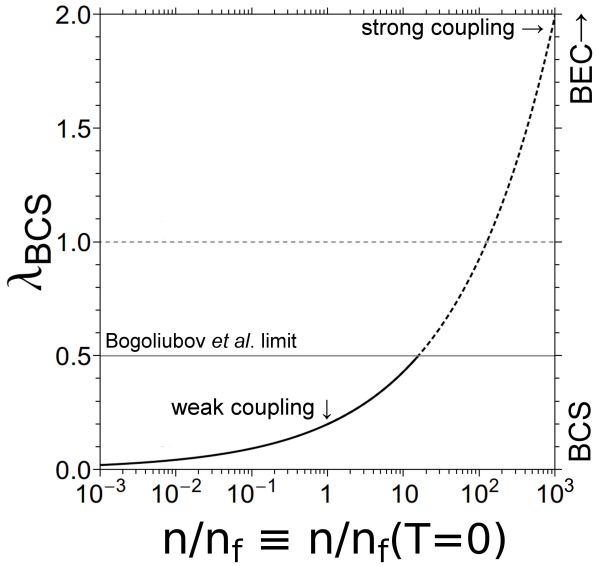

Figure 3.4: λ_{BCS} *vs.* n/n_f here plotted (3.8) with $\hbar\omega_D/E_F = 10^{-3}$. In the weak-coupling extreme, i.e., $n/n_f = 1$, all electrons are unbound, while in the strong-coupling extreme $n/n_f \to \infty$ one has an ideal Bose gas made up of 2eCPs. Note that to relatively higher dimensionless number density one has a higher λ_{BCS}. The Bogoliubov *et al.* limit is shown for comparison purposes.

To contruct the extended crossover phase diagram of T_c/T_F *vs.* n/n_f we must solve each case cited above with the set {(3.3), (3.4)} for 100-0 proportions, {(3.3), (3.5)} for 0-100 proportions and {(3.3), (3.4), (3.5)} for 50-50 proportions. This is shown in Fig.3.5 [139]. One should note that the critical temperature for all cases increases with respect to the BEC curve, which in turn represents that all particles are bounded as Cooper pairs in the well known limit $T_c/T_F \simeq 0.218$. Then, each case has a T_c's limit when all particles are bounded as CPs since no unbound particles remain. When $n/n_f \to \infty$ those limits are: for 100-0 (2eCPs only) $T_c/T_F \to 0.701$; for 0-100 (2hCPs only) $T_c/T_F \to 1.507$; and for 50-50 is $T_c/T_F \to 0.988$.

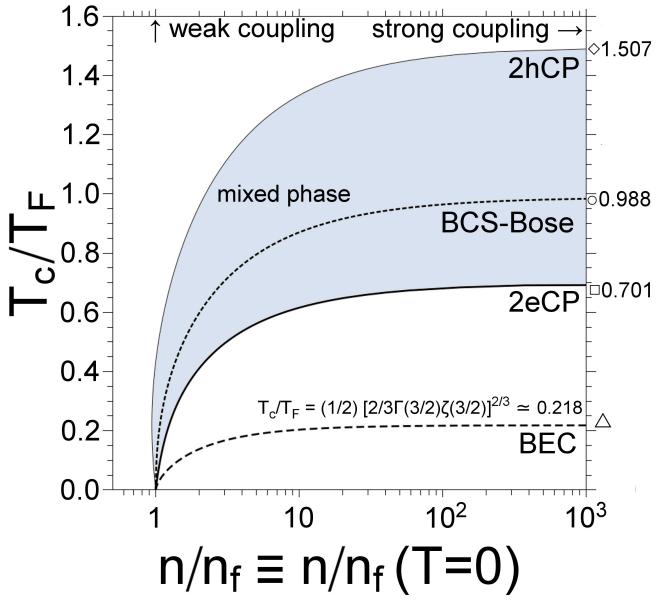

Figure 3.5: Extended BCS-Bose Crossover diagram T_c/T_F *vs.* n/n_f for each case cited in text. Thick curve labeled 2eCP is the 100-0 proportions solving (3.4) with (3.3). Thin curve labeled 2hCP is the 0-100 proportions which corresponds to (3.5) with (3.3), between those curves lies the mixed phase (blue-online shaded area) with arbitrary proportions between 2eCP and 2hCP. And as a special case the ideal perfect 50-50 symmetry corresponds to the dotted curve. Also presented here is the BEC curve (dashed curve) for comparison purposes only. Symbols at right corresponds to the limit of T_c/T_F for each phase when $n/n_f \to \infty$, or e.g., $n_f \to 0$ where no unbound electron remain in the system since all are bounded as Cooper pairs, for 2eCPs ($\square$) one has $T_c/T_F \to 0.701$ for 50-50 ($\circ$) one has $T_c/T_F \to 0.988$, for 2hCPs ($\diamond$) one has $T_c/T_F \to 1.507$ and finally for BEC curve ($\triangle$) is $T_c/T_F \to 0.218$. The weak coupling extreme is at $n/n_f = 1$ when all electrons are unbound (or correlated as in BCS theory) and the strong coupling extreme is $n/n_f \to \infty$. Figure taken from [139].

3.2 On the dimensionless number density n/n_f

So far we have investigating the behavior of the dimensionless number density which is the ratio between the total electron number density n and that of number density of unbound electrons at zero temperature $n_f \equiv n_f(T=0)$. Therefore, the dimensionless number density (3.3) is simply

$$n/n_f = \left[2n_0(T) + 2n_{B+}(T) - 2m_0(T) - 2m_{B+}(T) + n_f(T)\right]/n_f \tag{3.9}$$

Let's analyze the following cases for any T: a) $n/n_f = 1$; b) $n/n_f > 1$; c) $n/n_f < 1$ and d) $n/n_f \to \infty$. From (a) it is implied that

$$\begin{aligned} 1 &= n/n_f = \left[2n_B(T) - 2m_B(T) + n_f(T)\right]/n_f \qquad \Rightarrow \\ 2m_B(T)/n_f &= \left[2n_B(T) + n_f(T)\right]/n_f \end{aligned} \tag{3.10}$$

namely, $2m_0(T)$ along with $2m_{B+}(T)$, condensed and excited, respectively, are equals in number to 2eCPs

$2n_0(T)$ together with $2n_{B+}(T)$ condensed and excited, respectively, plus the unbound electrons $n_f(T)$. In other words, the difference between 2hCPs and 2eCPS are equal to the unbound electrons at any T. Iff $2n_0(T) = 2m_0(T)$ and $2n_{B+}(T) = 2m_{B+}(T)$ the total electron number density coincides precisely with that of unbound electrons at any T, this leads to the *weak coupling extreme*.

From (b) one has

$$\begin{aligned} 1 &< n/n_f = \left[2n_B(T) - 2m_B(T) + n_f(T)\right]/n_f \qquad \Rightarrow \\ 2m_B(T)/n_f &< \left[2n_B(T) + n_f(T)\right]/n_f \end{aligned} \tag{3.11}$$

implying that 2hCPs are less than 2eCPs alongside with the unbound electrons, i.e., in the region $n/n_f > 1$ 2eCPs predominates over 2hCPs.

From (c) one has

$$\begin{aligned} 1 &> n/n_f = \left[2n_B(T) - 2m_B(T) + n_f(T)\right]/n_f \qquad \Rightarrow \\ 2m_B(T)/n_f &> \left[2n_B(T) + n_f(T)\right]/n_f \end{aligned} \tag{3.12}$$

this implies that 2hCPs are greater than 2eCPs plus unbound electrons, i.e., in this region 2hCPs predominates over 2eCPs.

From (d) $n/n_f \to \infty$, e.g., $n_f \to 0$ which means that no unbound electrons remain in the system, all electrons are paired into CPs leaving an ideal Bose gas, this is the so-called *strong coupling regime*.

Later in this chapter, will be discuss the contribution of each kind of particle either 2eCPs or 2hCPs. Since in this survey will be theoretically predicted a Bose-Einstein condensate of 2hCPs, this may have nonphysical sense. Nevertheless, in a recent paper [140] appears the negative (effective) mass of a Bose-Einstein condensate, in this paper the single-band model reproduces the experiment, although it is applied to a spin-orbit coupled (SOC) system.

Boson-fermion interaction function

The BF interaction functions $f_{\pm}(\epsilon)$ in (2.73) and (2.74) are defined as constant [81, 82] over a specific interaction range. Implying that dimensionless strength parameter G [81, 82] is related with the BF function interaction as $G \equiv f^2 m^{3/2}/2^{5/2}\pi^2\hbar^3 E_f^{1/2}$. If one made dimensionless (2.73) with Fermi energy instead of E_f gives

$$f_+(\tilde{\epsilon}) = \begin{cases} f & \text{if} \quad E_f/E_F < \tilde{\epsilon} < E_f/E_F + \delta\tilde{\epsilon} \\ 0 & \text{otherwise} \end{cases}.$$

where tildes means dimensionless with respect to E_F. Or, equivalently

$$f_+(\tilde{\epsilon}) = \begin{cases} f & \text{if} \quad (n/n_f)^{-2/3} < \tilde{\epsilon} < (n/n_f)^{-2/3} + \delta\tilde{\epsilon} \\ 0 & \text{otherwise} \end{cases}. \tag{3.13}$$

and likewise to (2.74) one gets

$$f_{-}(\tilde{\epsilon}) = \begin{cases} f & \text{if} \quad (n/n_f)^{-2/3} - \delta\tilde{\epsilon} < \tilde{\epsilon} < (n/n_f)^{-2/3} \\ 0 & \text{otherwise} \end{cases} . \tag{3.14}$$

Then, the interaction function $f(\tilde{\epsilon})$ is now defined by a dimensionless interaction range given by the dimensionless number density with the dimensionless interaction range energy $\delta\tilde{\epsilon}$. Therefore, the interaction range is defined as $(n/n_f)^{-2/3} \pm \delta\tilde{\epsilon}$.

Fig. 3.6a shows the interaction $f_{\pm}(\tilde{\epsilon})$ for a fixed value $\delta\tilde{\epsilon} = 10^{-3}$. When $n/n_f = 1$, $\delta\tilde{\epsilon}$ is negligible in the two inequalities above. However, as n/n_f increases, $\delta\tilde{\epsilon}$ becomes more significant. But he main feature here is that the interaction f decreases as n/n_f increases. Thus, one has that $f \to 0$ as $n/n_f \to \infty$. This is agree with the assertion in Ref. [81], eq. (22), for a noninteracting BF gas.

Fig. 3.6b shows the interaction range of $f_{\pm}(\tilde{\epsilon})$ between $-10^{-3} < \delta\tilde{\epsilon} < 10^{-3}$. Approximately has the same behavior if the dimensionless interaction range energy was fixed. This figure exhibits the electron/two-electron CP vertex interaction $f_{+}(\tilde{\epsilon})$ (blue-online shaded sheet) as well as $f_{-}(\tilde{\epsilon})$ for the hole/two-hole CPs vertex interaction (yellow-online shaded sheet). On can observes when $\delta\tilde{\epsilon} \to 0$ one has a symmetric interaction between electrons and holes. Nevertheless, both kinds of interactions tend to zero as n/n_f increases.

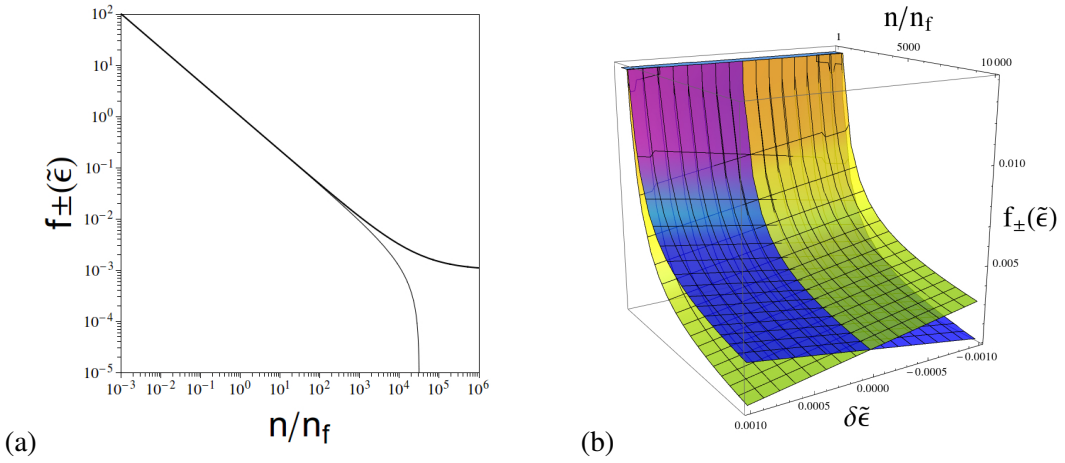

Figure 3.6: Illustrates the limits on the BF interaction $f_{\pm}(\tilde{\epsilon})$ *vs.* dimensionless number density n/n_f. (a) Shows the two kinds of interactions: thick curve for $(n/n_f)^{-2/3} + \delta\tilde{\epsilon}$ and thin curve for $(n/n_f)^{-2/3} - \delta\tilde{\epsilon}$. Here was used $\delta\tilde{\epsilon} = 10^{-3}$. Note that $f \to 0$ as $n/n_f \to \infty$, e.g., $n_f \to 0$ meaning no unbound electrons remain in the system, thus leaves an ideal Bose gas of 2eCPs as assumed in Ref. [81]. (b) Shows the BF interactions $f_{\pm}(\tilde{\epsilon})$ bounded by $(n/n_f)^{-2/3} \pm \delta\tilde{\epsilon}$. The color sheets represents both kinds of interaction in the range $-0.001 < \delta\tilde{\epsilon} < 0.001$. The blue-online shaded sheet corresponds to the e-2eCP vertex interaction $f_{+}(\tilde{\epsilon})$ while the yellow-online shaded one corresponds to h-2hCP vertex interaction $f_{-}(\tilde{\epsilon})$, both types of interaction have the same behavior, namely $f \to 0$ as $n/n_f \to \infty$. Hence, the strong-coupling regime is recovered.

At the precise value $n/n_f = 1$ one recovers the more familiar interaction limits

$$f(\tilde{\epsilon}) = \begin{cases} f & \text{if} \quad -\delta\tilde{\epsilon} < \tilde{\epsilon} < \delta\tilde{\epsilon} \\ 0 & \text{otherwise} \end{cases}$$

and make perfect contact with BCS theory if one puts $\delta\epsilon = \hbar\omega_D$ the Debye energy of the ionic lattice.

On the other hand, if one takes the limit $n/n_f \to \infty$ (BEC limit), or $n_f \to 0$ which implies no unbound electrons remaining in the system, then $f \to 0$ and one recovers the strong-coupling limit. Thus, $f_{\pm}(\tilde{\epsilon})$ is the interaction function spanning a coupling range which in turn is related with n/n_f the *new* dimensionless coupling constant of the extended BCS-Bose crossover [138] subsumed in the GBEC theory.

"*The phase transition is driven by the particle statistics and not their interactions*" [99]. Although one can initiate with a weak (phonon-electron) interaction system, the resulting Cooper pairs may suffer a phase transition not for a strong interaction but by its statistics. Here one can observes, when $n/n_f \to \infty$, or $n_f \to 0$, there is no unbound electrons remain in the system since one has a whole boson system compound by CPs, this can be seen if one takes eqs (3.4) and (3.3) without excited $m_{B+}(T)$. "Einstein realized that as soon as the chemical potential μ, becomes zero the number of particles in the lowest energy quantum state becomes infinite. More precisely we can say that out of a total of N particles in the gas, a macroscopic number N_0 occupy the one quantum state with $\epsilon_k = 0$. By a 'macroscopic number' we mean that N_0 is proportional to the system volume, so that there is a finite fraction of all of the particles, N_0/N, are in the one quantum state" [99].

On the meaning of $n/n_f < 1$ and excited bosonic pairs

Our study included the temperature range $0 \leq T \leq T_c$. Taking the extreme when $T = T_c$ implies $\Delta(T_c) = f\sqrt{n_0(T_c)} + f\sqrt{m_0(T_c)} = 0$, namely the condensed bosonic pairs 2e/2hCPs vanished and one has the contribution of excited 2e/2hCPs only. In the coupling extreme $n/n_f \to \infty$ one has an ideal Bose gas and one has a non-interacting boson-fermion gas with the following cases:

i) Ignoring excited 2hCPs, i.e., $m_{B+}(T_c) = 0$ therefore one has a non-interacting BF gas composed by unbound electrons and 2eCPs, i.e., a binary ideal gas with limit $T_c/T_F \to 0.988$ when $n/n_f \to \infty$, see Fig.3.5.

ii) Ignoring excited 2eCPs, i.e, $n_{B+}(T_c) = 0$ implies that one has a non-interacting BF gas composed by unbound electrons and 2hCPs, once again a binary ideal gas. However, with no bounds in the critical temperature, i.e., $T_c/T_F \to +\infty$.

iii) Taking both excited pairs, one has a noninteracting ternary gas composed by 2eCPs, 2hCPs and unbound electrons. From this case one has the limit $T_c/T_F \to 0.704$ for 100-0 (2eCPs only) case. The other limit occurs at $T_c/T_F \to 1.504$ for 0-100 (2hCPs only) case.

When $n/n_f < 1$ the number density of unbound electrons is greater than the total electron number density, this seems has no physical sense. However, if one analyzes the relation $(E_F/E_f)^{3/2} < 1$ which is equivalent to latter expression, several cases appear if E_f changes with respect to Fermi energy. From the electronic structure in solids one has the following considerations: If E_f is the pseudo-Fermi energy of the unbound electrons and E_F is the Fermi energy, both at zero temperature. One can choose arbitrarily E_f, i.e., putting the pseudo-Fermi energy above or below Fermi energy, this yields to

i) $E_f = E_F$ one has the perfect ideal symmetry with 50-50 proportions between 2eCPs and 2hCPs, thus one has that all electrons are unbounded.

ii) $E_f > E_F$ all bosonic energy levels of excited 2eCPs are filled, i.e., the total number density of excited 2hCPs are greater than 2eCPs. Then, the number density of excited 2hCPs are greater than excited 2eCPs plus unbound electrons, this leads to the concept of a mono gas composed by excited 2hCPs

iii) $E_f < E_F$ all bosonic energy levels of excited 2eCPs are unoccupied, namely the total number density of excited 2eCPs plus unbound electrons are greater than excited 2hCPs, this leads to a binary gas with excited 2eCPs and unbound electrons but if one considers the excited 2hCPs one has a ternary gas.

At zero temperature the excited CPs vanished, then one has the following considerations:

i) $E_f = E_F$ one has the perfect ideal symmetry with 50-50 proportions between 2eCPs and 2hCPs, thus

$$[2n_0(T) + n_f(0)]/n_f = 2m_0(T) + 1$$

implying $2n_0(T) = 2m_0(T)$ since $n_f(T = 0) \equiv n_f$.

ii) $E_f > E_F$ the bosonic energy levels of condensed 2hCPs are partially filled, this implies that total number density of condensed 2hCPs are greater than condensed 2eCPs, then

$$n/n_f = [2n_0(0) - 2m_0(0)]/n_f + 1 < 1$$

implying

$$2n_0(0)/n_f < 2m_0(0)/n_f$$

Therefore, the energy gap of 2hCPs is greater than the energy gap of 2eCPs $\Delta_m(0) > \Delta_n(0)$ implying $m_0(0) > n_0(0)$ for $n/n_f < 1$ at zero temperature. This result will be discuss in next section.

iii) $E_f < E_F$ bosonic energy levels of condensed 2eCPs are partially filled, namely the total number density of condensed 2eCPs are greater than condensed 2hCPs, gives

$$n/n_f = [2n_0(0) - 2m_0(0)]/n_f + 1 > 1$$

then

$$2n_0(0)/n_f > 2m_0(0)/n_f$$

In opposite sense with previous case, the energy gap of 2eCPs are greater than 2hCPs $\Delta_n(0) > \Delta_m(0)$ when $n/n_f > 1$ at zero temperature this implies that $n_0(0) > m_0(0)$, this result will be discuss in the energy gap section.

The analysis of three cases between E_f and E_F from the point of view of the energy dispersion relation is illustrated in Fig.3.7 for $T > 0$. Is plotted the energy dispersion relation of bosonic 2e/2hCPs, $E_{\pm}(K) = E_{\pm}(0) \pm \hbar^2 K^2/4m$ with $E_{\pm}(0) = 2E_f \pm \delta\epsilon$, where E_f is the pseudo-Fermi energy of unbound electrons at zero temperature and $\delta\epsilon$ is a shell energy around E_f where the boson-fermion interactions occur. The energy dispersion relation for excited $n_{B+}(T)$ and $m_{B+}(T)$ is simply $\mathcal{E}_{\pm}(\varepsilon) = \varepsilon \pm E_{\pm}(0) \mp 2\mu$ with $\varepsilon = \hbar^2 K^2/4m$.

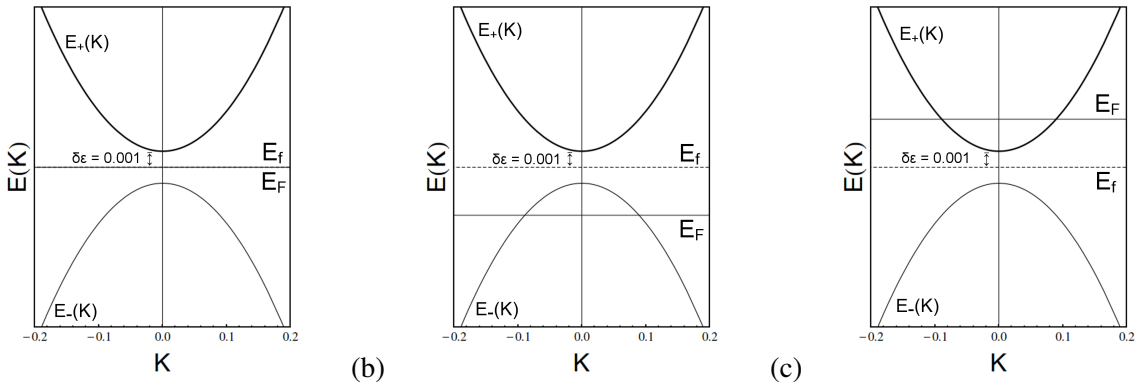

Figure 3.7: Energy dispersion relation $E_{\pm}(K)$ *vs.* K the wave number of excited bosonic pairs 2eCPs and 2hCPs for $T > 0$. With $E_{\pm}(K) = E_{\pm}(0) \pm \hbar^2 K^2/4m$ and $E_{\pm}(0) = 2E_f \pm \delta\epsilon$, here was used $\delta\epsilon = 0.001$ and letting $\hbar = m = 1$. (a) $E_f = E_F$ one has the the perfect ideal symmetry between 2eCPs and 2hCPs. (b) $E_f > E_F$ number density of 2hCPs are greater than 2eCPs. (c) $E_f < E_F$ number density of 2eCPs are greater than 2hCPs as discussed in text.

At any T, the three cases holds the BF ternary mixture, i.e, guarantees charge conservation. Also, for any n/n_f holds the BF ternary mixture, although $n/n_f < 1$ predominates 2hCPs over 2eCPs, and $n/n_f > 1$ predominates 2eCPs over 2hCPs.

3.3 Role of excited CPs

In this section we discuss the role of excited bosonic pairs of 2hCPs and 2eCPs. In Fig.3.5 we already construct the phase diagram of T_c/T_F *vs.* n/n_f for three extreme cases i) 100-0 (2eCPs only) ii) 0-100 (2hCPs only) and the simplest case of 50-50 proportions, namely an ideal perfect symmetry between 2eCPs and 2hCPs. Also we already constructed a phase diagram of the energy gap at zero temperature made dimensionless with respect to Fermi energy $\Delta(0)/E_F$ *vs.* n/n_f again for the same cases. Let's analyze the 100-0 case with or without the contributions of both excited pairs at $T = T_c$ as follows

i) $n/n_f = \left[n_f(T_c) + 2n_{B+}(T_c)\right]/n_f$ (excited 2eCPs contribution)

ii) $n/n_f = \left[n_f(T_c) - 2m_{B+}(T_c)\right]/n_f$ (excited 2hCPs contribution)

iii) $n/n_f = [n_f(T_c) + 2n_{B+}(T_c) - 2m_{B+}(T_c)]/n_f$ (both kind contribution)

iva) $n/n_f = n_f(T_c)/n_f$ (no contribution)

The 0-100 case with both kinds of contributions, yields to

v) $n/n_f = [n_f(T_c) - 2m_{B+}(T_c)]/n_f$ (excited 2hCPs contribution)

vi) $n/n_f = [n_f(T_c) + 2n_{B+}(T_c)]/n_f$ (excited 2eCPs contribution)

vii) $n/n_f = [n_f(T_c) + 2n_{B+}(T_c) - 2m_{B+}(T_c)]/n_f$ (both kind contribution)

ivb) $n/n_f = n_f(T_c)/n_f$ (no contribution)

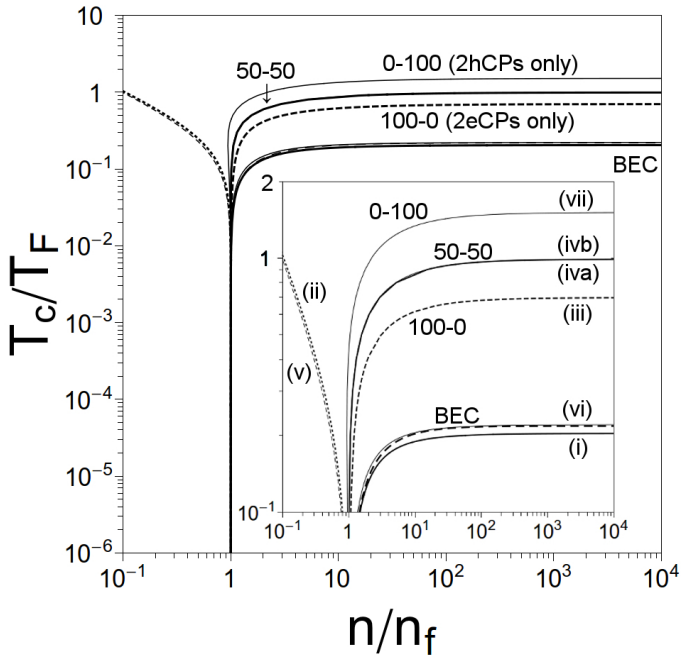

Figure 3.8: Phase diagram T_c/T_F vs n/n_f for different cases cited in text. BEC curve is presented for comparison. Inset shows both kinds of cases with contributions as mentioned in text. The 100-0 case are: (**i**) ignores excited 2hCPs, i.e., $2m_{B+}(T) = 0$ with limit $T_c/T_F = 0.204$ when $n/n_f \to \infty$, this is a binary gas. (**ii**) ignores excited 2eCPs, this curve diverges to $T_c/T_F \to \infty$ when $n/n_f \to 0$. (**iii**) counts both contributions and has the limit $T_c/T_F = 0.704$ when $n/n_f \to \infty$, this is ternary gas and is the so-called 100-0 case. (**iva**) ignores both excited pairs with limit $T_c/T_F = 0.988$, this curve resembles the perfect ideal symmetry. The 0-100 cases are: (**ivb**) with no contribution of excited pairs, i.e., $n_{B+}(T) = m_{B+}(T) = 0$ and tends to the limit of the 50-50 case. (**v**) ignores excited 2eCPs as case (**ii**) and diverges to $T_c/T_F \to +\infty$ when $n/n_f \to 0$. (**vi**) ignores 2hCPs an its limit resembles a BEC curve. (**vii**) counted both kinds of contribution with limit $T_c/T_F \to 1.507$, this is a ternary gas and is the 0-100 case.

Fig.3.8 shows T_c/T_F *vs.* n/n_f for each case above. All curves were calculated with $f_{\pm}(\epsilon) \neq 0$. Then, we analyze the 100-0 case in the interaction range of (3.13) with the following considerations:

– Curve labeled (**i**) ignores the excited 2hCPs and its behavior is similar to the BEC curve, which is an ideal Bose gas composed of 2eCPs with $T_c/T_F \to 0.204$ when $n/n_f \to \infty$, this curve is calculated with the interaction function $f_{\pm}(\epsilon) \neq 0$ instead of $f = 0$ as in Ref. [81]. This curve is slightly below with respect BEC curve with the familiar limit $T_c/T_F \to 0.218$ when $n/n_f \to \infty$ since there are still "some" interactions between electrons (as fermions) and bosons (2eCPs), namely, ignoring excited 2hCPs leads to a binary gas

– Curve labeled (**ii**) ignores the contribution of the excited 2eCPs, i.e., $n_{B+}(T) = 0$. This curve suddenly turns to left with respect to $n/n_f = 1$ and diverges to $T_c/T_F \to \infty$ as $n/n_f \to 0$. This curve represents a binary gas and suggest that for $n/n_f < 1$ predominates 2hCPs over 2eCPs

– Curve labeled (**iii**) consider both kinds of contribution of the excited bosonic CPs. Note that the mere presence of 2hCPs (excited) increase the critical temperatures with respect to BEC curve, this curve still remain as ternary ideal gas when $n/n_f \to \infty$ and has the limit $T_c/T_F \to 0.702$, this curve is the 100-0 proportions

– Curve labeled (**iva**) ignores both kinds of excited CPs, i.e., $n_{B+}(T) = m_{B+}(T) = 0$, and coincides with 50-50 proportions and $T_c/T_F \to 0.988$ when $n/n_f \to \infty$. Although the contribution of excited pairs was ignored, the entire behavior of this case resembles the perfect ideal symmetry.

Analyzing the 0-100 case with electronic energies in the interaction range (3.14) one has the following considerations:

– Curve labeled (**ivb**) has no contribution of excited pairs, i.e, $n_{B+}(T) = m_{B+}(T) = 0$, and again coincides precisely with 50-50 proportions

– Curve labeled (**v**) ignores the contribution of excited 2eCPs, namely $2n_{B+}(T) = 0$, the curve diverges to $T_c/T_F \to +\infty$ when $n/n_f \to 0$. This suggests that the absence of excited 2eCPs makes that the entire system falls in the region of $n/n_f < 1$, in this range the 2hCPs predominates over 2eCPs. Besides, this mixture corresponds to a binary gas of unbound electrons and excited 2hCPs

– Curve labeled (**vi**) ignores the excited 2hCPs ($m_{B+}(T) = 0$) and surprisingly tends to the BEC curve. Here, the interaction was taken as (3.14) (for 2hCPs) but the mixture is a binary gas composed of electrons with the contribution of excited 2eCPs, just as in case (**i**)

– Curve labeled as (**vii**) has both kinds of contribution of excited pairs $2n_{B+}(T)$ as well $2m_{B+}(T)$ with limit $T_c/T_F \to 1.507$ when $n/n_f \to \infty$, both kinds of excitations increase critical temperature. Specifically, the excited 2eCPs drives the entire system *above* the Fermi temperature, this is the 0-100 proportions case and is a ternary gas.

The role playing the excited 2eCPs as well 2hCPS is increase the critical temperature with respect to the BEC curve, namely, if one ignores specifically a kind of contribution of excited pairs, each curve will be change. For example, if one ignores the excited 2hCPs, i.e., $m_{B+}(T) = 0$ both cases (100-0 and 0-100)

tend to be a BEC curve, another example: if one ignores excited 2eCPS, i.e, $n_{B+}(T) = 0$ in both cases (100-0 and 0-100) critical temperature diverges to $T_c/T_F \to +\infty$ when $n/n_f \to 0$, the meaning behind of this behavior is that in this region ($n/n_f < 1$) the 2hCPs predominates over 2eCPs. On the other hand, in $n/n_f > 1$, if one ignores the excited 2hCPs, therefore the curves tends to be an ideal Bose gas composed of 2eCPs, in this region 2eCPs predominates over 2hCPs.

GBEC Condensate Fraction

To known the condensate fraction of GBEC one takes (2.69) at $T = 0$ and made dimensionless with total number of particles n instead of that of unbound electrons at $T = 0$ this gives

$$\left(\frac{2}{n}\right)\left[n_0(T=0) - m_0(T=0)\right] = 1 - \left(\frac{n}{n_f}\right)^{-1} \tag{3.15}$$

where $[n_0(T=0) - m_0(T=0)]/n$ is the **GBEC condensate fraction.** It includes both, total condensed bosonic 2eCP and 2hCPs. Taking $n/n_f \to 1$ in (3.15) gives $n_0(T=0) = m_0(T=0)$, i.e., the ideal perfect symmetry, then the condition that all particles are unbounded is recovered and one obtains the weak-coupling extreme at precisely $n/n_f = 1$, since $2[n_0(T=0)/n - m_0(T=0)/n] \to 0$. On the other hand, taking $n/n_f \to \infty$ in (3.15) gives

$$\left(\frac{2}{n}\right) n_0(T=0) = 1 - \left(\frac{2}{n}\right) m_0(T=0)$$

the left-hand-side essentially corresponds to the condensate fraction of an ideal Bose gas (strong coupling extreme) composed by two-electron pairs. Thus, the dimensionless number density n/n_f can be in principle, correlated with *any* other dimensionless coupling constant. In Fig.3.9 shows the GBEC condensate fraction *vs*. dimensionless number density and λ_{BCS}. Note that at relatively large number density, i.e., about $n/n_f \simeq 10^2$ most of the particles are condensed. Also shows the Bogoliubov *et al*. upper limit of $\lambda_{BCS} = 1/2$.

Fig. 3.10 compares the BCS dimensionless order parameter, i.e, the energy gap $\Delta(T)/\Delta(0)$ *vs*. T/T_c with the BEC order parameter that is just the condensate fraction $N_0/N = 1 - (T/T_c)^{3/2}$. Also shown is the extended crossover order parameter as $\Delta(T)/\Delta(0) = \sqrt{n_0(T)/n_0(0)}$ for 50-50 proportions, since $n_0(T) = m_0(T)$ implying $\Delta(T) = 2f\sqrt{n_0(T)} = 2f\sqrt{m_0(T)}$. Note that the extended crossover curve lies *between* the weak-coupling theory (BCS) and the strong-coupling theory (BEC). The GBEC theory with 50-50 proportions is described by two equations: the gap-like (3.4) plus (3.5) and (3.3). Thus, BCS theory is described by the gap equation while BEC theory by a number equation only. This suggests that the extended BCS-Bose crossover theory covers the weak, strong and intermediate coupling regimes.

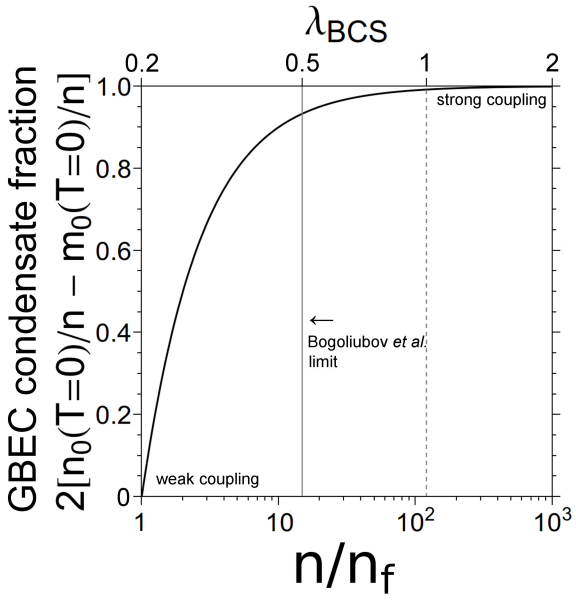

Figure 3.9: GBEC condensate fraction (3.15) *vs.* n/n_f. When $n/n_f = 1$ the condensate fraction vanishes and one recovers the weak-coupling extreme where all electrons are unbound. At the other extreme $n/n_f \to \infty$ one has strong-coupling. The Bogoliubov *et al.* upper limit of $\lambda_{BCS} = 1/2$ it shows for comparison purposes.

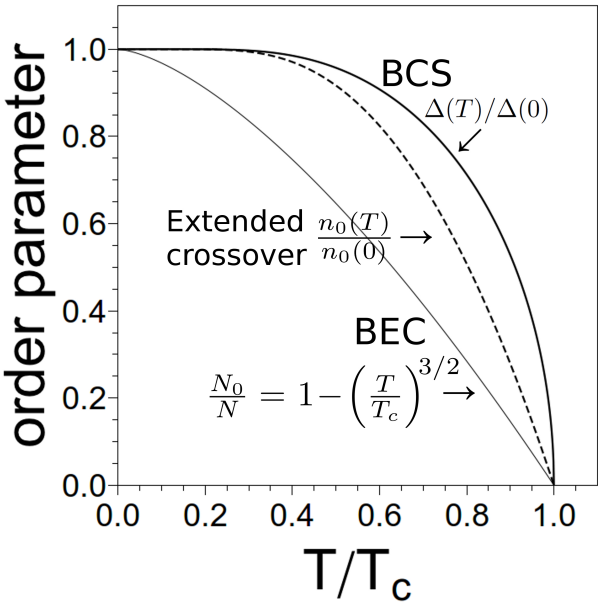

Figure 3.10: Order parameter *vs.* T/T_c of BCS theory, the energy gap $\Delta(T)/\Delta(0)$ (thick curve); BEC theory, the condensate fraction N_0/N (thin curve) and GBEC theory $n_0(T)/n_0(0)$ (dashed curve) where $n_0(T)$ is the number density of the condensed 2eCPs. The extended crossover order parameter comes from $\Delta(T) = f_+\sqrt{n_0(T)} + f_-\sqrt{m_0(T)}$, where $f_\pm$ is the BF vertex interaction function and here is taken as $f_+ = f_- = f$. GBEC curve shows the 50-50 proportions at $n/n_f = 1$. Note that the extended crossover order parameter curve lies between the BCS-energy gap (weak-coupling) and the BEC condensate fraction (strong-coupling) curves.

3.4 Energy gap for any T and the gap-to-T_c ratio

To construct the energy gap $\Delta(T)$ of the extended crossover it is necessary to solve simultaneously at least two equations: the gap-like (3.4), (3.3) for 100-0 proportions, the gap-like (3.5) and (3.3) for 0-100 and (3.4) plus (3.5) with (3.3) for 50-50 proportions. As experimental parameters one have the energy $\delta\epsilon$ which in turn can be related with $\hbar\omega_D$, the Debye energy of ionic lattice and the GBEC dimensionless interaction 'strength' parameter $\tilde{G}$. In principle be related with the dimensionless electron-phonon coupling constant of BCS theory as $\lambda_{BCS} = 2\tilde{G}/(\hbar\omega_D/E_F)$ for $n/n_f = 1$.

Fig. 3.11 shows the theoretical energy gap $\Delta(T)/\Delta(0)$ *vs.* T/T_c for 50-50 proportions and 100-0 proportions both with $n/n_f = 1$. The 50-50 curve coincides precisely with BCS energy gap curve. Also is plotted the 100-0 proportions with $n/n_f = 1.0001$. One can observe that the latter curve is near to the 50-50 proportions. Later will be shown that changing n/n_f slightly from unity one can adjust to experimental data.

The gap-to-T_c ratio, $2\Delta(0)/k_BT_c$ is an universal accepted value of the coupling strength, for weak coupling (BCS) regime is $2\Delta(0)/k_BT_c \simeq 3.53$, the 50-50 proportions reproduces quiet well this ratio, while for 100-0 case is $2\Delta(0)/k_BT_c \simeq 2.18$. As well the energy gap that changes if one changes n/n_f, also the gap-to-T_c ratio changes. For 100-0 proportions with $n/n_f = 1.0001$ the gap-to-T_c ratio changes to $2\Delta(0)/k_BT_c \simeq 3.17$.

Noting the following: i) ignoring the 2hCPs, i.e., taking the 100-0 proportions (2eCPs only), the energy gap curve substantially falls below from that of 50-50 symmetry, this suggest that 2hCP are *indispensable* to describing superconductivity; ii) changing n/n_f slightly from unity one can adjust the gap-to-T_c ratio, i.e., one changes the coupling strength if one changes n/n_f. With a slightly change in the dimensionless number density one can adjust to experimental data, in the following chapter will be presented this result.

It was shown that the energy gap at zero temperature for the perfect ideal symmetry lies precisely at $n/n_f = 1$, as shown in Fig.3.2. Furthermore, the critical temperature dimensionless with Fermi temperature T_c/T_F has an identical behavior around $n/n_f = 1$. In Fig.3.12 illustrates each case around $n/n_f = 1$ for $\Delta(0)/E_F$ and T_c/T_F *vs.* n/n_f. The energy gap for 50-50 proportions has a solely value at $n/n_f = 1$ which reproduces quite well the experiment, while the 100-0 and 0-100 proportions not reproduce the experiment data at $n/n_f = 1$. In the following chapter will be present this results.

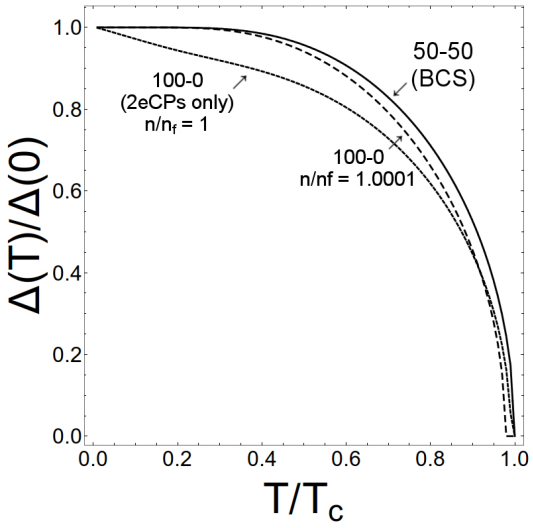

Figure 3.11: $\Delta(T)/\Delta(0)$ *vs.* T/T_c for ideal perfect symmetry with 50-50 proportions of the extended crossover which coincides precisely with BCS theory, holding $2\Delta(0)/k_BT_c \simeq 3.53$. Also, shows the 100-0 proportions (short-dashed) curve with $n/n_f = 1$ with $2\Delta(0)/k_BT_c \simeq 2.18$ and 100-0 proportions (long-dashed) curve with $n/n_f = 1.0001$ with $2\Delta(0)/k_BT_c \simeq 3.17$. If one ignores 2hCPs the energy gap curve is below of 50-50 proportions. This suggests that 2hCPs plays a key role to describes superconductivity.

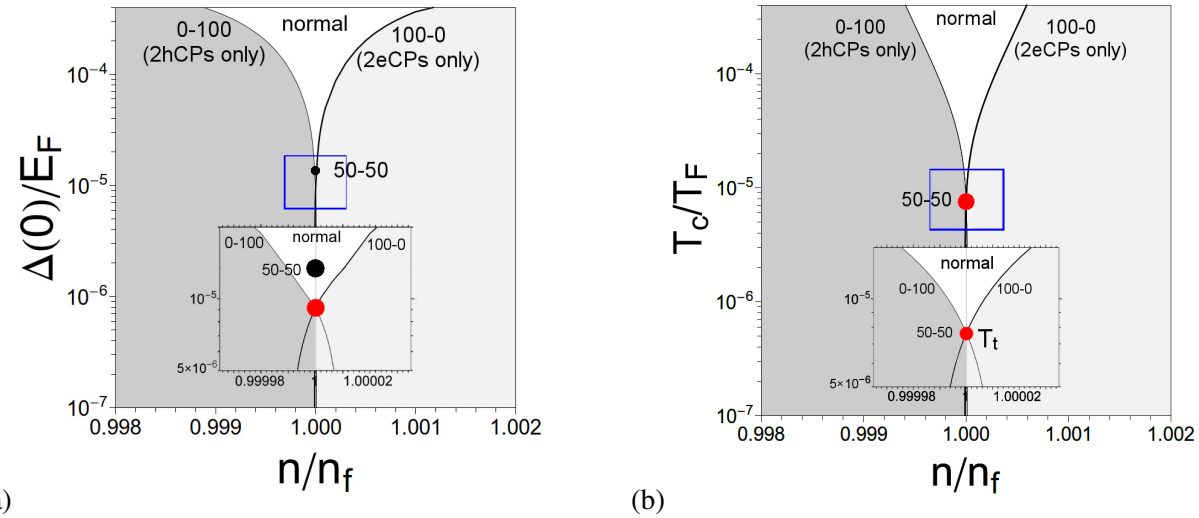

(a) (b)

Figure 3.12: (a) Energy gap $\Delta(0)/E_F$ *vs.* n/n_f for 50-50 proportions (black circle); the 100-0 proportions (thick curve); and 0-100 proportions (thin curve), different shade-gray areas corresponds to different phases. Blue (online) square marks the bottom inset and shows the same three cases. The red (online) circle marks where 100-0 and 0-100 proportions crosses and has the same value of $\Delta(0)/E_F = 9.11 \times 10^{-6}$ at $n/n_f = 1$, while that for the 50-50 symmetry has $\Delta(0)/E_F = 1.13 \times 10^{-5}$ (b) Critical temperature T_c/T_F *vs.* n/n_f for 50-50 red (online) circle, 100-0 proportions (thick curve) and 0-100 proportions (thin curve). All the three cases crossing (red online circle) at $T_t \equiv T_c/T_F = 7.64 \times 10^{-6}$ at precisely $n/n_f = 1$.

Chapter 4

Experimental data and the dimensionless number density

In this chapter the extended BCS-Bose crossover equations are solved to predicts the energy gap curve and of course the critical temperature for some elemental superconductors. The theoretical curves are compared with experimental data. If one changes slightly the dimensionless number density this results fit quite well with experiment. Showing that, e.g. the universal ratio $2\Delta(0)/k_BT_c$ can be adjust changing n/n_f. Furthermore is presented experimental data of Gallium films and the corresponding theoretical curves which reproduces the experimental data.

4.1 Extended crossover compared with experimental data

Table 4.1 lists some elemental SCs such as Al, In, Sn, Hg, Pb and Nb (ascending temperature order). It shows the theoretical T_c/T_F predicted by the extended crossover for each SC and compared with experiment and BCS theory. The BCS values of T_c/T_F are calculated via the BCS gap-T_c ratio $2\Delta(0)/k_BT_c \simeq 3.53$ using empirical data for the energy gap at $T = 0$. Extended crossover values for T_c/T_F are calculated by solving the three equations (3.4), (3.5) and (3.3) for perfect 50-50 symmetry, i.e., $n/n_f = 1$. The extended crossover predicts critical temperatures for the aforementioned SCs quite well, even for the so-called "bad actors" of BCS theory [141].

Here one solves three equations instead of the two equations as suggested by Keldysh *et. al* [34], Popov [35], Friedel *et. al* [36], Eagles [37] and Leggett [38], assuming $\mu \neq E_F$ as was implemented originally in BCS theory. Also shown is the experimental gap-to-T_c ratio for the listed SCs (tenth column) and is compared with that of the extended crossover (eleventh column). These values of the extended crossover are obtained by varying n/n_f slightly from unity (twelfth column) even for Hg and Pb, the so-called "bad actors" of BCS theory. This was done follows the charge-carrier sign from Ref. [142] according to whether n/n_f is greater or less than unity. The last column illustrates how the dimensionless number density n/n_f acting about as a dimensionless coupling constant, since with a slightly change the resulting gap-to-T_c ratio can be

adjusted to coincides with experiment. Here we did not supposed a strong coupling correction, such as the retardation effect of the Eliashberg-Migdal theory. Notice something important, n/n_f increases alongside with critical temperature.

Table 4.1: Experimental data for some conventional (i.e., presumed electron-phonon driven) SCs compared with results from the *extended* BCS-Bose crossover theory. Debye (Θ_D), Fermi (T_F) and critical temperatures (T_c) are in kelvin units (K) and λ_{BCS} is the dimensionless BCS coupling parameter. Here λ_{BCS} is determined via the BCS gap equation. Remarkably, the values obtained vindicated the Bogoliubov *et. al* upper limit $\lambda_{BCS} \leq 1/2$. The BCS gap-to-T_c ratio formula $2\Delta(0)/k_BT_c \simeq 3.53$ was used to calculate BCS T_c/T_F values, using empirical data of the energy gap at $T = 0$ in meV units. T_c/T_F values predicted by the extended crossover are given for $n/n_f = 1$, while calculated $2\Delta(0)/k_BT_c$ values were adjusted with a n/n_f value near unity as shown in last column. In **bold** are the BCS "bad actors" [141]. Table taken from [139].

	Θ_D	T_F	T_c	λ_{BCS}	$2\Delta(0)$	T_c/T_F ($\times 10^{-5}$)			$2\Delta(0)/k_BT_c$		
		($\times 10^5$)[a]				expt	BCS	Extended crossover	expt	Extended Crossover	n/n_f
Al	394[a]	1.36	(1.17 ± 0.003)[e]	0.17	(3.20 ± 0.03)[j]	0.87	0.82	0.87	3.17	3.17	1.0000075
In	108[b]	1.00	(3.41 ± 0.001)[f]	0.28	(1.05 ± 0.03)[j]	3.40	3.64	3.42	3.57	3.57	1.0000480
Sn(w)	195[b]	1.18	(3.72 ± 0.001)[f]	0.24	(1.11 ± 0.03)[j]	3.15	3.26	3.13	3.46	3.46	1.0000410
Hg	88[b]	0.83	(4.15 ± 0.001)[d]	0.31	(1.55 ± 0.07)[i]	**5.00**	**6.48**	**4.99**	**4.33**	**4.33**	1.0000975
Pb	96[b]	1.10	(7.20 ± 0.8)[g]	0.37	(2.68 ± 0.06)[j]	**6.54**	**8.45**	**6.53**	**4.32**	**4.32**	1.0001263
Nb	276[b]	0.62	(9.25 ± 0.010)[c]	0.28	(3.05 ± 0.05)[h]	14.96	17.12	14.90	3.83	3.83	1.0002692

Experimental data are from
[a] N.W. Ashcroft and N.D. Mermin, *Solid State Physics* (Saunders College Publishing, USA, 1976) pp. 38 and 729.
[b] C.P. Poole, Jr., H.A. Farah, R.J. Creswick & R. Prozorov, *Superconductivity* (Academic Press, Elsevier, New York, 2007) pp.2-3 and 62
[c] D.K. Finnemore, T.F. Stromberg, & C.A. Swenson, Phys. Rev. **149**, 231 (1966) [d] D.K. Finnemore, D.E. Mapother, & R.W. Shaw, Phys. Rev. **118**, 127 (1960)
[e] T. E. Faber, Proc. R. Soc. Lond. A **231**, 353 (1955) [f] D.K. Finnemore, & D.E. Mapother, Phys. Rev. **140**, A507 (1965)
[g] B.J.C. Van der Hoeven, Jr. & P.H. Keesom, Phys. Rev. **137**, A103 (1965) [h] P. Townsend & J. Sutton, Phys. Rev. **128**, 591 (1962)
[i] P. Richards & M. Tinkham, Phys. Rev. **119**, 575 (1960) [j] I. Giaver & K. Megerle, Phys. Rev. **122**, 1101 (1961)

Fig. 4.1 shows experimental T_c/T_Fs (ninth column in Table 4.1) as function of $\Delta n \equiv n/n_f - 1$ compared with two pairs of theoretical curves of the extended crossover: a) pair upper curves labeled $\lambda_{BCS} = 1/2$ correspond to the Bogoliubov *et al.* upper limit with $\hbar\omega_D/E_F = 0.002$, b) pair bottom curves are for $\lambda_{BCS} = 1/5$ with $\hbar\omega_D/E_F = 0.001$. These values of $\hbar\omega_D/E_F$ are typical for elemental SCs; black dots refer to experimental values of T_c/T_F for each SC associated with perfect ideal symmetry between 2eCPs and 2hCPs, i.e., $\Delta n = 0$ or weak-coupling regime. One sees that SC empirical data of T_c/T_F falls within the theoretical curves of the extended crossover. Thus, vindicated the Bogoliubov *et. al* upper limit $\lambda_{BCS} \leq 1/2$.

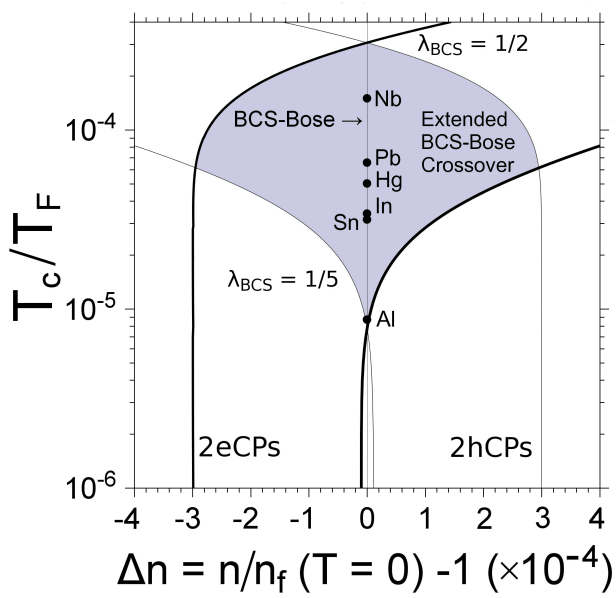

Figure 4.1: Theoretical curves of extended crossover compared with experimental values of T_c/T_F for the aforementioned SCs. Thick curves labeled as 2eCPs (100-0 proportions) are obtained by simultaneously solving (3.4) with (3.3); thin curves labeled 2hCPs (0-100 proportions) by solving (3.5) with (3.3). Black dots mark experimental T_c/T_F values with $\Delta n = 0$ where the error bars fall within dot size. Pair upper curves labeled $\lambda_{BCS} = 1/2$ (the Bogoliubov *et al.* upper limit, with $\hbar\omega_D/E_F = 0.002$) while pair bottom curves are for $\lambda_{BCS} = 1/5$ with $\hbar\omega_D/E_F = 0.001$. These Debye-energy values made dimensionless with Fermi energy are typical for elemental superconductors. Figure taken from [139].

4.2 The extended BCS-Bose crossover energy gap

The extended BCS-Bose crossover picture for the electronic gap $\Delta(T)$ is

$$\Delta(T) = f\sqrt{n_0(T)} = f\sqrt{m_0(T)} \tag{4.1}$$

where f is a boson-fermion vertex interaction coupling constant inherent to the GBEC theory. All three functions $\Delta(T)$, $n_0(T)$ and $m_0(T)$ have common "half-bell-shaped" forms. Namely, they vanish above a certain critical temperature T_c, and rise monotonically upon cooling (i.e., lowering T) to maximum values $\Delta(0)$, $n_0(0)$ and $m_0(0)$ at $T = 0$. The energy gap $\Delta(T)$ is the order parameter describing the SC condensed state, while $n_0(T)$ and $m_0(T)$ are the BEC order parameters depicting the macroscopic occupation that occurs below T_c in a BE condensate. This $\Delta(T)$ is *precisely* the BCS energy gap if one takes the perfect ideal symmetry between 2eCPs and 2hCPs and the BF vertex interaction functions is taken as $f \equiv \sqrt{2V\hbar\omega_D}$ where V and $\hbar\omega_D$ are the two parameters of the BCS model interelectronic interaction. Evidently then, the BCS and BEC T_cs are essentially equivalent.

Writing (4.1) for $T = 0$ and dividing this into (4.1) gives the much simpler *f-independent* relation involving order parameters, as well as temperatures T, normalized to unity in the interval $[0, 1]$, namely $\Delta(T)/\Delta(0) = \sqrt{n_0(T)/n_0(0)} = \sqrt{m_0(T)/m_0(0)}$. The first equality, apparently first obtained in Ref. [62],

connects in a simple way the two heretofore unrelated "half-bell-shaped" order parameters of the BCS and the BEC theories. The second equality implies that a BCS condensate is precisely a BE condensate of equal numbers of 2eCPs and 2hCPs.

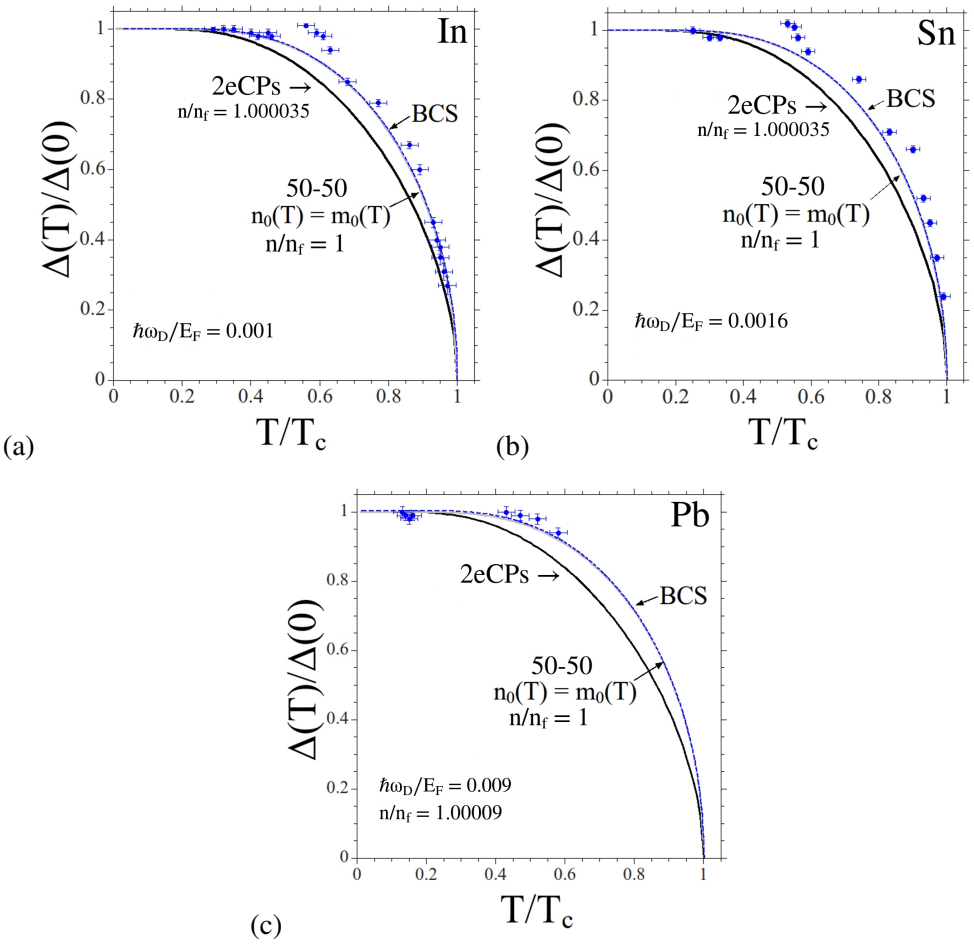

Figure 4.2: Energy-gap curves $\Delta(T)/\Delta(0)$ *vs.* T/T_c of the extended BCS-Bose crossover for (a) In (b) Sn and for (b) Pb with $n/n_f = 1$, i.e., the 50-50 symmetry, which coincides precisely with BCS energy-gap curve. The 2eCPs curve is obtained by simultaneously solving (3.4) and (3.3), with a different n/n_f from unity value, i.e., slightly different from the 50-50 symmetry. Note that the 2eCPs curve now falls substantially *near* to 50-50 curve agreeing quite well with experiment. Here experimental values of $\hbar\omega_D/E_F$ for In, Sn and Pb as well as gap experimental data were taken from Ref. [143]. Figure (a) and (b) taken from [138].

Here we solve at least two equations of the extended crossover instead just one as in the BCS theory, this giving the energy gap $\Delta(T)/\Delta(0)$ *vs.* T/T_c for any superconductor with a specific value of n/n_f. Fig.4.2 shows energy-gap curves for In and Sn and compared with experimental data [143], also is presented the energy gap for Pb [144]. It shows the 50-50 symmetry curve corresponding with BCS, obtained by solving (3.4) plus (3.5) with (3.3) when $n/n_f = 1$. Also shown in Fig.4.2 is the 2eCPs (100-0) case with $\Delta(T) = f\sqrt{n_0(T)}$, here were ignored 2hCPs, namely $m_0(T) = 0$. Both cases In and Sn was used $n/n_f = 1.000035$, for Pb was used $n/n_f = 1.00009$. These curves falling below but *near* to the 50-50

proportions. Clearly then, 2hCPs plays an *indispensable*, albeit intriguing [145] role in describing SCs.

So far, the energy gap curves $\Delta(T)$ has been presented in units of the energy gap at zero temperature $\Delta(0)$. Henceforth, we analyze the energy gap in units of Fermi energy. The main purpose is to illustrate how ignoring the 2hCPs or 2eCPs contribution, the energy gap reduces with respect the perfect ideal symmetry, even reduces with respect experimental data. In Table 4.2 shown the values of critical temperature T_c/T_F, the energy gap dimensionless with Fermi energy $\Delta(0)/E_F$ and $2\Delta(0)/k_BT_c$ for the aforementioned superconductors. Here were ignored the 2hCPs contribution.

Table 4.2: Experimental values of T_c/T_F, $\Delta(0)/E_F$ and $2\Delta(0)/k_BT_c$ for the aforementioned elemental superconductors compared with that values predicted by the extended crossover. Here were ignored the 2hCPs contribution, namely $m_0(T) = 0$. Note that all values for the 100-0 (2eCPs only) case falls below from the experimental data.

	$\Delta(0)/E_F$ ($\times 10^{-5}$)			T_c/T_F($\times 10^{-5}$)			$2\Delta(0)/k_BT_c$		
	exptl	**50-50**	**100-0**	**exptl**	**50-50**	**100-0**	**exptl**	**50-50**	**100-0**
Al	1.37	1.49	1.03	0.86	0.84	0.84	3.18	3.53	2.44
In	6.10	6.05	3.78	3.41	3.43	3.43	3.57	3.53	2.21
Sn	5.41	5.34	3.47	3.15	3.03	3.03	3.43	3.53	2.29
Pb	14.1	11.5	6.64	6.55	6.51	6.51	4.32	3.54	2.04
Hg	10.8	8.80	5.28	5.00	4.99	4.98	4.34	3.53	2.12
Nb	28.6	25.3	15.8	15.0	14.9	1.49	3.83	3.40	2.12

The 50-50 proportions contains in equal footing two-electron Cooper pairs and two-hole Cooper pairs. However, if one consider only the 2eCPs contribution, the energy gap, critical temperature and the gap-to-T_c ratio reduces with respect the experiment data. This suggests that 2hCPs are *indispensable* to describe superconductivity.

In Table 4.2 shows how reduces the predicted values of the extended crossover if one ignores the 2hCPs. But now, in Fig. 4.3 shows the theoretical energy gap curves $\Delta(T)/E_F$ *vs.* T/T_c for the aforementioned elemental superconductors. To plot these curves we use the experimental values of Debye energy $\hbar\omega_D$, Fermi energy E_F and the GBEC strength parameter G for each superconductor. Notably, one sees that the 100-0 proportions curve is below from that of 50-50 symmetry curve.

In Fig. 4.4 shows the extended crossover curves of the energy gap $\Delta(0)/E_F$ compared with experimental data [143, 146–148]. Solving (3.4) plus (3.5) and (3.3) one obtains the curve labeled 50-50, i.e., the perfect ideal symmetry. For 100-0 proportions was solved (3.4) and (3.3), and for 100-0* proportions was solved the same equations but now changing slightly n/n_f with respect unity.

For example, taking the aluminum case, one sees that the 50-50 curve is slightly up from experimental data [146], and 100-0 curve is substantially below. However, changing dimensionless number density as $n/n_f = 1.0000075$ (following the 12th column in Table 4.1) labeled 100-0* curve, fits very good to experimental data. This suggests that 2eCPs has a major contribution than 2hCPs since 50-50 curve is slightly up from experimental data. This behavior is repeated in Pb [143], Hg [147], and Nb [148], since the 100-0*

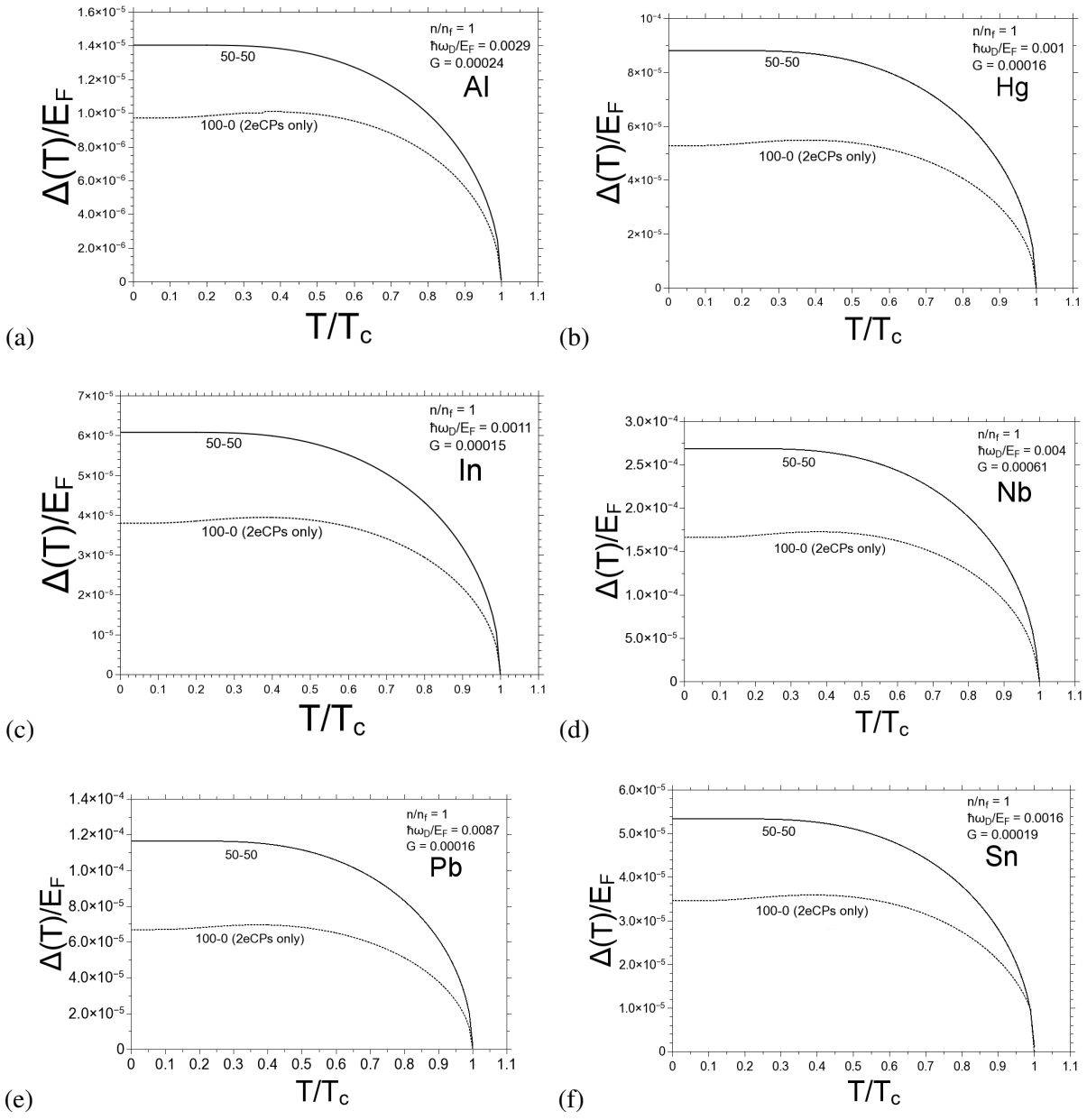

Figure 4.3: Energy gap $\Delta(T)/E_F$ vs T/T_c for (a) Al, (b) Hg, (c) In, (d) Nb, (e) Pb, and (f) Sn. Solid curve is the 50-50 proportions, i.e, $n_0(T) = m_0(T)$ and $n_{B+}(T) = m_{B+}(T)$. Dotted curve is for 100-0 case, ignoring 2hCPs, i.e., $m_0(T) = 0$. Note that latter curve is substantially below from the 50-50 symmetry curve which coincides precisely with experimental data. In all cases was used $n/n_f = 1$. Debye energy dimensionless with Fermi energy and the GBEC dimensionless strength parameter $\tilde{G}$ is labeled in each case.

curve fits better than 50-50 curve. For Indium and Tin the 50-50 curve depicts much better the experimental data [143]. In the next section we analyze the 0-100 case and compare with a superconductor with positive charge carriers.

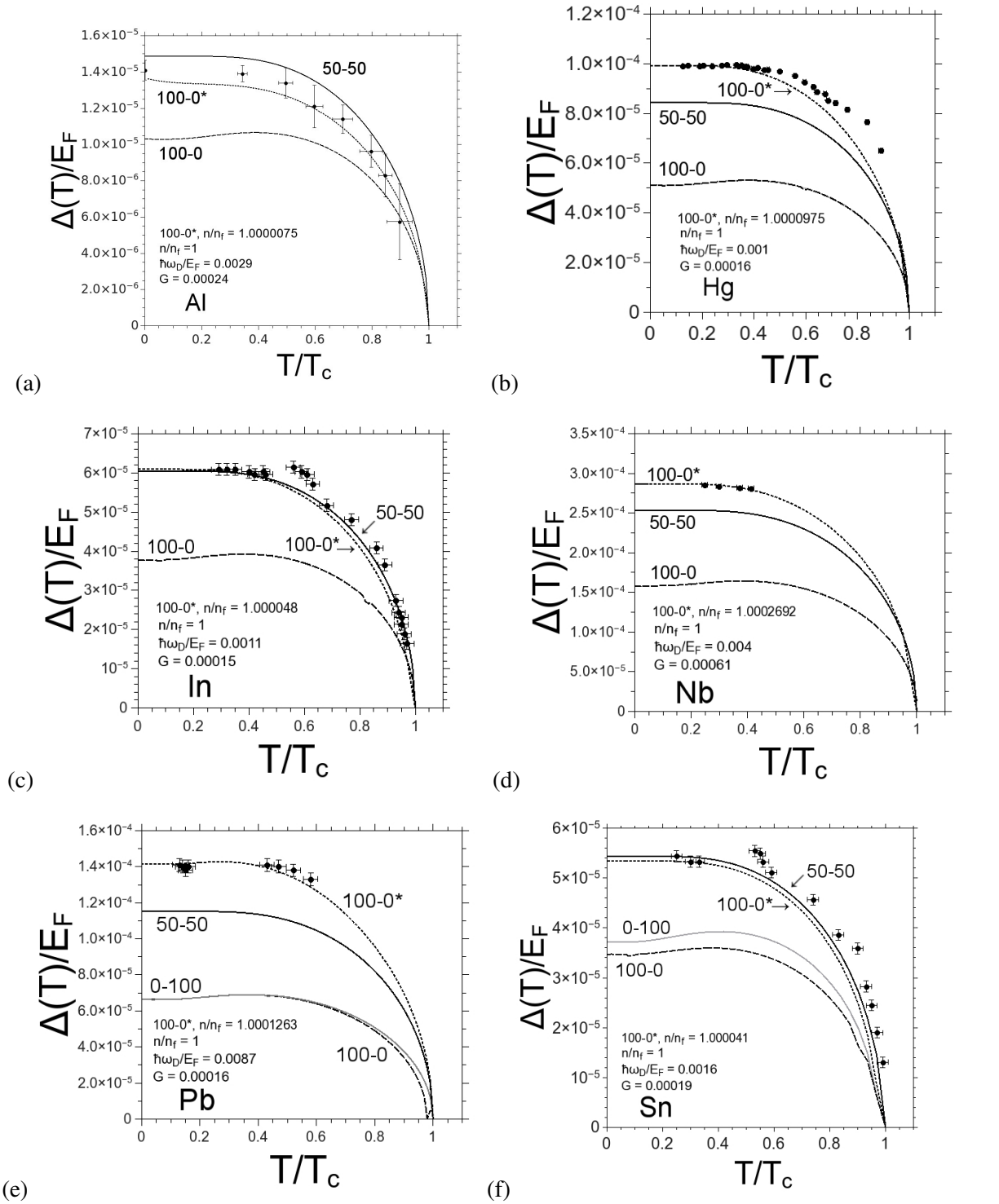

Figure 4.4: Energy gap $\Delta(T)/E_F$ vs T/T_c for (a) Al, (b) Hg, (c) In, (d) Nb, (e) Pb, and (f) Sn. Solid curve is the 50-50 proportions, i.e, $n_0(T) = m_0(T)$ and $n_{B+}(T) = m_{B+}(T)$. Gray curve is for 0-100 proportions, i.e, $n_0(T) = 0$. Dashed curve is for 100-0 proportions, ignoring 2hCPs, i.e., $m_0(T) = 0$. Note that latter curve is substantially below from the 50-50 symmetry curve but in some cases coincides with experimental data [143, 146–148]. Dashed curve 100-0* shows a slightly change in the dimensionless number density following the twelfth column of Table 4.1 to fit experiment. Each figure has labeled with its corresponding n/n_f.

4.2.1 Superconducting Gallium

In previous section, the SCs presented has a negative charge carriers according to [142]. Energy gap and critical temperature can be described with the 50-50 ideal perfect symmetry but in some cases with 100-0 (2eCPs only). To extend the crossover theory we are included explicitly the 2hCPs, namely the 0-100 proportions. There is a few elemental superconductors that have positive charge carriers, one of them is Gallium (Ga) [4]. Ga has a $T_c = 1.08$ K, while the energy gap is $\Delta(0) = 0.16$ meV [149]. The universal gap-to-T_c ratio exhibits the value $2\Delta(0)/k_BT_c \simeq 3.5$, i.e., is a weak-coupling superconductor. But Ga expose three different energy gaps according to Cohen *et. al* [149], those energy gaps labeled as Ga_{ord}, for ordinary Gallium and others labeled here as Ga_1, Ga_2, Ga_3, for different gallium films with critical temperatures of $T_c^1 = 6.4$ K, $T_c^2 = 7.9$ K, $T_c^3 = 8.4$ K, respectively and with energy gap values $\Delta(0)^1 = 1.03$ meV, $\Delta(0)^2 = 1.38$ meV, $\Delta(0)^3 = 1.53$ meV, respectively. The films labeled with (1), (2) and (3) shown a gap-to-T_c ratio above of BCS, but specially one, the Ga_2 exhibits the strong-coupling regime.

If we assuming that charge carriers were holes, we choose to use the 0-100 proportions, i.e., 2hCPs only. Furthermore we will change the dimensionless number density slightly from the unity to fit experimental values. In Fig. 4.5 shown the experimental data of the energy gap for Ga_1 and Ga_2, figure was taken from [149].

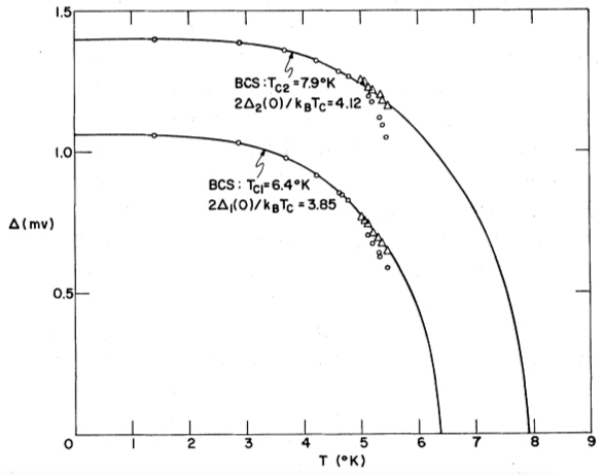

Figure 4.5: Energy gap Δ *vs.* absolute temperature T for Ga_1 and Ga_2 films according to [149]. Solid lines represents the BCS temperature dependence. Also is labeled the apparently strong coupling value compared with the universal gap-to-T_c ratio above of 3.53. The authors pointed out that they have corrected experimental data (triangles).

In Fig. 4.6 is plotted the energy gap dimensionless with Fermi energy *vs.* T/T_c for 50-50 symmetry of superconductor Ga, and the 100-0 curve with $n/n_f = 1$ alongside with experimental data of Ga_1 and Ga_2 films. The 50-50 curve predicts quiet well the energy gap of ordinary Ga, $\Delta(0)_{ord} = 1.41 \times 10^{-5} E_F$, but the 0-100 curve not. Nevertheless, this two curves are substantially below from the experimental energy gap data for Ga_1 and Ga_2. If one changes the dimensionless number density as $n/n_f = 0.9998929$ for Ga_1 and $n/n_f = 0.9998393$ for Ga_2 the energy gap curve for each film changes to fit experimental data. The criterion

to adjust the curves was fitted to energy gap value at zero temperature.

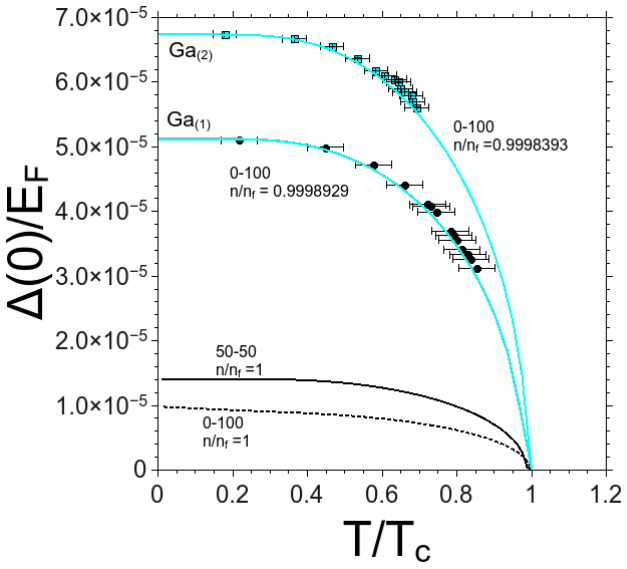

Figure 4.6: Energy gap dimensioless with Fermi energy $\Delta(T)/E_F$ vs. T/T_c for Ga_1 and Ga_2 films according to [149]. Black curve represents the 50-50 curve for the ordinary Ga with experimental $\Delta(0)_{ord} \simeq 1.55 \times 10^{-5} E_F$ while 50-50 predicts $\Delta(0)_{50-50} = 1.41 \times 10^{-5} E_F$. Dashed curve for 0-100 proportions with $\Delta(0)_{100-0} \simeq 9.8 \times 10^{-6} E_F$. Light gray curves represent the 0-100 proportions changing n/n_f, for Ga_1 with $n/n_f = 0.9998929$, for Ga_2 with $n/n_f = 0.9998393$. Note that if one changes solely the dimensionless number density, one can fit to experimental data, here n/n_f is illustrated as dimensionless coupling constant.

Cohen *et al.* [149] asserts that the change in the energy gaps so as their critical temperatures is due to a change in the density of states (DOS), which in turn is related with the number density of particles. Furthermore, they computed the BCS coupling constants via the BCS weak-coupling formula using different DOS. Surprisingly, the λ_{BCS} for different Ga films is below of the Bogoliubov *et al.* upper limit $\lambda_{BCS} \leq 1/2$. Cohen *et al.* arguing that they have different dirty films but the modifications to High-T_c films observed by others authors were for amorphous Ga [150], γ Ga [151] and β Ga [152], has the values presented in their work is very close to the aforementioned Ga phases. This suggests that number density of particles changes two important properties of superconductors, the energy gap and the critical temperature. Properties that has been studied in this thesis work.

If one changes the dimensionless number density slightly from unity one can be able to fit to experimental data with both kind of Cooper pairs, i.e., we can choose the 100-0 (2eCPs only) or the 0-100 (2hCPs only) proportions. This means that the perfect ideal symmetry between 2eCPs and 2hCPs (which coincides precisely with BCS theory) *only predicts* the energy gap at zero temperature or critical temperature at $n/n_f = 1$ as clearly illustrates in Fig. 3.12. Hence the requirement of the number equation to predicts correctly, the energy gap as well as the critical temperature.

Furthermore, the results presented here are consistent with experimental findings by Uemura *et al* [153]. as well as by Božović *et al.* [154] where it was concluded that critical temperatures T_c are driven by the superfluid number density.

Conclusions

In the GBEC theory is subsumed the BCS-Bose crossover extended with explicit inclusion of 2hCPs, starting from an ideal BF ternary gas with specific boson-fermion vertex interactions. The extended crossover is defined by two thermodynamic-equilibrium requirements along with a well-known result from statistical mechanics that guarantees charge conservation which lacking in BCS theory. Upon increasing the dimensionless number density n/n_f one increases T_c several orders higher wrt BCS theory and also the well-known BEC ratio $T_c/T_F \simeq 0.218$, with T_c the transition temperature of an ideal Bose gas composed by paired fermions.

Two coupling extremes emerge by varying n/n_f: a weak-coupling regime at $n/n_f = 1$, all electrons are unbound (or *correlated* as in BCS theory); a strong-coupling regime at $n/n_f \to \infty$, or, e.g., $n_f \to 0$ meaning that no unbound electrons remain in the system since all electrons are paired up into bosons. Of course, the intermediate coupling whenever $1 < n/n_f < \infty$. The GBEC dimensionless number density n/n_f can in principle be correlated with any other dimensionless coupling constant such as the BCS λ_{BCS}. Ignoring 2hCPs the energy-gap curve departs substantially below from the curve with 50-50 symmetry and most importantly from the data meaning, unequivocally, that 2hCPs are *indispensable* in describing superconductivity. Guided by the Bogoliubov *et al.* upper limit of $\lambda_{BCS} \leq 1/2$ one finds that the extended crossover predicts T_c/T_F values of several elemental superconductors with perfect ideal symmetry between 2eCPs and 2hCPs which agree reasonably well with experimental data. Furthermore, the analysis of Ga shows the role played by 2hCPs, which can be varied slightly from unity via n/n_f to match the data even for strong-coupling superconductors. Besides, it evidences the critical role played by both kinds of excited pairs such as increased T_cs.

Also shown is that n/n_f slightly varied can give the correct gap-to-T_c ratio even for the BCS "bad actors" Hg and Pb. Also the results presented here is consistent with the experimental assertion by Uemura *et al*. as well as I. Božović *et al*. that the number density of charge carriers driven the critical temperature of a superconductor. This study leads to the important conclusion that changing the total electron number particles, even with the assumption that CPs have been formed with electron-phonon dynamics the whole system changes from weak-coupling regime to strong-coupling regime.

Future work is to compare the extended BCS-Bose crossover thermodynamic properties with experimental data for the aforementioned superconductors, e.g., the critical magnetic field which is an essential part of superconductivity either as a thermodynamic property or by adding a magnetic-energy term to the Hamiltonian. Also, we plan to study a boson-fermion mixture with at least two-energy bands in the electronic structure.

Appendix A

"Electron" and "hole" Fermi and Bose Creation/Annihilation Operators

A.1 Fermions

For single fermions, as for any Fermi-particles, we are able to use two alternative mathematically equivalent *representations* – so-called "electron" and "hole" ones. Thus we can speak instead of "electrons" of "holes," which fermions remain vacant after themselves, as about new individual Fermi-particles.

Indeed, it is always possible to perform the *canonical transformation* (i.e. taking invariant the form of canonical anticommutation relations) of fermion creation and annihilation operators in such a way that we shall consider the creation operator as the annihilation one, and the annihilation operator as the creation one, i.e. we can consider new so-called "hole" Fermi-operators (designate with a special superscript index "h"). Specifically,

$$a^{+h}_{\mathbf{k},s} = a_{\mathbf{k},s} \qquad a^{h}_{\mathbf{k},s} = a^{+}_{\mathbf{k},s}. \tag{A.1}$$

Obviously, "hole fermion" operators satisfy Fermi anticommutation relations

$$\begin{aligned}
\left\{a^{+h}_{\mathbf{k},s},\, a^{+h}_{\mathbf{k}',s'}\right\} &= a^{+h}_{\mathbf{k},s}a^{+h}_{\mathbf{k}',s'} + a^{+h}_{\mathbf{k}',s'}a^{+h}_{\mathbf{k},s} = 0 \\
\left\{a^{h}_{\mathbf{k},s},\, a^{h}_{\mathbf{k}',s'}\right\} &= a^{h}_{\mathbf{k},s}a^{h}_{\mathbf{k}',s'} + a^{h}_{\mathbf{k}',s'}a^{h}_{\mathbf{k},s} = 0 \\
\left\{a^{h}_{\mathbf{k},s},\, a^{+h}_{\mathbf{k}',s'}\right\} &= a^{h}_{\mathbf{k},s}a^{+h}_{\mathbf{k}',s'} + a^{+h}_{\mathbf{k}',s'}a^{h}_{\mathbf{k},s} = \delta_{\mathbf{k}',\mathbf{k}}\delta_{s',s}.
\end{aligned} \tag{A.2}$$

The particle and hole occupation number operators are connected with each other by the simple relation

$$\begin{aligned}
\hat{n}^{h}_{\mathbf{k},s} &= 1 - \hat{n}_{\mathbf{k},s} \\
\hat{n}^{h}_{\mathbf{k},s} \equiv a^{+h}_{\mathbf{k},s}a^{h}_{\mathbf{k},s} \qquad \hat{n}_{\mathbf{k},s} &\equiv a^{+}_{\mathbf{k},s}a_{\mathbf{k},s}.
\end{aligned} \tag{A.3}$$

Eigenvalues of either operators $\hat{n}_{\mathbf{k},s}$ and $\hat{n}^{h}_{\mathbf{k},s}$ take on values 0 or 1. These eigenvalues are connected with

each other by the same relation as operators themselves: because the same one-particle states $\mathbf{k}, s$ are eigenstates for each of them.

If the state $\mathbf{k}, s$ is occupied by an "electron," i.e., $n_{\mathbf{k},s} = 1$, then this state lacks a "hole," i.e., $n^h_{\mathbf{k},s} = 0$. And vice versa, if the state $\mathbf{k}, s$ is empty of an "electron," i.e., $n_{\mathbf{k},s} = 0$, then it is occupied by a "hole," i.e., $n^h_{\mathbf{k},s} = 1$. This can be easily seen with the application of (A.3) to the vacuum state and consequently when we change "electron" creation and annihilation operators to "hole" creation and annihilation operators the Hamiltonian of system of noninteracting fermions transforms as

$$\hat{H} \equiv \sum_{\mathbf{k},s} \epsilon_k a^+_{\mathbf{k},s} a_{\mathbf{k},s} = -\sum_{\mathbf{k},s} \epsilon_k a^{+h}_{\mathbf{k},s} a^h_{\mathbf{k},s} \tag{A.4}$$

and the total number of fermions as

$$\hat{N} \equiv \sum_{\mathbf{k},s} a^+_{\mathbf{k},s} a_{\mathbf{k},s} = -\sum_{\mathbf{k},s} a^{+h}_{\mathbf{k},s} a^h_{\mathbf{k},s}. \tag{A.5}$$

Note the appearance of minus signs on both right hand sides.

Thus, fermions as well as any Fermi-particles in the second quantization representation can be described equally well in "electron" or in the "hole" representation; both descriptions are mathematically equivalent. In the present paper, following tradition, we will use only "electron" representation for fermions, not "hole" one.

A.2 Bosons

For 2e or 2h, as for any Bose particles, as well as for Fermi particles, we can also use one of two mathematically equivalent alternative representations, "electron" or "hole." In contrast with Fermi-particles, however, now "hole Bose" operators do *not* satisfy ordinary Bose commutation relations, and for this reason we must talk now about "hole bosons" as a special kind of individual quantum particles. The transformation from "electron" to "hole" bosons is *not* canonical now (i.e., does *not* conserve invariant the commutation relations for creation and annihilation operators).

Let us suppose that he creation "electron" operator is precisely the annihilation "hole" operator, and vice versa, namely

$$c^\dagger_{\mathbf{K}} = b_{\mathbf{K}} \qquad c_{\mathbf{K}} = b^\dagger_{\mathbf{K}} \tag{A.6}$$

where we have used the letter "c" to designate "hole Bose" operators. These operators satisfy the commutation relations

$$\begin{aligned} \left[c^\dagger_{\mathbf{K}},\, c^\dagger_{\mathbf{K}'}\right] &= c^\dagger_{\mathbf{K}} c^\dagger_{\mathbf{K}'} - c^\dagger_{\mathbf{K}'} c^\dagger_{\mathbf{K}} = 0 \\ \left[c_{\mathbf{K}},\, c_{\mathbf{K}'}\right] &= c_{\mathbf{K}} c_{\mathbf{K}'} - c_{\mathbf{K}'} c_{\mathbf{K}} = 0 \\ \left[c_{\mathbf{K}},\, c^\dagger_{\mathbf{K}'}\right] &= c_{\mathbf{K}} c^\dagger_{\mathbf{K}'} - c^\dagger_{\mathbf{K}'} c_{\mathbf{K}} = -\delta_{\mathbf{K}',\mathbf{K}} \end{aligned} \tag{A.7}$$

which we obtain immediately from the ordinary Bose commutation relations valid for operators $b^{+}_{\mathbf{K}}$ and $b_{\mathbf{K}}$. In contrast with Bose relations the commutation relations now obtained (for "hole Bose-operators") have *minus signs* before Kronecker symbol $\delta_{\mathbf{K}',\mathbf{K}}$ on the right hand side of the last equation. This means in particular that occupation numbers of hole Bose operators $\hat{M}_{\mathbf{K}} = c^{\dagger}_{\mathbf{K}} c_{\mathbf{K}}$ have negative eigenvalues: $0, -1, -2, \cdots -\infty$.

For the Hamiltonian of noninteracting hole bosons and for the operator of total number of them we have formulas:

$$\begin{aligned} \hat{H} &= \sum_{\mathbf{K}} E_{-}(K) c^{\dagger}_{\mathbf{K}} c_{\mathbf{K}} \\ \hat{M} &= \sum_{\mathbf{K}} c^{\dagger}_{\mathbf{K}} c_{\mathbf{K}} \end{aligned} \tag{A.8}$$

where $E_{-}(K) = E_{-}(0) - \hbar^2 K^2/2(2m)$, with $\hat{M}$ the hole boson number particle operator and $E(0)$ is the energy of *motionless* or center-momentum-of-mass of hole boson (positive or negative), m is the effective mass of hole Boson which itself is *negative* (because hole Boson has *negative kinetic energy*).

Eigenvalues of operators $\hat{H}$ and $\hat{N}$ we can write as follows:

$$E_{\ldots N_{\mathbf{K}} \ldots} = \sum_{\mathbf{K}} E_{+}(K) N_{\mathbf{K}}, \qquad N_{\ldots N_{\mathbf{K}} \ldots} = \sum_{\mathbf{K}} N_{\mathbf{K}}. \tag{A.9}$$

where $N_{\mathbf{K}}$ is the electron boson number particle operator, this implies that $M_{\mathbf{K}} = -N_{\mathbf{K}}$, these formulas (A.9) become

$$E_{\ldots M_{\mathbf{K}} \ldots} = -\sum_{\mathbf{K}} E_{-}(K) M_{\mathbf{K}}, \qquad M_{\ldots M_{\mathbf{K}} \ldots} = -\sum_{\mathbf{K}} M_{\mathbf{K}}. \tag{A.10}$$

Thus in "electron" representation of "hole bosons"' for their Hamiltonian and the operator of total number of particles we have

$$\hat{H} = \sum_{\mathbf{K}} \varepsilon_K c^{\dagger}_{\mathbf{K}} c_{\mathbf{K}} \qquad \hat{M} = -\sum_{\mathbf{K}} c^{\dagger}_{\mathbf{K}} c_{\mathbf{K}} \tag{A.11}$$

where $\varepsilon_K = -E_{-}(K) = E(0) + \hbar^2 K^2/2(2m)$. "Electron" representation of Bose operators in this paper we use both for *2h* and for 2e.

Appendix B

GBEC Thermodynamic Properties

The thermodynamic properties can be found from (2.61) as follows, the pressure is

$$P(T,n) = -\frac{\Omega}{L^3} \tag{B.1}$$

the entropy

$$\frac{S(T,n)}{L^3} = -\frac{\partial}{\partial T}\left(\frac{\Omega}{L^3}\right) \tag{B.2}$$

the specific heat

$$C_V(T,n) = T\frac{\partial}{\partial T}\left(\frac{S(T,n)}{L^3}\right) = -T\frac{\partial^2}{\partial T^2}\left(\frac{\Omega}{L^3}\right) \tag{B.3}$$

the Helmholtz free energy

$$F(T,n) = -P(T,n) + n\,\mu(T,n) \tag{B.4}$$

since $F(T,L^3,n) \equiv \Omega + \mu N$. This leads to find out the Helmholtz free energy at superconducting and normal state for any finite temperature, specifically $E_{cond}(T,n) = [F_{\mathsf{s}}(T,n) - F_{\mathsf{n}}(T,n)]/L^3F_F$ as

$$\begin{aligned} E_{cond} &\equiv \frac{F_{\mathsf{s}}(T,n)}{L^3} - \frac{F_{\mathsf{n}}(T,n)}{L^3} \\ &= P_{\mathsf{s}}(T,n) - P_{\mathsf{n}}(T,n) + n\,[\mu_{\mathsf{s}}(T,n) - \mu_{\mathsf{n}}(T,n)] \end{aligned} \tag{B.5}$$

where subindex s and n denote superconductor and normal phases, respectively.

B.1 GBEC state equation

From (B.1) one can find the state equation of GBEC as follows, the pressure is

$$\begin{aligned} P(T,n) &= -\int_0^\infty d\epsilon N(\epsilon)\left[\epsilon-\mu-E(\epsilon)\right]+2k_BT\int_0^\infty d\epsilon N(\epsilon)\ln\left\{1+\exp\left[-\beta E(\epsilon)\right]\right\} \\ &- \left[E_+(0)-2\mu\right]n_0-k_BT\int_0^\infty d\varepsilon M(\varepsilon)\ln\left\{1-\exp\left[-\beta\mathcal{E}_+(\varepsilon)\right]\right\} \\ &- \left[2\mu-E_-(0)\right]m_0-k_BT\int_0^\infty d\varepsilon M(\varepsilon)\ln\left\{1-\exp\left[-\beta\mathcal{E}_-(\varepsilon)\right]\right\} \end{aligned} \tag{B.6}$$

dimensionless with respect to Fermi energy E_F and multiplying both sides by $1/k_BT$ one has

$$\begin{aligned} \frac{P(T,n)}{nk_BT} &= -\frac{3}{4}\int_0^\infty d\tilde{\epsilon}\frac{\sqrt{\tilde{\epsilon}}}{\tilde{T}}\left[\tilde{\epsilon}-\tilde{\mu}-\sqrt{(\tilde{\epsilon}-\tilde{\mu})^2+\tilde{\Delta}^2}\right] \\ &+ \frac{6}{4}\int_0^\infty d\tilde{\epsilon}\sqrt{\tilde{\epsilon}}\ \ln\left\{1+\exp\left[\frac{\sqrt{(\tilde{\epsilon}-\tilde{\mu})^2+\tilde{\Delta}^2}}{\tilde{T}}\right]\right\} \\ &- \frac{n_0(\tilde{T})}{n}\left[\frac{2(n/n_f)^{-2/3}+\delta\tilde{\epsilon}-2\tilde{\mu}}{\tilde{T}}\right]-\frac{m_0(\tilde{T})}{n}\left[\frac{-2(n/n_f)^{-2/3}+\delta\tilde{\epsilon}+2\tilde{\mu}}{\tilde{T}}\right] \\ &- \frac{6}{2^{3/2}}\int_0^\infty d\tilde{\varepsilon}\sqrt{\tilde{\varepsilon}}\ \ln\left\{1-\exp\left[-\frac{\tilde{\varepsilon}+2(n/n_f)^{-2/3}+\delta\tilde{\epsilon}-2\tilde{\mu}}{\tilde{T}}\right]\right\} \\ &- \frac{6}{2^{3/2}}\int_0^\infty d\tilde{\varepsilon}\sqrt{\tilde{\varepsilon}}\ \ln\left\{1-\exp\left[-\frac{\tilde{\varepsilon}-2(n/n_f)^{-2/3}+\delta\tilde{\epsilon}+2\tilde{\mu}}{\tilde{T}}\right]\right\} \end{aligned} \tag{B.7}$$

where tilde means dimensionless with respect to Fermi energy and $n_0(\tilde{T})/n$, $m_0(\tilde{T})/n$ are the condensate fraction for 2eCPs and 2hCPs respectively.

B.2 GBEC Entropy

The entropy is

$$\frac{S(T,n)}{L^3}=-\frac{\partial}{\partial T}\left(\frac{\Omega}{L^3}\right) \tag{B.8}$$

taking the first derivative of (2.61), implies

$$\begin{aligned} \frac{S(T,n)}{L^3} &= 2\int_0^\infty d\epsilon N(\epsilon)\left[\frac{E(\epsilon)}{T}\frac{\exp[-\beta E(\epsilon)]}{\exp[-\beta E(\epsilon)]+1}+k_B\ln\left\{1+\exp[-\beta E(\epsilon)]\right\}\right] \\ &+ 2\int_0^\infty d\varepsilon M(\varepsilon)\left[\frac{\mathcal{E}_+(\varepsilon)}{T}\frac{\exp[-\beta\mathcal{E}_+(\varepsilon)]}{1-\exp[-\beta\mathcal{E}_+(\varepsilon)]}-k_B\ln\left\{1-\exp[-\beta\mathcal{E}_+(\varepsilon)]\right\}\right] \\ &+ 2\int_0^\infty d\varepsilon M(\varepsilon)\left[\frac{\mathcal{E}_-(\varepsilon)}{T}\frac{\exp[-\beta\mathcal{E}_-(\varepsilon)]}{1-\exp[-\beta\mathcal{E}_-(\varepsilon)]}-k_B\ln\left\{1-\exp[-\beta\mathcal{E}_-(\varepsilon)]\right\}\right] \end{aligned} \tag{B.9}$$

made dimensionless with Fermi energy one has

$$
\begin{aligned}
S(T,n)/L^3 &= \frac{2}{2^{1/2}} S_F \int_0^\infty d\tilde{\epsilon}\sqrt{\tilde{\epsilon}} \left(\frac{\sqrt{(\tilde{\epsilon}-\tilde{\mu})^2+\tilde{\Delta}^2}}{\tilde{T}} \right) \\
&\times \left[\frac{\exp[-\frac{\sqrt{(\tilde{\epsilon}-\tilde{\mu})^2+\tilde{\Delta}^2}}{\tilde{T}}]}{\left(1+\exp[-\frac{\sqrt{(\tilde{\epsilon}-\tilde{\mu})^2+\tilde{\Delta}^2}}{\tilde{T}}]\right)} - \ln\left\{1+\exp[-\frac{\sqrt{(\tilde{\epsilon}-\tilde{\mu})^2+\tilde{\Delta}^2}}{\tilde{T}}]\right\} \right] \\
&+ 2S_F \int_0^\infty d\tilde{\varepsilon}\sqrt{\tilde{\varepsilon}} \left(\frac{(\tilde{\varepsilon}+2(n/n_f)^{-2/3}+\delta\tilde{\epsilon}-2\tilde{\mu})}{\tilde{T}} \right) \\
&\times \left[\frac{\exp[-\frac{\tilde{\varepsilon}+2(n/n_f)^{-2/3}+\delta\tilde{\epsilon}-2\tilde{\mu}}{\tilde{T}}]}{\left(1-\exp[-\frac{\tilde{\varepsilon}+2(n/n_f)^{-2/3}+\delta\tilde{\epsilon}-2\tilde{\mu}}{\tilde{T}}]\right)} - \ln\left\{1-\exp[-\frac{\tilde{\varepsilon}+2(n/n_f)^{-2/3}+\delta\tilde{\epsilon}-2\tilde{\mu}}{\tilde{T}}]\right\} \right] \\
&+ 2S_F \int_0^\infty d\tilde{\varepsilon}\sqrt{\tilde{\varepsilon}} \left(\frac{(\tilde{\varepsilon}-2(n/n_f)^{-2/3}+\delta\tilde{\epsilon}+2\tilde{\mu})}{\tilde{T}} \right) \\
&\times \left[\frac{\exp[-\frac{\tilde{\varepsilon}-2(n/n_f)^{-2/3}+\delta\tilde{\epsilon}+2\tilde{\mu}}{\tilde{T}}]}{\left(1-\exp[-\frac{\tilde{\varepsilon}-2(n/n_f)^{-2/3}+\delta\tilde{\epsilon}+2\tilde{\mu}}{\tilde{T}}]\right)} - \ln\left\{1-\exp[-\frac{\tilde{\varepsilon}-2(n/n_f)^{-2/3}+\delta\tilde{\epsilon}+2\tilde{\mu}}{\tilde{T}}]\right\} \right]
\end{aligned}
$$

where $S_F = k_B m^{3/2} E_F^{3/2}/\pi^2\hbar^3$. Made dimensionless with $S_f = k_B m^{3/2} E_f^{3/2}/\pi^2\hbar^3$ the entropy of unbound electrons gives

$$
\begin{aligned}
\frac{S(T,n)}{L^3\, S_f} &= \frac{2}{2^{1/2}} \left(\frac{n}{n_f}\right)^{3/2} \int_0^\infty d\tilde{\epsilon}\sqrt{\tilde{\epsilon}} \left(\frac{\sqrt{(\tilde{\epsilon}-\tilde{\mu})^2+\tilde{\Delta}^2}}{\tilde{T}} \right) \\
&\times \left[\frac{\exp[-\frac{\sqrt{(\tilde{\epsilon}-\tilde{\mu})^2+\tilde{\Delta}^2}}{\tilde{T}}]}{\left(1+\exp[-\frac{\sqrt{(\tilde{\epsilon}-\tilde{\mu})^2+\tilde{\Delta}^2}}{\tilde{T}}]\right)} - \ln\left\{1+\exp[-\frac{\sqrt{(\tilde{\epsilon}-\tilde{\mu})^2+\tilde{\Delta}^2}}{\tilde{T}}]\right\} \right] \\
&+ 2\left(\frac{n}{n_f}\right)^{3/2} \int_0^\infty d\tilde{\varepsilon}\sqrt{\tilde{\varepsilon}} \left(\frac{(\tilde{\varepsilon}+2(n/n_f)^{-2/3}+\delta\tilde{\epsilon}-2\tilde{\mu})}{\tilde{T}} \right) \\
&\times \left[\frac{\exp[-\frac{\tilde{\varepsilon}+2(n/n_f)^{-2/3}+\delta\tilde{\epsilon}-2\tilde{\mu}}{\tilde{T}}]}{\left(1-\exp[-\frac{\tilde{\varepsilon}+2(n/n_f)^{-2/3}+\delta\tilde{\epsilon}-2\tilde{\mu}}{\tilde{T}}]\right)} - \ln\left\{1-\exp[-\frac{\tilde{\varepsilon}+2(n/n_f)^{-2/3}+\delta\tilde{\epsilon}-2\tilde{\mu}}{\tilde{T}}]\right\} \right] \\
&+ 2\left(\frac{n}{n_f}\right)^{3/2} \int_0^\infty d\tilde{\varepsilon}\sqrt{\tilde{\varepsilon}} \left(\frac{(\tilde{\varepsilon}-2(n/n_f)^{-2/3}+\delta\tilde{\epsilon}+2\tilde{\mu})}{\tilde{T}} \right) \\
&\times \left[\frac{\exp[-\frac{\tilde{\varepsilon}-2(n/n_f)^{-2/3}+\delta\tilde{\epsilon}+2\tilde{\mu}}{\tilde{T}}]}{\left(1-\exp[-\frac{\tilde{\varepsilon}-2(n/n_f)^{-2/3}+\delta\tilde{\epsilon}+2\tilde{\mu}}{\tilde{T}}]\right)} - \ln\left\{1-\exp[-\frac{\tilde{\varepsilon}-2(n/n_f)^{-2/3}+\delta\tilde{\epsilon}+2\tilde{\mu}}{\tilde{T}}]\right\} \right]
\end{aligned}
\tag{B.10}
$$

where $S_F/S_f = (n/n_f)^{3/2}$.

B.3 GBEC Specific Heat

The specific heat at constant volume in equilibrium state by T and n is given by

$$\frac{C(T,n)}{L^3} = T\frac{\partial}{\partial T}\left(\frac{S(T,n)}{L^3}\right)_{V,\mu} \tag{B.11}$$

Then the specific heat is

$$\frac{C(T,n)}{L^3} = -T\frac{\partial^2}{\partial T^2}\left(\frac{\Omega}{L^3}\right)_{V,\mu} \tag{B.12}$$

this implies that

$$\begin{aligned}\frac{C(T,n)}{L^3} &= 2\int_0^\infty d\epsilon N(\epsilon)\left(\frac{E^2(\epsilon)}{k_BT^2}\right)\left[\frac{\exp[\beta E(\epsilon)]}{(\exp[\beta E(\epsilon)]+1)^2}\right] \\ &+ 2\int_0^\infty d\varepsilon M(\varepsilon)\left(\frac{\mathcal{E}_+^2(\varepsilon)}{k_BT^2}\right)\left[\frac{\exp[\beta\mathcal{E}_+(\varepsilon)]}{(\exp[\beta\mathcal{E}_+(\varepsilon)]-1)^2}\right] \\ &+ 2\int_0^\infty d\varepsilon M(\varepsilon)\left(\frac{\mathcal{E}_-^2(\varepsilon)}{k_BT^2}\right)\left[\frac{\exp[\beta\mathcal{E}_-(\varepsilon)]}{(\exp[\beta\mathcal{E}_-(\varepsilon)]-1)^2}\right].\end{aligned} \tag{B.13}$$

made dimensionless with Fermi energy gives

$$\begin{aligned}\frac{C(T,n)}{L^3} &= \frac{2}{2^{1/2}}\int_0^\infty d\tilde{\epsilon}\, C_F\left(\frac{\sqrt{\tilde{\epsilon}}}{\tilde{T}^2}\right)[(\tilde{\epsilon}-\tilde{\mu})^2+\tilde{\Delta}^2]\left(\frac{\exp\left[\frac{\sqrt{(\tilde{\epsilon}-\tilde{\mu})^2+\tilde{\Delta}^2}}{\tilde{T}}\right]}{\left(\exp\left[\frac{\sqrt{(\tilde{\epsilon}-\tilde{\mu})^2+\tilde{\Delta}^2}}{\tilde{T}}\right]+1\right)^2}\right) \\ &+ 2\int_0^\infty d\tilde{\varepsilon}\, C_F\left(\frac{\sqrt{\tilde{\varepsilon}}}{\tilde{T}^2}\right)\left[\tilde{\varepsilon}+2(n/n_f)^{-2/3}+\delta\tilde{\epsilon}-2\tilde{\mu}\right]^2 \\ &\times \left(\frac{\exp\left[\frac{\tilde{\varepsilon}+2(n/n_f)^{-2/3}+\delta\tilde{\epsilon}-2\tilde{\mu}}{\tilde{T}}\right]}{\left(\exp\left[\frac{\tilde{\varepsilon}+2(n/n_f)^{-2/3}+\delta\tilde{\epsilon}-2\tilde{\mu}}{\tilde{T}}\right]-1\right)^2}\right) \\ &+ 2\int_0^\infty d\tilde{\varepsilon}\, C_F\left(\frac{\sqrt{\tilde{\varepsilon}}}{\tilde{T}^2}\right)\left[\tilde{\varepsilon}-2(n/n_f)^{-2/3}+\delta\tilde{\epsilon}+2\tilde{\mu}\right]^2 \\ &\times \left(\frac{\exp\left[\frac{\tilde{\varepsilon}-2(n/n_f)^{-2/3}+\delta\tilde{\epsilon}+2\tilde{\mu}}{\tilde{T}}\right]}{\left(\exp\left[\frac{\tilde{\varepsilon}-2(n/n_f)^{-2/3}+\delta\tilde{\epsilon}+2\tilde{\mu}}{\tilde{T}}\right]-1\right)^2}\right)\end{aligned} \tag{B.14}$$

where $C_F \equiv k_B m^{3/2} E_F^{3/2}/\pi^2\hbar^3$. Finally one can dimensionless with specific heat of unbound electrons $C_f \equiv k_B m^{3/2} E_f^{3/2}/\pi^2\hbar^3$, this gives

$$\begin{aligned}
\frac{C(T,n)}{L^3 C_f} &= \frac{2}{2^{1/2}}\left(\frac{n}{n_f}\right)^{3/2}\int_0^\infty d\tilde{\epsilon}\,\left(\frac{\sqrt{\tilde{\epsilon}}}{\tilde{T}^2}\right)[(\tilde{\epsilon}-\tilde{\mu})^2+\tilde{\Delta}^2] \\
&\times \left(\frac{\exp\left[\frac{\sqrt{(\tilde{\epsilon}-\tilde{\mu})^2+\tilde{\Delta}^2}}{\tilde{T}}\right]}{\left(\exp\left[\frac{\sqrt{(\tilde{\epsilon}-\tilde{\mu})^2+\tilde{\Delta}^2}}{\tilde{T}}\right]+1\right)^2}\right) \\
&+ 2\left(\frac{n}{n_f}\right)^{3/2}\int_0^\infty d\tilde{\varepsilon}\,\left(\frac{\sqrt{\tilde{\varepsilon}}}{\tilde{T}^2}\right)\left[\tilde{\varepsilon}+2(n/n_f)^{-2/3}+\delta\tilde{\epsilon}-2\tilde{\mu}\right]^2 \\
&\times \left(\frac{\exp\left[\frac{\tilde{\varepsilon}+2(n/n_f)^{-2/3}+\delta\tilde{\epsilon}-2\tilde{\mu}}{\tilde{T}}\right]}{\left(\exp\left[\frac{\tilde{\varepsilon}+2(n/n_f)^{-2/3}+\delta\tilde{\epsilon}-2\tilde{\mu}}{\tilde{T}}\right]-1\right)^2}\right) \\
&+ 2\left(\frac{n}{n_f}\right)^{3/2}\int_0^\infty d\tilde{\varepsilon}\,\left(\frac{\sqrt{\tilde{\varepsilon}}}{\tilde{T}^2}\right)\left[\tilde{\varepsilon}-2(n/n_f)^{-2/3}+\delta\tilde{\epsilon}+2\tilde{\mu}\right]^2 \\
&\times \left(\frac{\exp\left[\frac{\tilde{\varepsilon}-2(n/n_f)^{-2/3}+\delta\tilde{\epsilon}+2\tilde{\mu}}{\tilde{T}}\right]}{\left(\exp\left[\frac{\tilde{\varepsilon}-2(n/n_f)^{-2/3}+\delta\tilde{\epsilon}+2\tilde{\mu}}{\tilde{T}}\right]-1\right)^2}\right)
\end{aligned} \tag{B.15}$$

since $C_F/C_f = (n/n_f)^{3/2}$.

B.4 Helmholtz Free Energy

From (2.61) the Helmholtz free energy is

$$F(T,n) = -P(T,n) + n\,\mu(T,n)$$

since $F(T,L^3,n) \equiv \Omega + \mu N$. Therefore

$$\begin{aligned}
\frac{F(T,n)}{L^3} &= \int_0^\infty d\epsilon N(\epsilon)\,[\epsilon-\mu-E(\epsilon)] \\
&- 2k_BT\int_0^\infty d\epsilon N(\epsilon)\ln\{1+\exp[-\beta E(\epsilon)]\} \\
&+ [E_+(0)-2\mu]n_0 + k_BT\int_0^\infty d\varepsilon M(\varepsilon)\ln\{1-\exp[-\beta\mathcal{E}_+(\varepsilon)]\} \\
&+ [2\mu-E_-(0)]m_0 + k_BT\int_0^\infty d\varepsilon M(\varepsilon)\ln\{1-\exp[-\beta\mathcal{E}_-(\varepsilon)]\} + n\mu(T)
\end{aligned}$$

made dimensionless with Fermi energy gives

$$\begin{aligned}
\frac{F(T,n)}{L^3} &= \frac{3}{4}F_F\int_0^\infty d\tilde{\epsilon}\frac{\sqrt{\tilde{\epsilon}}}{\tilde{T}}\left[\tilde{\epsilon}-\tilde{\mu}-\sqrt{(\tilde{\epsilon}-\tilde{\mu})^2+\tilde{\Delta}^2}\right] \\
&- \frac{6}{4}F_F\int_0^\infty d\tilde{\epsilon}\sqrt{\tilde{\epsilon}}\,\ln\left\{1+\exp\left[-\frac{\sqrt{(\tilde{\epsilon}-\tilde{\mu})^2+\tilde{\Delta}^2}}{\tilde{T}}\right]\right\} \\
&+ \frac{n_0(\tilde{T})}{n}F_F\left[\frac{2(n/n_f)^{-2/3}+\delta\tilde{\epsilon}-2\tilde{\mu}}{\tilde{T}}\right] \\
&+ \frac{m_0(\tilde{T})}{n}F_F\left[\frac{-2(n/n_f)^{-2/3}+\delta\tilde{\epsilon}+2\tilde{\mu}}{\tilde{T}}\right] \\
&+ \frac{6}{2^{3/2}}F_F\int_0^\infty d\tilde{\varepsilon}\sqrt{\tilde{\varepsilon}}\,\ln\left\{1-\exp\left[-\frac{\tilde{\varepsilon}+2(n/n_f)^{-2/3}+\delta\tilde{\epsilon}-2\tilde{\mu}}{\tilde{T}}\right]\right\} \\
&+ \frac{6}{2^{3/2}}F_F\int_0^\infty d\tilde{\varepsilon}\sqrt{\tilde{\varepsilon}}\,\ln\left\{1-\exp\left[-\frac{\tilde{\varepsilon}-2(n/n_f)^{-2/3}+\delta\tilde{\epsilon}+2\tilde{\mu}}{\tilde{T}}\right]\right\}+\frac{2}{3}\,\frac{\tilde{\mu}}{\tilde{T}}
\end{aligned} \tag{B.16}$$

where $F_F = 2^{1/2}m^{3/2}E_F^{5/2}/\pi^2\hbar^3$. Made dimensionless with $F_f = 2^{1/2}m^{3/2}E_f^{5/2}/\pi^2\hbar^3$ the Helmholtz free energy of unbound electrons gives

$$\begin{aligned}
\frac{F(T,n)}{L^3} &= \frac{3}{4}\left(\frac{n}{n_f}\right)^{2/3}\int_0^\infty d\tilde{\epsilon}\frac{\sqrt{\tilde{\epsilon}}}{\tilde{T}}\left[\tilde{\epsilon}-\tilde{\mu}-\sqrt{(\tilde{\epsilon}-\tilde{\mu})^2+\tilde{\Delta}^2}\right] \\
&- \frac{6}{4}\left(\frac{n}{n_f}\right)^{2/3}\int_0^\infty d\tilde{\epsilon}\sqrt{\tilde{\epsilon}}\,\ln\left\{1+\exp\left[-\frac{\sqrt{(\tilde{\epsilon}-\tilde{\mu})^2+\tilde{\Delta}^2}}{\tilde{T}}\right]\right\} \\
&+ \frac{n_0(\tilde{T})}{n}\left(\frac{n}{n_f}\right)^{2/3}\left[\frac{2(n/n_f)^{-2/3}+\delta\tilde{\epsilon}-2\tilde{\mu}}{\tilde{T}}\right] \\
&+ \frac{m_0(\tilde{T})}{n}\left(\frac{n}{n_f}\right)^{2/3}\left[\frac{-2(n/n_f)^{-2/3}+\delta\tilde{\epsilon}+2\tilde{\mu}}{\tilde{T}}\right] \\
&+ \frac{6}{2^{3/2}}\left(\frac{n}{n_f}\right)^{2/3}\int_0^\infty d\tilde{\varepsilon}\sqrt{\tilde{\varepsilon}}\,\ln\left\{1-\exp\left[-\frac{\tilde{\varepsilon}+2(n/n_f)^{-2/3}+\delta\tilde{\epsilon}-2\tilde{\mu}}{\tilde{T}}\right]\right\} \\
&+ \frac{6}{2^{3/2}}\left(\frac{n}{n_f}\right)^{2/3}\int_0^\infty d\tilde{\varepsilon}\sqrt{\tilde{\varepsilon}}\,\ln\left\{1-\exp\left[-\frac{\tilde{\varepsilon}-2(n/n_f)^{-2/3}+\delta\tilde{\epsilon}+2\tilde{\mu}}{\tilde{T}}\right]\right\}+\frac{2}{3}\,\frac{\tilde{\mu}}{\tilde{T}}
\end{aligned} \tag{B.17}$$

Therefore one can find the condensation energy for any $0 < T < T_c$, thus $E_{cond}(T,n) = F_{\mathsf{s}}(T,n)/L^3F_F -$

$F_{\mathsf{n}}(T,n)/L^3F_F$ is

$$
\begin{aligned}
E_{cond}(T,n) &= \frac{3}{4}\left(\frac{n}{n_f}\right)^{2/3}\int\limits_{(n/n_f)^{-2/3}-\delta\tilde{\epsilon}}^{(n/n_f)^{-2/3}+\delta\tilde{\epsilon}} d\tilde{\epsilon}\frac{\sqrt{\tilde{\epsilon}}}{\tilde{T}}\left[\tilde{\epsilon}-\tilde{\mu}-\sqrt{(\tilde{\epsilon}-\tilde{\mu})^2+\tilde{\Delta}^2}\right] \\
&- \frac{6}{4}\left(\frac{n}{n_f}\right)^{2/3}\int\limits_{(n/n_f)^{-2/3}-\delta\tilde{\epsilon}}^{(n/n_f)^{-2/3}+\delta\tilde{\epsilon}} d\tilde{\epsilon}\sqrt{\tilde{\epsilon}}\,\ln\left\{1+\exp\left[-\frac{\sqrt{(\tilde{\epsilon}-\tilde{\mu})^2+\tilde{\Delta}^2}}{\tilde{T}}\right]\right\} \\
&+ \frac{n_0(\tilde{T})}{n}\left(\frac{n}{n_f}\right)^{2/3}\left[\frac{2(n/n_f)^{-2/3}+\delta\tilde{\epsilon}-2\tilde{\mu}}{\tilde{T}}\right] \\
&+ \frac{m_0(\tilde{T})}{n}\left(\frac{n}{n_f}\right)^{2/3}\left[\frac{-2(n/n_f)^{-2/3}+\delta\tilde{\epsilon}+2\tilde{\mu}}{\tilde{T}}\right] \\
&+ \frac{6}{2^{3/2}}\left(\frac{n}{n_f}\right)^{2/3}\int_0^{\infty} d\tilde{\varepsilon}\sqrt{\tilde{\varepsilon}}\,\ln\left\{1-\exp\left[-\frac{\tilde{\varepsilon}+2(n/n_f)^{-2/3}+\delta\tilde{\epsilon}-2\tilde{\mu}}{\tilde{T}}\right]\right\} \\
&+ \frac{6}{2^{3/2}}\left(\frac{n}{n_f}\right)^{2/3}\int_0^{\infty} d\tilde{\varepsilon}\sqrt{\tilde{\varepsilon}}\,\ln\left\{1-\exp\left[-\frac{\tilde{\varepsilon}-2(n/n_f)^{-2/3}+\delta\tilde{\epsilon}+2\tilde{\mu}}{\tilde{T}}\right]\right\}.
\end{aligned}
\tag{B.18}
$$

since the normal and superconducting state are in equilibrium the contribution of chemical potential is zero.

Bibliography

[1] P.C.W. Chu, Sci. Am., **273**, 162 (1995)

[2] H.K. Onnes, Comm. Phys. Lab. Univ. Leiden **12**, 120 (1911)

[3] W. Meissner and R. Ochsenfeld. Naturwissenschaften **21** 44, 787 (1933)

[4] J. Hirsch, M.B. Maple, and F. Marsiglio, Physica C **514**, 1 (2015)

[5] C.P. Poole, Jr., H.A. Farach, R.J. Creswick, R. Prozorov, *Superconductivity*, 2nd. ed., (Academic Press, London, 2007)

[6] M.K. Wu, M.K. Wu, J.R. Ashburn, C.J. Torng *et al*. Phys. Rev. Lett. **58**, 908 (1987)

[7] F. London and H. London, Proc. Roy. Soc. A, **149**, 71 (1935)

[8] V.L. Ginzburg and L.D. Landau, Zh. Eksp. Teor. Fiz. (J. Exp. & Theo. Phys.) **20**, 1064 (1950)

[9] L. Landau and E. Lifshitz, *Física Estadística*, Volume 5, 2nd. Ed., (Ed. Revertè, México, 1964), p. 522

[10] E. Maxwell, Phys. Rev. **78**, 477 (1950)

[11] C.A. Reynolds, B. Serin, W. H. Wright, and L. B. Nesbitt, Phys. Rev. **78**, 487 (1950)

[12] H. Frölich, Phys. Rev. **79**, 845 (1950)

[13] H. Frölich , Proc. Roy. Soc, **A215**, 291 (1952)

[14] L.N. Cooper, Phys. Rev. **104**, 1189 (1956)

[15] L. P. Gor'kov, Zh. Eksp. Teor. Fiz. **36**, 1364 (1959)

[16] G.J. Bednorz and K.A. Müller, Z. Phys.B - Cond. Matt. **64**, 189 (1986)

[17] L. Gao, Y.Y. Xue, F. Chen, Q. Xiong, R.L. Meng, D. Ramírez, C.W. Chu, J.H. Eggert, and H.K. Mao, Phys Rev B **50**, 4260 (1994)

[18] D.A. Papaconstantopoulos, B.M. Klein, M.J. Mehl, and W.E. Pickett, Phys Rev B **91**, 184511 (2015)

[19] M.H. Anderson, J.R. Ensher, M.R. Wieman, and E.A. Cornell, Science **269**, 198 (1995)

[20] C.C. Bradley, C.A. Sackett, J.J. Tollett, and R.G. Hulet, Phys. Rev. Lett. **75**, 1687 (1995)

[21] K.B. Davis, M.O. Mewes, M.R. Andrews, N.J. van Drutten, D.S. Durfee, D.M. Kurn, and W. Ketterle, Phys. Rev. Lett. **75**, 3969 (1995)

[22] D.G. Fried, T.C. Killian, L. Willmann, D. Landhuis, S.C. Moss, D. Kleppner, and T.J. Greytak, Phys. Rev. Lett. **81**, 3811 (1998)

[23] S.L. Cornish, N.R. Claussen, J.L. Roberts, E.A. Cornell, and C.E. Wieman, Phys. Rev. Lett. **85**, 1795 (2000)

[24] F. Pereira Dos Santos, J. Léonard, J. Wang, C.J. Barrelet, F. Perales, E. Rasel, C.S. Unnikrishnan, M. Leduc, and C. Cohen-Tannoudji, Phys. Rev. Lett. **86**, 3459 (2001)

[25] G. Mondugno, G. Ferrari, G. Roati, R.J. Brecha, A. Simoni, and M. Inguscio, Science **294**, 1320 (2001)

[26] T. Weber, J. Herbig, M. Mark, H.C. Nagel, and R. Grimm, Science **299**, 232 (2003)

[27] A. Griesmaier, J. Werner, S. Hensler, J. Stuhler, and T. Pfau, Phys. Rev. Lett. **94**, 160401 (2005)

[28] Y. Takasu, K. Maki, K. Komori, T. Takano, K. Honda, M. Kumakura, T. Yabuzaki, and Y. Takahashi, Phys. Rev. Lett. **91**, 040404 (2003)

[29] T. Fukuhara, S. Sugawa, and Y. Takahashi, Phys. Rev. A **76**, 051604 (2007)

[30] T. Fukuhara, S. Sugawa, Y. Takasu, and Y. Takahashi, Phys. Rev. A **79**, 021601 (2009)

[31] S. Stellmer, M.K. Tey, R. Grimm, and F. Schreck, Phys. Rev. A **82**, 041602 (2010)

[32] A. Rosencwaig, Phys. Rev. B **67**, 184514 (2003)

[33] J.R. Schrieffer, *Theory of Superconductivity* (Benjamin, New York, 1963) p. 41

[34] L.V. Keldysh and Yu. V. Kopaev, Sov. Phys. Sol. St. **6**, 2219 (1965)

[35] V.N. Popov, Sov. Phys. JETP **50**, 1034 (1966)

[36] J. Labbé, F. Barisic, and J. Friedel, Phys. Rev. Lett. **19**, 1039 (1967)

[37] D.M. Eagles, Phys. Rev. **186**, 456 (1969)

[38] A.J. Leggett, J. Phys. (Paris). Colloq. **41** C7-19 (1980)

[39] For a review see M. Randeria in: *Bose-Einstein Condensation*, ed. A. Griffin *et al.* (Cambridge University, Cambridge, 1995) p. 355

[40] R.M. Carter, M. Casas, J.M. Getino, M. de Llano, A. Puente, H. Rubio, and D. van der Walt, Phys. Rev. B **52**, 16149 (1995)

[41] J. Bardeen, L. N. Cooper, and J. R. Schrieffer, Phys. Rev. **108**, 1175 (1957)

[42] M. Casas, M. Fortes, M. de Llano, A. Puente, and M.A. Solís, Int. J. Theor. Phys. **34**, 707 (1995)

[43] K. Miyake, Prog. Theor. Phys. **69**, 1794 (1983)

[44] M. de Llano, A. Salazar, and M.A. Solís, Rev. Mex. Fís. **51**, 626 (2005)

[45] P. Gosdzinsky and R. Tarrach, Am. J. Phys. **59**, 70 (1991)

[46] P. Nozières and S. Schmitt-Rink, J. Low. Temp. Phys. **59**, 195 (1985)

[47] J. Ranninger, R. Micnas, and S. Robaszkiewicz, Ann. Phys. Fr. **13**, 455 (1988)

[48] M. Randeria, J.M. Duan, and L.Y. Shieh, Phys. Rev. Lett. **62**, 981 (1989)

[49] D. van der Marel, Physica C **165**, 35 (1990)

[50] Y. Bar-Yam, Phys. Rev. B **43** 359 and 2601 (1991)

[51] M. Drechsler and W. Zwerger, Ann. der Physik **1**, 15 (1992)

[52] R. Haussmann, Phys. Rev. B **49**, 12975 (1994)

[53] F. Pistolesi and G.C. Strinati, Phys. Rev. B **53**, 15168 (1996)

[54] R.M. Quick, C. Esebbag and M. de Llano, Phys. Rev. B **47**, 11512 (1993)

[55] M.R. Schafroth, Phys. Rev. **96**, 1442 (1954)

[56] M.R. Schafroth, S.T. Butler, and J.M. Blatt, Helv. Phys. Acta **30**, 93 (1957)

[57] M.R. Schafroth, Sol. State Phys. **10**, 293 (1960)

[58] J.M. Blatt, *Theory of Superconductivity* (Academic Press, New York, 1964)

[59] N.N. Bogoliubov, JETP **34**, 41 (1958)

[60] N.N. Bogoliubov, V.V. Tolmachev, and D.V. Shirkov, Fortschr. Phys. **6**, 605 (1958); and also in *A New Method in the Theory of Superconductivity* (Consultants Bureau, NY, 1959)

[61] J. Ranninger and S. Robaszkiewicz, Physica B **135**, 468 (1985)

[62] J. Ranninger, R. Micnas, and S. Robaszkiewicz, Ann. Phys. Fr. **13**, 455 (1988)

[63] R. Micnas, J. Ranninger, and S. Robaszkiewicz, Revs. Mod. Phys. **62**, 113 (1998)

[64] R. Micnas, S. Robaszkiewicz, and A. Bussmann-Holder, Phys. Rev. B **66**, 104516 (2002)

[65] R. Micnas, S. Robaszkiewicz, and A. Bussmann-Holder, Struct. Bond **114**, 13 (2005)

[66] R. Friedberg and T.D. Lee, Phys. Rev. B **40**, 6745 (1989)

[67] R. Friedberg, T.D. Lee, and H.C. Ren, Phys. Rev. B **42**, 4122 (1990)

[68] R. Friedberg, T.D. Lee, and H.C. Ren, Phys. Lett. A **152**, 417 and 423 (1991)

[69] R. Friedberg, T.D. Lee, and H.C. Ren, Phys. Rev. B **45**, 10732 (1992)

[70] M. Casas, A. Rigo, M. de Llano, O. Rojo, and M.A. Solís, Phys. Lett. A **245**, 5 (1998)

[71] B.S. Deaver, Jr. and W.M. Fairbank, Phys. Rev. Lett. **7**, 43 (1961)

[72] R. Doll and M. Näbauer, Phys. Rev. Lett. **7**, 51 (1961)

[73] C.E., Gough, M.S. Colclough, E.M. Forgan, R.G. Jordan, M. Keene, C.M. Muirhead, I.M. Rae, N. Thomas, J.S. Abell, and S. Sutton, Nature **326**, 855 (1987)

[74] C.W. Schneider, G. Hammerl, G. Logvenov, T. Kopp, J.R. Kirtly, P.J. Hirschfeld, and J. Mannhart, Europhys Lett. **68** 86 (2004)

[75] A.A. Aligia, A.P. Kampf, and J. Mannhart, Phys. Rev. Lett. **94**, 247004 (2005)

[76] S.I. Koh, Physica C **191**, 167 (1992)

[77] S.I. Koh, Phys. Rev. **49**, 8983 (1994)

[78] P. Tarasewicz, Eur. Phys. J. B **41** 185 (2004)

[79] Y.M. Bunkov, A.S. Chen, D.J. Cousins, and H. Godfrin, Phys. Rev. Lett. **85**, 3456 (2000)

[80] H.C. Ren, Physica C **303**, 115 (1998)

[81] V.V. Tolmachev, Phys Lett. A **266**, 400 (2000)

[82] M. de Llano and V.V. Tolmachev, Physica A **317** (2003) 546

[83] A.J. Leggett, Nature Physics **2**, 134 (2006)

[84] P. Ehrenfest, J.R. Oppenheimer, Phys. Rev. **37**, 333 (1931)

[85] P. Nozières, S.Schmitt-Rink, J. Low Temp Phys. **59**, 195 (1985)

[86] J. Batle, M. Casas, M. Fortes, M. de Llano, F.J. Sevilla, M.A Solís, and V.V. Tolmachev, Cond. Mat. Theories **18**, 111 (2003)

[87] M. de Llano and V.V. Tolmachev, Ukrainian J. Phys. **55**, 79 (2010) and refs. therein

[88] M. Grether, M. de Llano, and V.V. Tolmachev, Int. J. Quant. Chem. **112**, 3018 (2012)

[89] M. Casas, J.M. Getino, M. de Llano, A. Puente, R.M. Carter, H. Rubio, and D.M. van der Walt, Phys. Rev. B **50**, 15945 (1994)

[90] A.B. Migdal, JETP **34**, 1438 (1958), Soviet Phys. JETP **7**, 996 (1958)

[91] G.M. Eliashberg, Sov. Phys. JETP **11**, 696 (1960)

[92] J.P. Carbotte, Rev. Mod. Phys. **62**, 1027 (1990)

[93] W.L. McMillan, Phys. Rev. **167**, 331 (1968)

[94] P. Morel and P.W. Anderson, Phys. Rev. **125**, 1263 (1962)

[95] P.B. Allen and R.C. Dynes, Phys. Rev. B **12**, 905 (1975)

[96] N.N. Bogoliubov, Il Nuovo Cim. **7**, 794 (1958)

[97] V.V. Tolmachev and S.V. Tyablikov, Sov. Phys. JETP, **34**, 46 (1958)

[98] F. London and H. London, Proc. Roy. Soc. **A149**, 71 (1935)

[99] J.F. Annett, *Superconductivity, superfluids and condensates* (Oxford University Press, New York, 2004) p. 62

[100] M. Tinkham, *Introduction to Superconductivity*, 2nd Ed. (McGraw-Hill International Editions, 1996) p. 5

[101] W. Zwerger Editor, *The BCS-BEC Crossover and the Unitary Fermi Gas*, (Springer-Verlag Berlin Heidelberg 2012) p. 4

[102] M. Randeria, Nature Phys. **6**, 561 (2010)

[103] M. de Llano, Mecánica Cuántica 3a Ed. (UNAM, Ciudad de México 2015) p. 195

[104] C.A. Regal, M. Greiner, S. Giorgini, M. Holland, and D. S. Jin, Phys. Rev. Lett. **95**, 250404 (2005)

[105] I. Chávez, J. Ortega, M. de Llano and V.V. Tolmachev, in Superconductivity: Properties, Applications and New Developments, Editor: Paulette Grant. Chapter 4: "*Generalized Bose-Einstein Condensation Model of Superconductivity and Superfluidity*" pp. 91-134. ISBN: 978-1-63483-907-5 (Chapter book)

[106] M. Fortes, M. de Llano, M.A. Solís, to be published.

[107] V.C. Aguilera-Navarro, M. Fortes, and M. de Llano, Sol. St. Comm. **129**, 577 (2004)

[108] M. Fortes, M.A. Solís, M. de Llano, and V.V. Tolmachev, Physica C **364**, 95 (2001)

[109] N.W. Ashcroft and N.D. Mermin, *Solid State Physics* (Saunders College Publishing, USA, 1976)

[110] M. de Llano, F.J. Sevilla and S. Tapia, Int. J. Mod. Phys. **20**, 2931 (2006)

[111] C.E. Gough, M.S. Colclough, E.M. Forgan, R.G. Jordan, M. Keene, C.M. Muirhead, A.I.M. Rae, N. Thomas, J.S. Abell and S. Sutton, Nature **326**, 855 (1987)

[112] J.E. Hirsch, Physica C **2013**, 341 (2000) and refs. therein.

[113] A.A. Verheijen, J.M. van Ruitenbeek, R. de Bruyn Ouboter, and L.J de Jongh, Nature **345**, 418 (1990)

[114] J.E. Hirsch, Phys. Rev. B **68**, 012510 (2003)

[115] J. Colino, M.A.Gonzalez, J.I. Martín, M. Velez, D. Oyola, P. Prieto, and J.L. Vicent, Phys. Rev. B **49**, 3496 (1994)

[116] R. Jin and H.R. Ott, Phys. Rev. B **57**, 13872 (1998)

[117] W. Göb, W. Liebich, W.Lang, I. Puica, R. Sobolewski, R. Rössler, J.D. Pedarnig, and D. Büerle, Phys. Rev. B **62**, 9780 (2000) and refs. therein

[118] T.A. Mamedov and M. de Llano, J. Phys. Soc. of Japan **79**, 044706 (2010)

[119] T.A. Mamedov and M. de Llano, J. Phys. Soc. of Japan 074718, 074718 (2011)

[120] T.A Mamedov, M. de Llano, Phil. Mag. **93**, 2896 (2013)

[121] T.A. Mamedov, M. de de Llano, Phil. Mag. **94**, 4102 (2014)

[122] N.N. Bogoliubov, J. Phys. (USSR) **11**, 23 (1947)

[123] E.H. Lieb, R. Seiringer and J. Yngvason, Phys. Rev. Lett. **94**, 080401 (2005)

[124] Y. Nambu, Phys. Rev. **117**, 648 (1960)

[125] N.N. Bogoliubov, Nuovo Cim. **7**, 794 (1958)

[126] J. Valatin, Nuovo Cim. **7**, 843 (1958)

[127] J. Corson, R. Mallozo, J. Orenstein, J.N. Eckstein, and I. Boővić, Nature **398**, 221 (1999)

[128] J. Corson, J. Orenstein, S. Oh, J. O'Donnell, and J.N. Eckstein, Phys. Rev. Lett. **85**, 2569 (2000)

[129] M. Casas, M. de Llano, A. Puente, A. Rigo and M.A. Solis, J. Phys. and Chem. of Solids **63**, 2365 (2002)

[130] M. Casas, N.J. Davidson, M. de Llano, T.A. Mamedov, A. Puente, R.M. Quick, A. Rigo, and M.A. Solís, Physica A **295**, 146(2001)

[131] S. Fujita and S. Godoy, *Quantum Statistical Theory of Superconductivity*, (Plenum Press, New York 1996) p. 181

[132] R. Micnas and S. Robaszkiewickz, Cond. Matt. Phys. **13**, 89 (1998)

[133] R. Micnas and S. Robaszkiewickz, in "*Ordering phenomena in condensed matter physics"* (Eds. Z.M. Galaziewicz, A. Pekalski, World Scientific, 1991) p. 127

[134] R. Micnas and S. Robaszkiewickz, Phys. Rev. **B 45**, 9990 (1992); R. Micnas, S. Robaszkiewickz, and T. Kostyrko, Ibid **B 52**, 6863 (1995).

[135] M. Bronstein, "*Quantentheorie schwacher Gravitationsfelder*" Phys. Z. Sowjetunion **9**, 140 (1936)

[136] R.K. Pathria, *Statistical Mechanics*, 2nd. Ed. (Butterworth-Heinemann, Oxford, 1996)

[137] M. Casas, M. de Llano, A. Puente, A. Rigo, and M.A. Solís, Sol. State. Comm. **123**, 101 (2002)

[138] I. Chávez, L.A. García, M. Grether and M. de Llano Int. J. Mod. Phys. B **31**, 1745013 (2017)

[139] I. Chávez, L.A. García, M. Grether and M. de Llano Int. J. Mod. Phys. B **31**, 1745004 (2017)

[140] M.A. Khamehchi, Khalid Hossain, M.E. Mossman, Yongping Zhang, Th. Busch, Michael McNeil Forbes, and P. Engels, Phys. Rev. Lett. **118**, 155301 (2017)

[141] G.W. Webb, F. Marsiglio, and J.E. Hirsch, Physica C **514** 17 (2015)

[142] C.M. Hurd, *The Hall Effect in Metals and Alloys* (Plenum Press, New York, 1973) pp. 203-208 and refs. therein

[143] I. Giaver and K. Megerle, Phys. Rev. **122**, 1101 (1961); P. Richards and M. Tinkham, Phys. Rev. **119**, 575 (1960); P. Townsend and J. Sutton, Phys. Rev. **128**, 591 (1962)

[144] I. Chávez, Master Thesis, "*Predictions of the generalized Bose-Einstein condensation theory compared with superconductor experimental data*" Posgrado en Ciencia e Ingeniería de Materiales, UNAM (2013)

[145] M. Grether, M.de Llano, S. Ramírez, and O. Rojo, Int. J. Mod. Phys B. **22**, 4367 (2008)

[146] M. A. Biondi and M. P. Garfunkel, Phys. Rev. Lett **2**, 143 (1959)

[147] D.K. Finnemore and D. E. Mapother, Phys. Rev. **140**, A507 (1965)

[148] C. Kittel, *Introduction to Solid State Physics*, 7th Ed. (John Wiley & Sons, New York 1996), p. 345

[149] R.W. Cohen, B. Abeles, and Gabriel S. Weisbarth, Phys. Rev. Lett. **18**, 336 (1967)

[150] W. Buckel and R. Hilsch, Z. Physik **138**, 118 (1954)

[151] J. Feder, S.R. Kiser, F. Rothwarf, J.P. Burger, and C. Valette, Solid State Commun. **4**, 611 (1966). In addition to γ gallium, there exists a high-pressure modification of Ga with $T_c = 7.5$K see W. Buckel and W. Gey, Z. Physik **176**, 336 (1963)

[152] L. Bosio, A. Defrain, J. Keyston, and J. Vallier, Compt, Rend. **261**, 5431 (1965). $T_c = 6.2 \pm 0.1$ K is the value for β gallium given by Feder *et al.* (see. [151]), Bosio *et al*. give the value $T_c = 6.0 \pm 0.1$ K, and Buckel and Hilsch (Ref. [150]) find for their crystalline modification $T_c = 6.3$ K

[153] Y.J. Uemura, J. Phys. Cond. Mat. **16**, S4515 (2004) and more recently in Physica B **1**, 374 (2006)

[154] I. Božović, C. He, J. Wu, and A.T. Bollinger, Nature **536**, 309 (2016).